UNIVERSITY OF OKLAHOMA

GRADUATE COLLEGE

EVALUATION OF LINER HANGER SEAL ASSEMBLY AND CEMENT SHEATH AS A DUAL BARRIER SYSTEM: IMPLICATIONS FOR INDUSTRY AND REGULATORS

A DISSERTATION

SUBMITTED TO THE GRADUATE FACULTY

in partial fulfillment of the requirements for the

Degree of

DOCTOR OF PHILOSOPHY

By

SHAWGI MOHMED ELZAKI AHMED
Norman, Oklahoma
2020

EVALUATION OF LINER HANGER SEAL ASSEMBLY AND CEMENT SHEATH AS A DUAL BARRIER SYSTEM: IMPLICATION FOR INDUSTRY AND REGULATORS

A DISSERTATION APPROVED FOR THE
MEWBOURNE SCHOOL OF PETROLEUM AND GEOLOGICAL ENGINEERING

BY THE COMMITTEE CONSISTING OF

Dr. Saeed Salehi, Chair

Dr. Catalin Teodoriu, Co-Chair

Dr. Harold L. Stalford

Dr. Ramadan Ahmed

Dr. Hamidreza Karami

Dedication

First and foremost, I would like to thank God Almighty for giving me the strength and ability to preserve and complete this study. Without his blessings, this achievement would not have been possible. I would also like to dedicate this PhD dissertation, to my parents, family, siblings, colleagues, and friends for their continuous and unparalleled love, help, and support.

Acknowledgement

I would like to take the opportunity to acknowledge the contribution of my advisor Dr. Salehi for the continuous support of my PhD study and related research, for his patience, motivation, and immense knowledge. His guidance helped me in all the time of research and writing of this thesis as well as technical articles.

I would like to express my sincere gratitude to my dissertation committee for accepting to be members of the committee. I am deeply indebted to my co-chair Dr. Catalin Teodoriu for his invaluable knowledge, expertise, and support. I am very thankful to my outside committee member, Prof. Harold L. Stalford, and your feedback on the material properties was very useful. My sincere thanks to Dr. Ramadan Ahmed for his valuable discussions and consultations. I credit Dr. Hamidreza Karami for his suggestions to improve the quality of my work and for insightful discussions. I would particularly like to acknowledge all of my committee members for their contributions, feedbacks and insightful comments you have given during my general exam.

I wish to extend my special thanks and recognition to Dr. Chinedum Ezeakacha, Dr. Raj Kiran, Dr. Harshkumar Patel, Mr. Musaab Elhag, colleagues, and my friends for their invaluable feedback, consultation, and encouragement. I am particularly thankful to Mr. Jeff McCaskill for his compassion, patience, and support. My sincere thanks also go to Dr. Ali Tinni, and Mr. Gary Stowe for their support during core samples preparation.

Finally, I deeply thankful to my dear wife, son, and daughters for their love, support, and sacrifices. I am grateful to my siblings for always being there whenever I need them. I am forever indebted to my parents for giving me the opportunities and experiences that have made me who I am.

Table of Contents

List of Tables

List of Figures

Abstract

Robust dual barrier systems are crucial for well integrity. Regulators and industry have consistently raised the concerns in such systems regarding the testing, qualification, and prediction of leakage pathways and failure modes. Liner hanger is an example of dual barrier system in which seal assembly and cement sheath act as two barrier elements.

The objective of this study is to evaluate the performance characteristics of the liner hanger dual barrier system and to identify the risks of failures that could compromise the wellbore integrity. In this study, the performance of the liner hanger dual barrier system was evaluated using experimental and numerical approaches. Results of experiments revealed that elastomers' sealability was not affected after they were exposed to a surfactant degradation. However, the seals failed the pressure tests when they had mechanical defects present and also after exposure to carbon dioxide. The results also revealed that neat Class H cement requires gas migration control additive to act as a primary barrier. In addition, wait-on-cement (WOC), pipe material and surface roughness play key roles in the strength of cement bonding.

Finite element analysis (FEA) models were developed to evaluate the performance of the liner hanger dual barrier system. The results disclosed that elastomer contact pressure (sealability) mainly depends on the compression ratio, seal materials, pipe materials, and volumetric swelling. The friction coefficient at the seal-casing interference has a minor effect on the contact pressure. Results also showed that tensile hoop stress is the most dominant factor which compromises the cement hydraulic and mechanical integrity.

The contribution of this research can advance performance evaluation guidelines of the liner hanger dual barrier system in terms of failure modes prediction and operational limits identification. In addition, the research highlighted some of the gaps in current industry standards and regulatory guidelines that need further considerations.

Chapter 1: Introduction

1.1 Overview of Liner Dual Barrier Systems

In recent decades, exploration and drilling operations have been venturing into harsh environments that pose significant challenges for operators and regulators, especially in the offshore deep and ultra-deepwater basins. The well construction in these environments requires a unique casing program that usually consists of a number of complex tubular and casing strings. In this context, liners and liner hangers are the most essential components of the well casing strings. Liners are usually deployed to penetrate the troublesome and sensitive formations, such as shallow gas-pressurized zones, salt domes, and depleted reservoirs. In addition, liners are a viable solution in the completion of wells with complicated trajectories, such as multilateral, s-shapes, and extended -reach wells. Mohamed and Al-Zuraigi (2013) claimed that deploying a liner in lieu of running a full casing string is a developing industry practice because liner provides many advantages. The advantages include but are not limited to cost-saving (less steel is used), reducing the load hung on the wellhead, requiring short running time, enabling high flow rate circulation while cementing operations, and assuring efficient completion of monobore wells.

API STD 65-2 (2010) defines liner as "A casing string that does not extend to the top of the well or to the wellhead." Technically, liners are correlated to their respective well depth or casing. For example, a liner installed to isolate the surface depth of a well is called a surface liner. Whereas the liners used to isolate the intermediate and productive depths are called intermediate and production liners respectively as shown in Figure 1.1. Liner is suspended or attached from inside the previous host casing string using a device called "liner hanger." The liner hanger technology started with the mechanical-set (conventional) liner hangers, which evolved into hydraulic-set liner hangers, balanced cylinder hangers, and expandable liner hangers (Mohamed

and Al-Zuraigi 2013). Among these types, the conventional and expandable versions will be briefly described herein, as they are commonly used in the oil and gas industry. The conventional hanger version consists of setting components called slip and cone that mechanically driven by the drilling string to energize the liner hanger seal assembly. In this technique, the process of slip-cone engagement always confronts technical issues that create leak pathways for the flow of uncontrolled formation fluids into the wellbore and/or to the surrounding environment. Therefore, the failure of the liner hanger system may impose a significant risk that could compromise the well integrity (Walvekar and Jackson, 2006: Ahmed et al. 2020a). To eliminate potential risk, the liner hanger seal assembly is usually supported by a cement sheath that collectively establishes a protection system called a dual barrier system as shown in Figure 1.1.

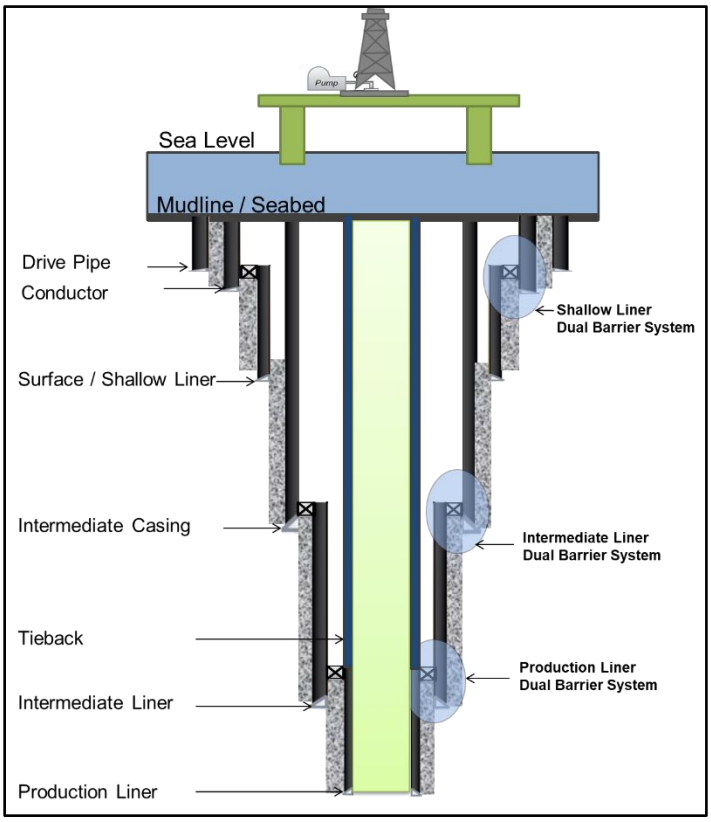

Figure 1.1: General representation of liner hanger dual barrier systems (seal assembly and cement sheath) for a deep water well

1.2 Problem Statement and Motivation

Current studies have revealed that most of the oil and gas incidents are caused by gas migration in shallow formations during drilling operations. These formations are commonly isolated by deploying surface liner(s) supported by a dual barrier system, consisting of seal assembly and cement sheath. Failure of this type of barrier system is always a hot topic for industry and regulators, especially failure in mechanical conventional liner hangers. In these versions, the failure rate of the top packers exceeds 40% (Nida 2005; Walvekar and Jackson 2006). The outcomes of an informal survey conducted in 1999 over several Gulf of Mexico (GoM) operators disclosed that 30% to 50% of pressure seals in overlaps failed (Moore et al. 2002). Van Dort (2009) stated that a failure of critical liner hanger seal assembly that serves in high pressure/high temperature (HPHT) environments has become a problematic issue and accounts for 18% of offshore wells integrity issues worldwide. Recently, Patel et al. (2019a) clarified that more than 46% of failure in secondary barriers originated in seal components.

In addition to the mentioned technical issues, the testing and verification of dual barrier system elements challenge industry and regulatory agencies because the seal assembly is placed ahead of the cement sheath as shown in Figure 1.2. It should be noted that this topic has not been fully addressed in the current literature. Following the introduction of liner hanger technology, most of liner hanger topics addressed by many researchers have focused on leak issues on liner top (Agnew and Klein 1984), liner cementing issues (Hebert 1986), design criteria and axial load capacity (Moore et al. 2002), sealing problems of conventional liner hangers (Walvekar and Jackson, 2006; Jackson and Smith, 2006; Williford and Smith, 2007), liner hangers technology (Mohamed and Al-Zuraigi 2013), and liner rating capacities (Payne et al. 2016). In addition, other studies have focused on liner hangers elastomeric swellable technology (Al-Yami et al. 2008; Pervez et al. 2009; Ma et al. 2014a), HPHT expandable liner hanger technology (Royer and Turney

2019), liner hangers setting and energization (Patel et al. 2019b), casing-liner overlap cementing (Al-Ramadan et al. 2019). From this screening, it is clear that testing and verification of dual-barrier system have not been addressed. Therefore, the scope of this study includes a thorough review of dual barrier system testing and verification as well as predicts the modes of failure that may occur during the barriers' life cycle.

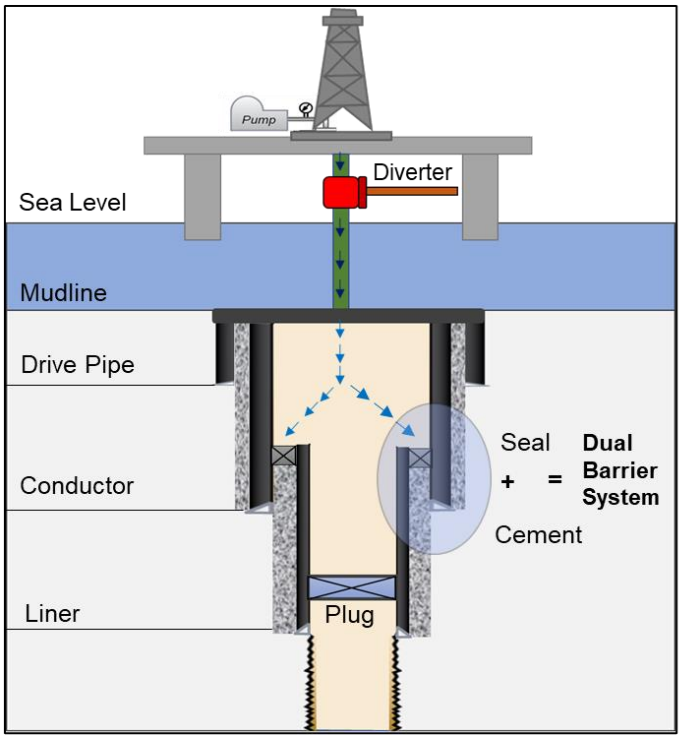

Figure 1.2: Pressure test arrangement for liner hanger dual barrier system (seal assembly and cement)

The motivation for this study is promoted by the incident that occurred in 2013 while drilling an offshore well located in Main Pass Block 295 (MP 295), Gulf of Mexico (GoM). The incident represented a critical event that has driven service companies, researchers and regulators, to conduct further studies in liner hangers' systems. The incident occurred because of the failure of the liner hanger dual barrier system. The barrier elements (seal and cement) were breached by a gas kick migrated while drilling a long open hole section in a gas-charged formation as shown in Figure 1.3. The root cause of the failure has not been well-identified due to the complex nature

of this type of barrier system. The findings of the United States, Bureau of Safety and Environmental Enforcement BSEE (2014) investigation report highlighted a number of unresolved issues that require a further research. The issues raised questions related to the testing and evaluation of the dual barrier system as well as the identification of the primary barrier (seal, cement, or both).

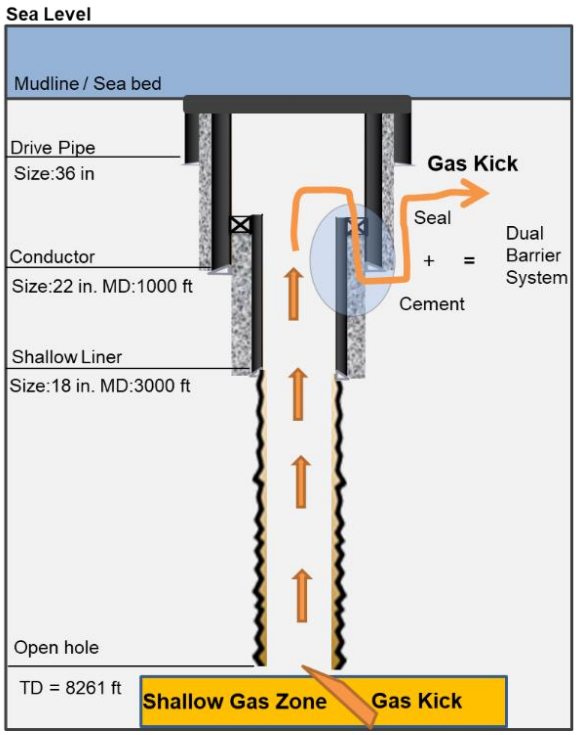

Figure 1.3:Wellbore schematic showing gas migration into liner seal/cement overlap (reproduced after Morris et al. 2015)

1.3 Research Objectives

The objective of this research is to evaluate the performance of a liner hanger dual barrier system that incorporates sealing assembly and cement sheath. To maintain the well integrity in terms of risk prevention, this barrier system must be robust, reliable, and functional. The specific objectives of this research are to:

- Study the validity of the pressure test for liners dual barrier system evaluation and review standards and regulations gaps.

- Define the primary barrier when a liner hanger seal assembly and cement are used as a dual barrier system to seal off a liner.

- Evaluate the performance of seal assembly/ elastomers at different downhole operating conditions and predict the failure scenarios.

- Assess the effect of pressure cycling upon the elastomers' performance.

- Evaluate the effect of using an anti-gas migration additive on cement sealability.

- Evaluate the performance of the cement sheath at different operating conditions and predict the potential failure scenarios.

1.4 Research Hypotheses

Based on the challenges raised by industry and regulators in terms of primary barrier identification in liner hanger dual barrier systems, the following hypotheses are considered for this research:

- Seal assembly can be identified as a primary barrier in the liner dual barrier hanger system if it is being selected, designed, manufactured, qualified, deployed and tested properly. In addition, it is maintained within its design envelope

- Cement can be identified as a primary barrier if it is properly designed, placed, and tested. In addition, it is maintained within its design envelope

1.5 Research Scope and Methodology

The methodology of this study was classified into three levels of investigations in order to cover the scope and to meet the objectives. The research levels include theoretical literature review, experimental investigation, and numerical modeling analysis. The relation interrelated these levels is structured in the framework shown in Figure 1.4. The scope of each investigation level is discussed in the following methodologies:

1. *Theoretical Review*: The objective of the theoretical analysis conducted in this study is to provide a comprehensive critical review of literature on wellbore barriers systems, specifically the liner hanger dual barrier system. The review focuses on the following: conducting a thorough investigation on the complexities of gas migration from shallow zones into the wellbore, the type of liner hanger seal materials that are used as barrier elements, the failure modes of liner hanger seal assemblies, liner hanger cement practices, and the measurements that can be applied to control the potential leaks, kicks, and blowouts. In addition, the gaps in current industry standards and government regulations are identified to advance improvements in liner hanger seal assemblies and cement integrity. The aim of this review is to provide an in-depth evaluation of the current state of the liner hanger issues and implications that challenge industry and regulatory agencies. Findings and outcomes from this review also assisted in establishing guidelines for performance evaluation techniques and approaches, such as laboratory experiments and numerical model simulations. These approaches are utilized to accomplish the objectives of this study.
2. *Laboratory Experiments*: In this study, two stages of experiments were conducted to evaluate the integrity of the liner hanger dual barrier system using an experimental setup.

In the first stage, pressure tests were conducted on elastomer samples that are commonly used in liner hanger technology. In this case, the elastomer seals were considered a single barrier system and the pressure tests were conducted considering two different experimental scenarios (regular and irregular conditions). Based on the outcomes of the first stage, the second stage of the experimental work was established. In the second stage, experiments were conducted to test both elastomer seals, and cement as a dual barrier. The details of all the experiments are described in Chapter 4.

3. *Numerical Modeling and Simulations*: The numerical modeling approach was validated by a lab-scale experimental work. FEA models were created to mimic the casing program of the shallow section of the well. The objective is to evaluate the performance of the liner hanger dual barrier system at various wellbore operating conditions as described in Chapter 6.

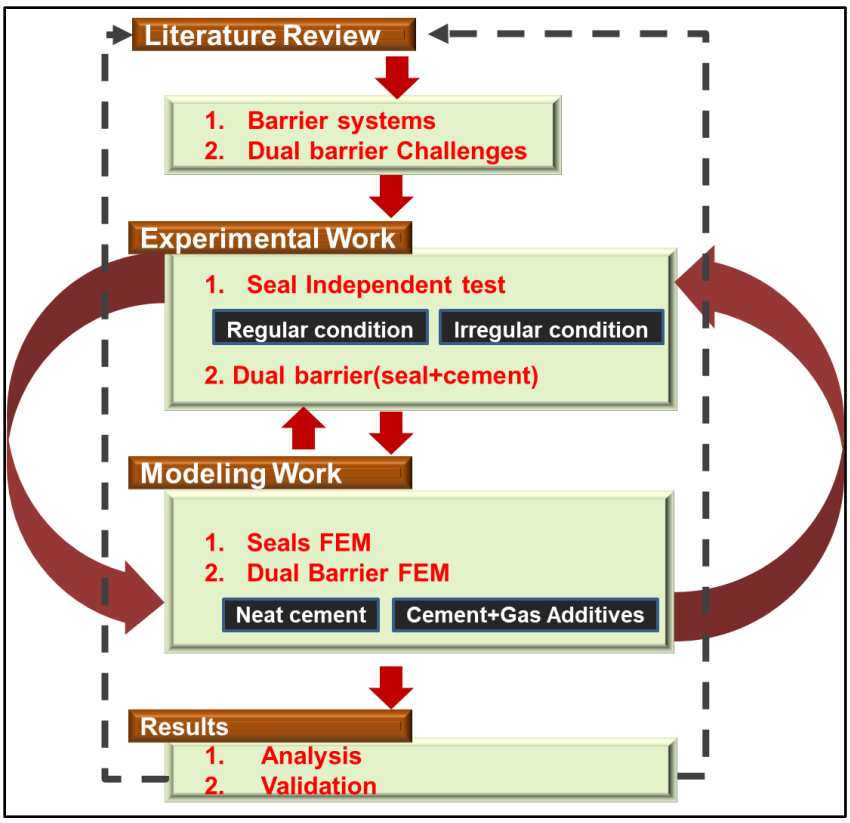

Figure 1.4: Methodology model used for performance evaluation of liner hanger dual barrier system

1.6 Dissertation Structure

The study is structured into eight chapters. Chapter 1 provides an overview of the liner hanger dual barrier system and underlines the problems related to this type of barrier. The motivation, scope, hypotheses, and objectives of the dissertation are also discussed. In Chapter 2, a comprehensive literature review of the wellbore barrier systems, with special emphasis on the liner hanger dual barrier system is presented. Various types of barrier systems established to maintain the integrity of the wellbore are thoroughly discussed. Chapter 3 describes the liner hangers technologies, sealing mechanisms, liner cementing techniques, cement key properties, and dominant failure mechanisms in the elements of the dual barrier system. The latest technologies, techniques, and materials invented to improve the barriers' performance are highlighted. The gaps in current standards and regulations relevant to testing and verification of the dual barrier system are

discussed extensively. Chapter 4 outlines the experimental work conducted to evaluate the performance of the liner hanger dual barrier system at different operation scenarios. Chapter 6 demonstrates the numerical approaches used to develop finite element models that utilized to predict potential failure scenarios and to demarcate safe wellbore operating envelopes. The results of the experimental and numerical work are presented in Chapter 5 and chapter 7 to establish a comparative analysis that assists in a better understanding of the performance of the barrier. Chapter 8 summarizes conclusions and recommendations that set to help in maintaining a robust, durable, and reliable dual barrier system.

Chapter 2: Literature Review of Wellbore Barrier Systems

2.1 Critical Events Affect the Integrity of the Wellbore

The well integrity can be compromised according to the occurrence of one or more undesirable critical events. Skogdalen et al. (2011) state that there are three categories of undesired events that may be encountered during the drilling operations. The first two categories are wellbore leakage/spills and unintentional well influx (kick). Whereas the third disastrous category is a blowout that mostly happens as a result of the loss of well control (LOWC). Due to their adverse impact on the well stability, these events are thoroughly discussed in the following subsections.

2.1.1 Leakage and Spills

A leak (also known as fugitive emissions), is defined as an unintended movement of fluid to or from a system (ISO16530-1 2017). Leakage is defined as visible passage of pressurized fluid from the inside to the outside of the pressure-containment area of the equipment being tested (API 16A 2017). Although a leak is well defined, and a variety of robust sealing systems have been developed to prevent fluid leakage, the exact mechanism of the surface roughness induced leakage is not well understood (Persson and Yang 2008). Watson and Bachu (2007); Davies et al. (2014) emphasized three main factors required for leakage initiation, a source, a driving mechanism (e.g. buoyancy, head differential), and a pathway. The leak pathway is usually created according to the interconnection of void spaces formed by the topographical variations of the static mating surfaces (Bauer 1965). In addition to lack of knowledge of the leak mechanism, currently, there is no accepted definition of the term "zero leakage". For instance, according to Advanced Technology Labs, zero leakage is defined as $< 10^{-8}$ cm ^{3}/ s of helium at atmospheric pressure. Whereas, according to the National Aeronautics and Space Administration (NASA), zero leakage defined as a flow rate not more than 1.4×10^{-3} cm ^{3}/ s of nitrogen at 300 psi and ambient temperature (Bilzzard

1990). For the well barriers serving in oil and gas wellbores, NORSOK D-010 (2013) states that the acceptable leak rate shall be zero unless specified otherwise in certain well barrier element acceptance criteria. As per ISO 16530-1 (2017), applying zero-leak-rate criteria during the well operational phase is unrealistic due to the pressure build-up as a result of the effects of temperature variation, air entrapment, and media compressibility. Therefore, NORSOK D-010 (2013) recommends establishing maximum allowable leak rate criteria for evaluating the well barriers performance. ISO 16530-1 (2017) includes a leak rate acceptance matrix for most of the wellbore barrier elements.

Feather (2011) claimed that well integrity is a global challenge mainly caused by leaks in (tubular, casing, valves, packers, and reservoir issues) and/or annular flow through (cement, packers, liner seal assemblies, and plugs). As shown in Figure 2.1, there are thousands of onshore and offshore wells leaking worldwide. The Norwegian Petroleum Safety Authority (PSA 2006) stated that in 482 gas wells at the North Sea, 18% of the wells were leaking. The U.S. Mineral Management Services database (MMS, 2000) showed that at 6650 gas wells in the Gulf of Mexico (GoM), 45% of the wells had leakage issues. The leaking wells were diagnosed with sustained casing pressure resulting from tubing and casing leaks. MMS (2000) surveyed 200,000 onshore wells, the results showed that 16.7% of the wells had leakage problems.

Over the years, spill incidents in the oil and gas sector have been considered critical environmental challenges. The consequences of these events have increased the technical and operational safety requirements and created more awareness of challenges resulting from spills in various operations. The Code of Federal Regulations (CFR 2016), Sec 254.46 (b) (2), obligates operators exploring in the U.S Outer Continental Shelf (OCS) to report any spill of one barrel or more. Spills above 50 barrels require more detailed reporting and monitoring. The spill events that

occurred over the years 2007-2016 were reported by BSEE (2016) showed an annual average of nine spills. The high number of spills recorded in 2008 was due to facilities damaged caused by Hurricanes. The main causal factors associated with the offshore platforms' spills are natural causes (e.g. weather), human error, external/other factors, equipment failure, and unknown. Equipment failure drives the spill events during the drilling and production phases (ABS 2016).

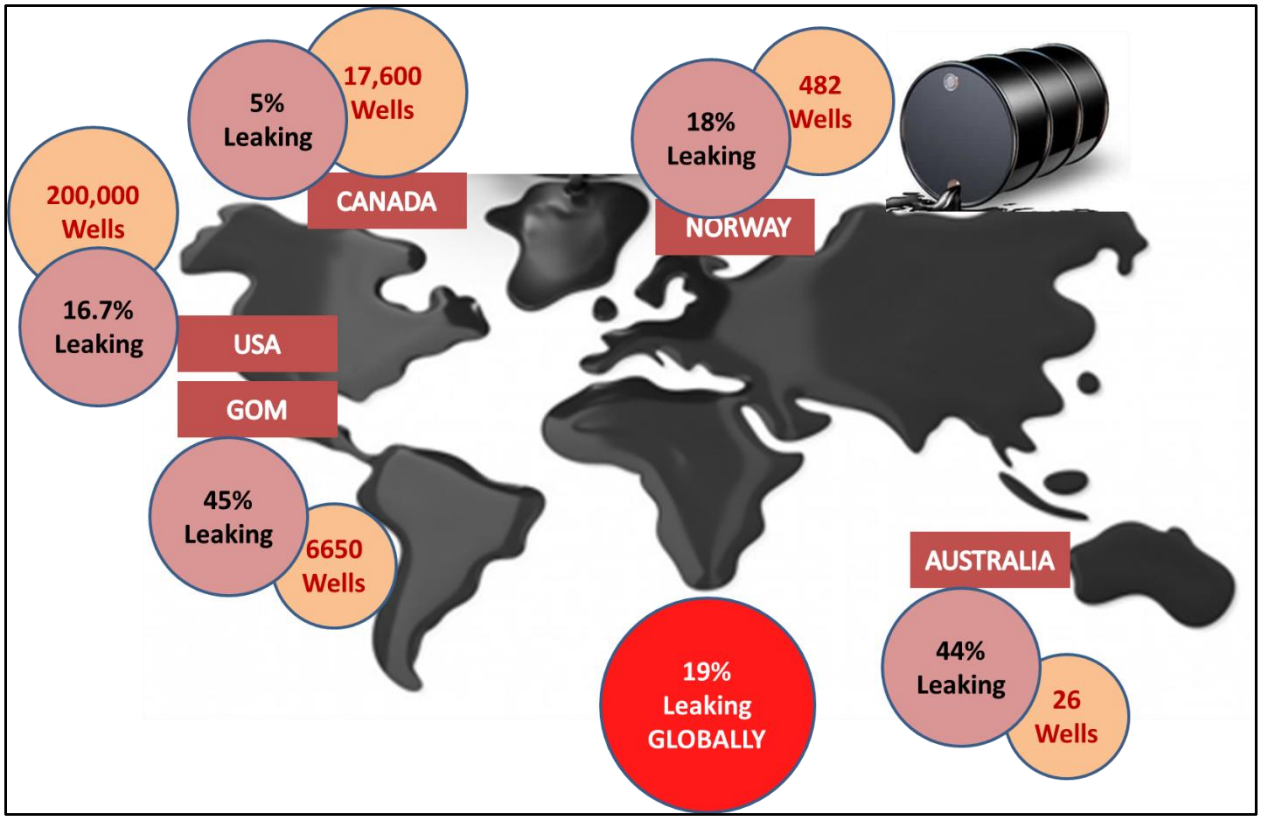

Figure 2.1: Oil and gas wells leak around the world

2.1.2 Gas Migration and Kick

Percolation of uncontrolled gas/kick into the wellbore is a common problem that has been confronted since the first oil well was drilled. The gas can migrate when potential risk sources are not completely isolated either at the drilling operation or later during the production phase. Dusseault et al. (2000) underlined that multiple strata rich in free gas usually found in any well. The gas can migrate through the flaws at cement-rock/casing interference that have circumferential

fracture aperture in the order of 10 to 20 micrometers. Watson and Bachu (2007); Dusseault et al. (2000) claimed that gas usually propagates into the wellbore and/or behind the casing string to the surface according to two mechanisms called surface casing vent flow (SCVF) and soil gas migration (GM), respectively (see Figure 2.2). GM is attributed to gas migration from shallow zones whereas SCVF is attributed to the gas migration from deep zones as shown in Figure 2.2.

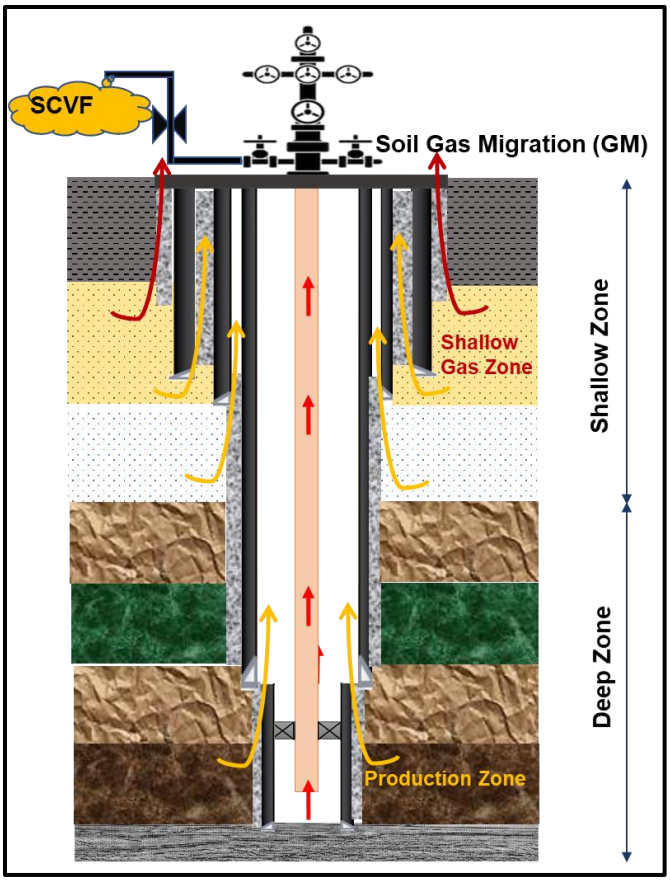

Figure 2.2: Gas migration mechanisms, SCVF and GM (reproduced after Watson and Bachu 2007)

NORSOK D-010 (2013) defines a shallow gas zone as any depth drilled before the surface casing has been deployed and the blowout preventer (BOP) has been mounted on the wellhead. Any zone penetrated after the BOP is installed is not considered a shallow gas zone. Gas is the predominant hydrocarbon fluid leaking source that can jeopardize the wellbore integrity. Prince

(1990) demonstrated that shallow gas kick most likely results in complex downhole conditions during the drilling operations because it cannot be detected, confirmed, and circulated using the conventional well control procedures. Shallow gas blowouts have been reported as the most disastrous worldwide events in the oil and gas industry. The Norwegian SINTEF Energy Research database showed that shallow gas is the major cause of kicks that led to 172 blowouts recorded around the world (Goins and Ables 1987). Prince (1990) declared that around one-third of the global blowouts have been initiated by a shallow gas kick. Skalle (2012) claimed that every 100th gas kick results in one blowout. Recently, Per Holand (2017), conducted a screening study for the kick events on exploration and developmental wells drilled in various regions. Figure 2.3 shows that the U.S. Outer Continental Shelf (OCS) kick frequency in 2011-2015 is higher than that of North Sea OCS (Norway and U.K.) in 2009-2014. The author attributed the difference to many factors such as incident reporting procedure, well controls policies, formation type, well depth, drilling margin, well monitoring technology, and personnel qualification requirements. Wells drilled in the U.S. OCS are characterized by deeper depths, narrow drilling margins, and very young formations. All these factors increase kick probability.

The most common causes of kick include, but are not limited to: insufficient drilling fluid density, swabbing during drilling in relatively low overbalance conditions, improper hole filling, loss of circulation, tripping out of the hole, tripping in of the hole, gas cut mud from drilled gas, drill stem testing, excessive drilling rate through gas sand, and drilling into neighboring producing well (API RP 59, 2018; Skalle 2012). Per Holland (2017) attributes the causes of a shallow kick to: too low drilling fluid density (seawater commonly used to drill shallow well sections), swabbing, cement hydrostatic decay that occurred during its transition from liquid to a solid phase, and improper cement placement. The main kick contributor factors are summarized in Figure 2.4.

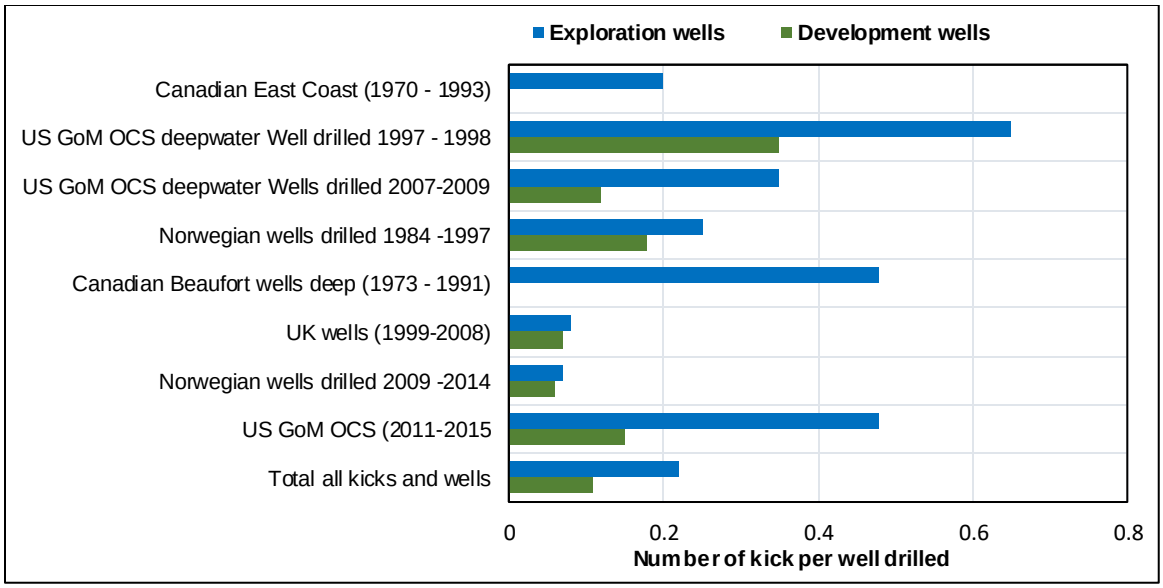

Figure 2.3: Overviews of kick frequencies from various countries (Modified after Per Holand 2017)

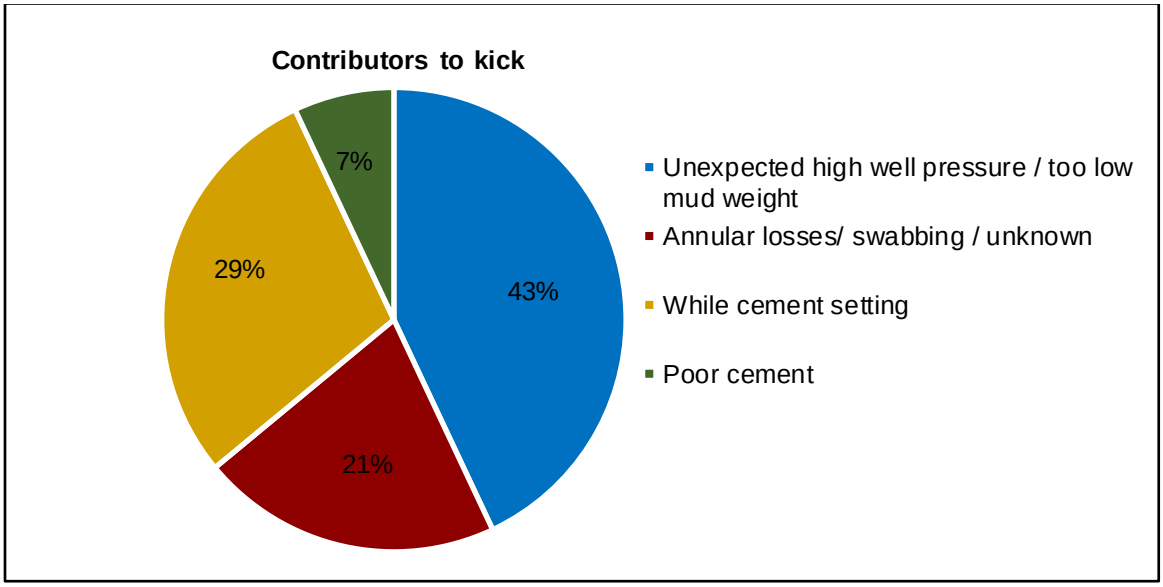

Figure 2.4: Causes of kick in shallow zones (Modified after Per Holand 2017)

2.1.3 Loss of Well Control (LOWC)

Maintaining a well under control is a primary and essential safety requirement that can be accomplished by stacked robust barrier systems. The well primary control can be lost in case the integrity of the barrier system is compromised during performing one of the major activities. Such

activities include but are not limited to: drilling, completion, production, abandonment, testing operations, wireline operations, coiled tubing operations, and snubbing. LOWC incidents can be categorized into four levels of events (CRF 2016; BSEE 2016):

- Aboveground/surface blowout
- Underground blowout
- Flow through a diverter
- Uncontrolled flow resulting from a failure of procedures or surface equipment

Statistical records based on the number of LOWC incidents reported by BSEE (2016) on the U.S. OCS from 2006 to 2016 (Figure 2.5) showed an average of five LOWC events occur each year. Figure 2.5 shows a continuous decrease trend from 2013 to 2016.

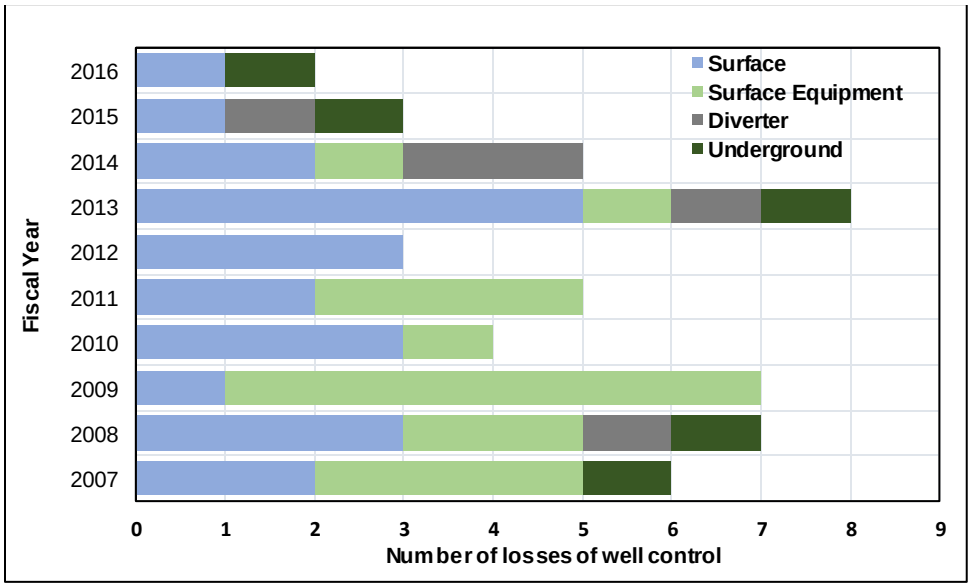

Figure 2.5: Causes of LOWC events occurred at U.S. OCS during 2006-2016 (Modified after BSEE 2016)

A blowout is an uncontrolled kick or uncontrolled influx into the wellbore (Skalle 2012). The author underlines that the kick can be controlled, whereas a blowout means the ability to control the kick is lost. Blowout is conventionally classified into above or underground. The underground blowout is defined as uncontrolled migration of formation fluids from a high-pressure zone into a

lower pressure zone (API RP 59 2018; API STD 53 2018). Underground blowout is mainly caused according to the fracture of the weak formation located just below the casing shoe (shown in Figure 2.6 (a)) that is triggered by excessive annulus backpressure. This phenomenon is very common during drilling the uppermost shallow gas zone(s). In these zones, the likelihood of experiencing blowouts from shallow gas kicks is more probable than e xperiencing kicks during drilling in deeper wellbore zone(s) for many reasons (Goins and Ables 1987; Byrom 2013). First, in a shallow depth, the overbalance margin is very minor and any slight deviation from this narrow margin can cause a substantial underbalanced condition that is most likely prompting the gas kick swabbing into the wellbore. Unlike the shallow formation zone(s), the deep formation sections of the wellbore can tolerate the deviation in the overbalance margin. The second reason is linked to the fact that the shallow casing strings provide slight protection against shallow gas kicks. The formations at the conductor or surface pipe are usually very young and have low fracture gradient values. Therefore, these formations are very weak and cannot withstand the wellbore pressure spike occurs in the event of the well is shut-in during kick invasion. The formation fracture most likely results in very complicated situations, such as loss of circulation, that end up with underground blowout fires as shown in Figure 2.6 (a). The uncontrolled gas kick can migrate to the surface and creates a gas crater around the rig as shown in Figure 2.6 (b). The crater can topple the jack-ups and platforms as shown in Figure 2.6 (b); hence they are the most vulnerable structure of the rig foundation. The crater can also cause critical evacuation implications because the gasified zone around the rig reduces the bouncy force needed to lift the lifeboats (Grace 2017).

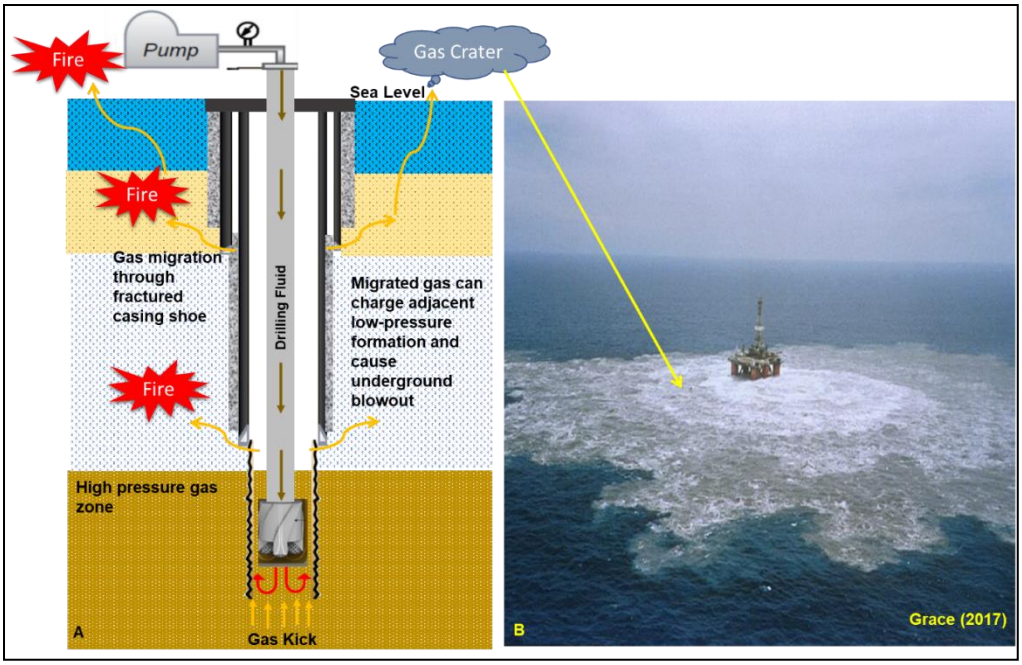

Figure 2.6 : Underground blowout mechanism (a), gas crater around semisubmersible ring (b)

2.2 Barrier Systems According to Current Standards

2.2.1 Overview of Wellbore Barrier Systems

Safety is a core value for the well integrity concept that recently has been introduced in the oil and gas industry to prevent risk during the life cycle of a well. According to Skogdalen et al. (2011), the technical, operational, and organizational measures to diminish the risk mentioned in NORSOK D-010 (2013) are called safety barriers. In this context, there is no common definition of the term "barrier" available in the literature, however, all terms share the same nuances as stated in the forthcoming definitions. A barrier is an obstacle or impediment to flow and/or pressure (API RP 19LH 2019). The Norwegian Petroleum Safety Authority (PSA 2013) defines barrier as "Technical, operational and organizational elements which are intended individually or collectively to reduce possibility/ for a specific error, hazard or accident to occur, or which limit its harm/disadvantages." Sklet (2005), defines the well safety barrier as a physical and/or a non-physical means planned to prevent, and/or control, and/or mitigate the occurrence of undesirable

events or accidents over the life cycle of the well. According to Sklet (2005) and ISO 13702 (2015) prevent, in the context of this definition, means to reduce the probability of the occurrence of hazardous events. "Control" refers to the processes of limiting the acceleration of the events in a very short duration. Meanwhile, "mitigate" refers to minimizing the consequences of hazardous events. API RP 96 (2013) defines a barrier as "Component or practice that contributes to the total system reliability by preventing formation fluid or gas flow." The standard states that when barriers are combined in one system and act collectively to prevent the influx of unintended fluids flow, the system is technically called the "barrier system." According to NORSOK D-010 (2013), the well barrier system is defined as "Envelope of one or several well barrier elements preventing fluids from flowing unintentionally from the formation into the wellbore, into another formation or to the external environment." As per API 65-2 (2010), well barrier system is defined as "One or more barriers that act in series to prevent flow." The standard highlights that well barriers that do not act in series are not considered part of a single well barrier system, as they do not work collectively to support total system reliability. In this context, the total system reliability refers to the likelihood of barrier success, or one minus likelihood to fail.

Sklet (2005) states that the barrier system is a system established (designed, installed, qualified, tested, verified, and managed) to perform one or multiple functions. Among others, the most essential objectives/ functions of the well barrier are (Torbergsen et al. 2012):

- Prevent a major wellbore fluid leakage to the surrounding environment
- Shut-in the wellbore on direct command during an emergency shutdown scenario to prevent formation fluid influx and migration in the well

To fulfill these objectives, a barrier must meet certain performance requirements, such as functionality, availability, reliability, capacity, effectiveness, integrity, ability to withstand loads,

robustness, accessibility, and response time (PSA 2013; ISO 16530-1 2017). In addition to these, failure mechanisms, failure consequences, operating conditions, and interactions with other systems should be considered as part of the performance standards (ISO 16530-1 2017).

According to API RP 96 (2013), well control is defined as activities or processes that are implemented to prevent or mitigate the unplanned release of formation fluids from the well to its environments. Industry and regulators agencies issued different guidelines and rules for well control. However, they agreed on a common rule for well control barriers specifying that: "at least, two tested independent barriers must be allocated between the reservoir and the environment at all times" (NORSOK D-010 2013; API RP 96 2013; ISO 16530-1 2017; API STD 53 2018). Application of this rule is also recommended by the U.S Code of Federal Regulations CFR (2016) and The Norwegian Petroleum Safety Authority (PSA 2013) regulations. It is a safety requirement for oil and gas operators to strictly apply the concept of two well barriers during all well operation activities. However, most of the investigations of the loss of well control incidents disclosed that most of the two well barriers were not maintained by the rig crew (Strand 2017).

The concept of establishing a robust barrier system incorporating several active and redundant barrier elements was introduced to enhance the integrity and reliability of the well (ISO 16530-1 2017). The number and types of well barriers are technically selected based on the downhole conditions and the governing regulations. However, it is commonly accepted safety practice to stack two independent barriers to enhance the protection layers (API RP 96 2013). Technically, the independent barriers provided are classified into primary and secondary barriers. Pertaining to the function it is intended to perform, the barrier can be classified as: permanent (e.g. casing, cement, hangers) or temporary (e.g. drilling fluid, diverter, BOP); active (human/BOP) or passive (seals); and on-line (continuous duty) or off-line(need to be activated) (Sklet 2005).

The primary barrier(s), defined as the first line of defense, formed by cascading a series of barrier element(s) to directly be in contact with the pressure/flow source. The secondary barrier(s) is characterized as a redundant set of barrier element(s) that do not directly contact the pressure/flow source. Technically, they are backup for the primary barrier (ISO 16530-1 2017). Backup in this context implies that an element or system is installed to function when the primary element or system is in a defective condition. The barrier can be identified as a primary or a secondary depending on the following factors:

- The direction of influx to be contained
- The operation phase of the well (e.g. drilling, completion, production, and abandonment)
- Drilling method (conventional, underbalanced, and managed pressure)

2.2.2 Special Requirements for Barriers Serve in Corrosive and Geothermal Environments

Drilling and completion operations at formations containing high concentrations of corrosive gases, such as H_2S, SO_2, CO_2, and CH_4, require the barrier systems to be designed, fabricated, installed, tested, and verified in very rigorous methods in order to maintain the well integrity. According to CFR (2016), Sec 250.490, the barrier installed to work at bottom-hole with H_2S must be manufactured from materials that resist or prevent sulfide stress cracking (also known as hydrogen embrittlement and stress corrosion cracking). Critical materials of wellbore barriers, such as tubular (drill pipes, tubing, casing, connections, and flanges) and BOP system elements shall be specified in accordance with NACE standard MR0175-1. The drill string must not be subjected to high stresses. Elastomer seal shall be manufactured from materials with high resistivity to H_2S. In addition, non-metallic materials of temporary barriers, such as bridge plugs and retrievable packers shall be designed to resist the harsh nature of H_2S gases. In this context API 17TR8 (2015) defines corrosion resistant materials (CRM) as “Ferrous or non-ferrous alloy

that is more corrosion-resistant than low-alloy steels." Examples of CRM are duplex, austenitic, martensitic stainless steels, and corrosion-resistant alloy.

CFR (2016), Sec 250.490 recommends the injection of corrosion inhibitors to control chemical reactions between barriers and H_2S. The code also states that, during drilling, completion, and work-over operations, sets of sensors shall be installed at some control points, such as mud return line, bell nipple, trip tank, shale shaker, and other areas where H_2S may accumulate.

Formations rich with acidic gas usually exist under high-pressure and high-temperature (HPHT) conditions (Bihua et al. 2018). Therefore, cement recipes designed for zonal isolation of these types of formations must be acid resistant with a high density. Many researches have been performed to develop slurries that meet the requirements of the regulations. Adding additives to the base cement is a common field practice, enhancing its acid resistance and improving the other cement tensile properties. Experimental results conducted by Ahmed et.al (2015) revealed that Class H based hydroxyapatite and magnesium oxide containing cement is the best formulation resisting acidic gas attack under HPHT environments. Cement resistance can be significantly enhanced by adding corrosion -resistant for Fe_2O_3-amended cement (Bihua et al. 2018) and adding pozzolan-amended cement (Zhang et al. 2013). Many researchers recommend the addition of silica flour to improve the properties of cement shear bond (Ahmed et al. 2015) and to prevent cement retrogression in geothermal wells (Kosinowski and Teodoriu 2012). To avoid cement retrogression at a temperature above 230°F, API RP 65-1 (2018) recommends the addition of approximately 35 % to 40 % crystalline silica by weight of cement. Allan and Philippacopoulos (1998) state that for geothermal applications, the cement requires to develop a 1000 psi after 24 WOC (this value must be well-maintained for at least 12 months) and to develop a bond strength of 100 psi to steel.

Chapter 3: Literature Review of Liner Hanger Dual Barrier System

3.1 Seal Assemblies of Liner Hanger Dual Barrier System

3.1.1 Overview of the Evolution of Liner Hanger Technology

A liner hanger is a device that is positioned at the top of the liner string to anchor the liner with previous casing. It supports the weight of the liner and is set by engaging the slip and cone using the drilling string as in the mechanical type (Figure 3.1(a)) or by external expansion using pressure force as in the expandable liner types as shown in Figure 3.1(b) and (c). Furthermore, the liner hangers seal off the annulus above and below the seal when an external seal is energized (API RP 65-2 2010; API RP 96 2013).

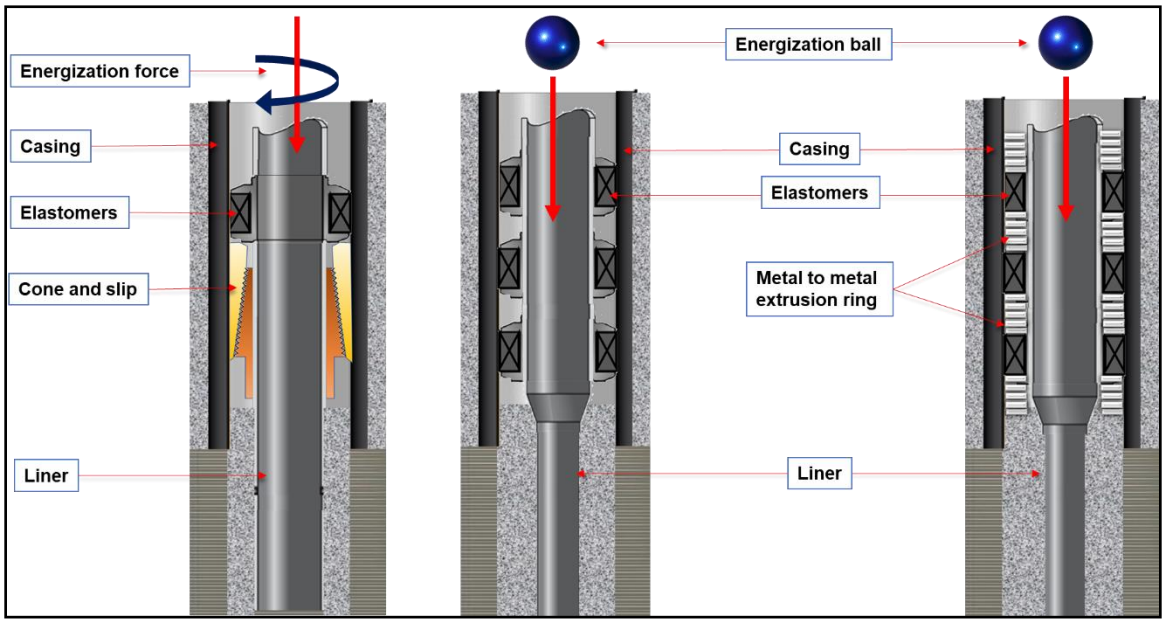

Figure 3.1: General representations of (a) conventional mechanical, (b) conventional expandable, and metal-to- metal (c)expandable liner hanger seal assemblies

Conventional mechanical liner hanger leak is still challenging the oil and gas industry even after the invention of the new generation of integrally liner top packers (Walvekar and Jackson 2006; Jackson and Smith 2006; Williford and Smith 2007). The authors attribute the issues of the

conventional hangers to the complexity of the mechanical elements they incorporated. Defective mechanical elements usually provide multiple leak paths.

In 1999 the technology of the expandable liners was developed to solve leakage problems in mechanical liner hangers. Expandable liners are superior because they do not contain complicated mechanical components (Mohamed and Al-Zurigi 2013). The setting mechanism of the expandable hanger depends on the energization procedure of the seal assembly incorporated on the hanger body (Byrom 2013). Despite the significant advantages of expandable liner hanger, it has the following limitations (Mohamed and Al-Zurigi 2013): long installation and setting time, requires sophisticated setting tools (need longer design lead time), and high manufacturing cost.

In 2015, a new generation of expandable liner hanger has been introduced (shown Figure 3.2) to overcome the challenges associated with drilling operations in extreme environments such as deepwater and ultra-deepwater. In these wells, the heavier host casing poses additional challenges to conventional expandable liner hangers. In this technology, the elastomer seal will not carry all the hang weight as in the conventional expandable liner hanger system. In fact, in this technology metal-to-metal seal with the hanger body carrying the hang weight and the elastomer forming the secondary seal. The liner hanger provides a gas-tight seal at temperatures beyond 350 °F and it can be an excellent candidate for geothermal wells (Halliburton 2015).

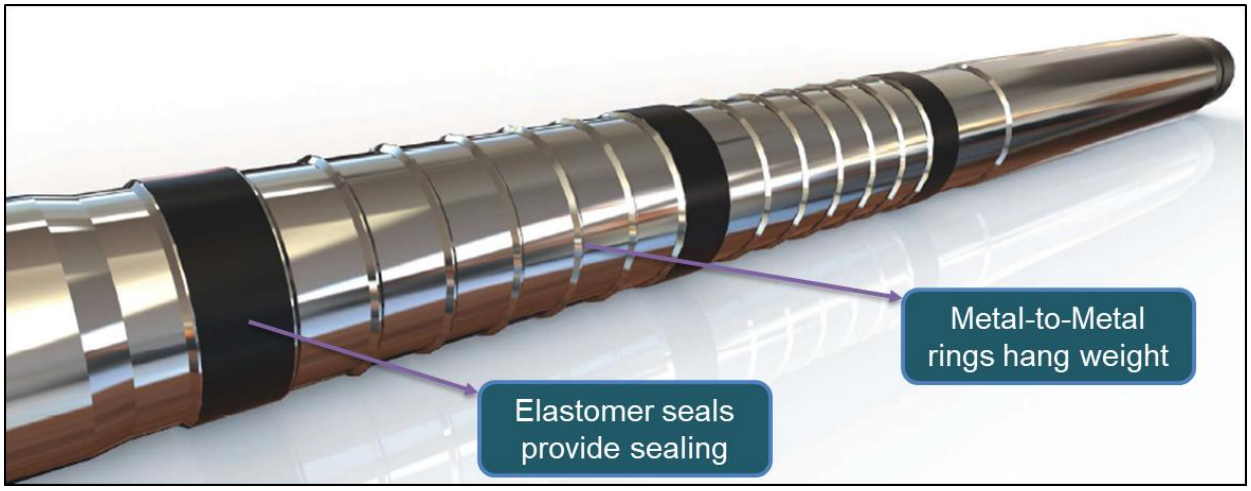

Figure 3.2: Metal-to-metal VersaFlex Xtreme Grip liner hanger (Halliburton 2015)

3.1.2 Types of Elastomeric Materials Used in Liner Hangers

An elastomer is defined as a material that can demonstrate a rapid and significant reversible strain in response to stress (Visakh et al. 2013). Elastomers are commonly used rubber materials in the oilfield applications. They are used to provide the sealing and/or hanging mechanisms in most of the wellbore barrier elements such as blowout preventers, diverters, liner hanger seal assemblies, sub-mudline liner hangers, casing hanger seal assemblies, packers, valves, and tubular connections as shown in Figure 3.3. In this section, details of the elastomeric materials of the liner hangers seal assemblies are presented to describe their types, properties, applications, limitations, and operating conditions. Technically, the performance of the seal assembly of the liner hanger depends on the elastomers' chemical compounding, physico-mechanical properties, design specifications, and compatibility with the downhole environment. Elastomers are arguably the most versatile materials used in oilfield applications due to their oil resistance, their tolerance to high-temperature and high-pressure (HTHP) environments, and the way they deform and recover under loads (Dolog et al. 2017). Types of elastomers used in drilling and completion equipment include, but are not limited to; neoprene (EPDM), nitrile elastomers (NBR), hydrogenated nitrile (HNBR), and

fluoroelastomers (FKM/Viton), tetrafluoroethylene (FEPM/Alfas), and perfluoroelastomer (FFKM/Kalrez) (Dolog et al. 2017; Ahmed et al. 2019b; Salehi et al. 2091; Patel et al. 2019b).

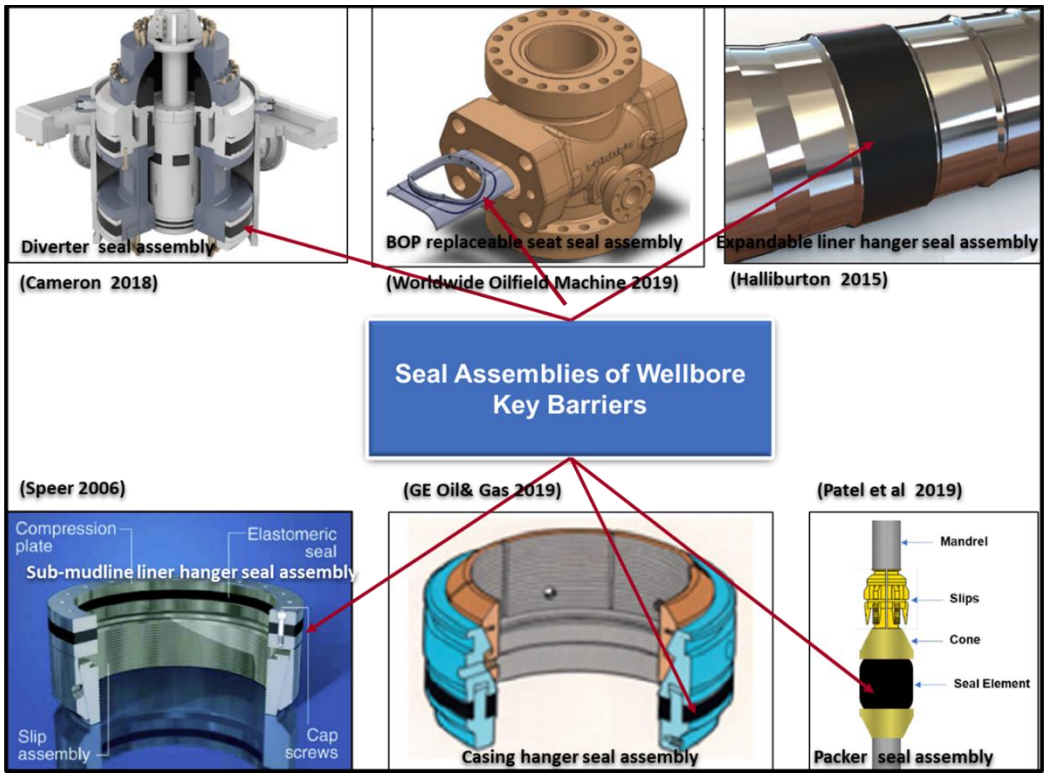

Figure 3.3: Elastomeric materials of wellbore main barrier systems

EPDM is used by some suppliers to replace the lead material used in lead seal liner hanger of the gravel packing units, where a slotted liner is deployed to complete the production zone. In 1979 a modified version of EPDM called "EPDM Y267" was developed. The elastomer proved an excellent performance in very hostile down holes with a temperature of 500°F. The elastomer also performed successfully when it utilized in some of the oil and gas components mainly, packer's seals (Hirasuna et.al 1983). Despite the aforementioned applications of EPDM, some suppliers have concerns about the use of EPDM in field applications. They are not recommended to use this elastomer in hydrocarbons, leaded gasoline, kerosene, fuel oils, and diesel oils because they believe EPDM is susceptible to hydrocarbons. Flitney (2014) also supports this consensus and

claims that EPDM lacks resistance to hydrocarbon liquids because it rapidly swells and structurally deforms when reacting with mineral oils. NBR is suitable for low duties and low-temperature environments. The elastomer operating temperature varies from -58°F to 230°F. NBR can serve in a wide range of media such as mineral oils, water, and hydraulic fluids. NBR is not suitable for working in an environment containing ketones, amines, and hydrogen sulfide (Walker 2009). In the oil and gas industry, NBR is frequently used to manufacture gas barrier elements, packers, sleeves, and gaskets (Najipoor et al. 2018). Fluoroelastomer (FKM/Viton) is a key sealing element in liner hanger seal assemblies, packers, mud motors, pumps, valves, and blowout preventers. It is a viable solution for critical problems in many sealing systems, especially where elastomers such as NBR or EPDM fail to function properly (DuPont 2013; 2017). (FKM/Viton) demonstrates good performance in severe downhole conditions e.g. H_2S, and temperature range of 392 °F to 599°F. However, it exhibits poor performance in hot water, steam, ketones, and amines (James 2009; DuPont 2013 and 2017). Tetrafluoroethylene (FEPM/Aflas) has introduced to deal with corrosive environments. It withstands sour oil and gas, amines, acids, and steam. However, it is sensitive to halohydrocarbons. The elastomer can work from medium to high downhole temperatures in the range of 41°F to 401°F (James 2009). Perfluoroelastomer (FFKM/Kalrez) elastomer is commonly used for HTHP applications (Walker 2009; DuPont 2013; 2017). FFKM can tolerate temperature up to 617°F (PPE 2019). The elastomer has outstanding resistance to sour oil and gas, ketones, and methyl tertiary-butyl ether (MTBE). However, it is very susceptible to alkali metal solutions. A comparison between elastomers' properties and application is presented in Table A2, Appendix B.

In conclusion, the selection of elastomeric materials for wellbore pressure-containing and controlling should consider many interrelated factors. However, according to the American Bureau of Shipping (ABS, 2018), more attention should be given to the following factors:

- Materials must be fit for services, withstand the operating temperature and pressure, and compatible with operating mediums.
- Handling and storage procedures should be well-identified, particularly for age-sensitive materials for critical components.

In addition to that the manufacturer's specifications shall minimum include (ABS, 2018):

- A generic base polymer as specified by ASTM D1418
- Mechanical properties requirements
- Storage and age control procedure and requirements
- Testing and nondestructive examination (NDE) requirements; acceptance and/or rejection criteria according to related recognized standard(s)

3.1.3 Unconventional Elastomeric Materials to Enhance the Barrier Performance

Currently, new unconventional elastomeric materials consisting of nanoparticles or nanocomposites have been proposed by many researchers to modify properties of commonly used conventional elastomeric materials in the oil and gas industry. Dolog et al. (2017) demonstrate that reinforcing fillers such as carbon black and silica have been used for many decades in the industry of conventional rubbers. However, the use of nano-sized fillers such as carbon nanotubes, nanosilica, nanoclays, and graphene has significantly improved the rubber properties. The authors claim that carbon nanotubes improved the performance of HNBR elastomers, particularly mechanical properties, wear resistance and RGD resistance. Welch et al. (2012) conducted laboratory studies on Nano-enhanced EPDM, Nano-enhanced-HNBR, and Nano-enhanced-FEPM to investigate their performance at HPHT corrosive gases in downhole environments. The authors claimed that nanotechnology would be beneficial for swellable packers because the results showed that the oil swelling rate could be significantly reduced to give operators greater flexibility in

setting the packers and minimize the intervention time. Denison et al. (2018) introduced a new nitrile elastomer (urethane) which has a high wear resistance. Urethane is used in the manufacturing of the packers used for sealing the slip joints of floating drilling rigs.

3.1.4 Sealing Mechanisms of Liner Hangers

The main function of the elastomeric materials incorporated in the wellbore liner hanger systems is to maintain an intact bonding between the liner and host casing or formation. There are two common techniques used to energize the elastomeric materials, mechanical and chemical. In mechanical technique, the sealing (bonding) mechanism can be achieved by elastically deforming an elastomeric material confined between two concentric casings, specifically the liner and the previous casing. Technically, maintaining a long-term stable bonding requires that the seal remains under sufficient compression loads. Akhtar et al. (2018) claimed that intact sealing (bonding) implies that the contact stress (pressure) at the seal-casing interface is greater than the differential fluid pressure across the seal ends. This can be inferred with a zero-leak rate or zero-pressure decline.

The procedure of elastomer activation/energization very much depends on the type of the liner hanger seal assembly. Mohamed and Al-Zuraigi (2013) demonstrated that there are two common seal assemblies used in well drilling and completion, mechanical/conventional and expandable versions. In the mechanical version, the sealing mechanism usually accomplished by engaging two mechanical components called cone and slip. The slip-cone engagement pushes the compression plate which automatically expands the elastomeric material to plug the annular space between the liner and the host casing. The drilling string normally utilized for applying an axial load to hook the cone and the slip. Alzebdeh et al. (2010) stated that in the expandable liner hanger version, a setting tool (solid mandrel with larger outer diameter than the internal diameter of

hanger) driven by differential pressure is run to expand the liner. As the liner expands, the elastomeric bands strain (compress) to fill the liner-casing annular space and eventually generates pressure zonal isolation (API RP 96, 2013).

The second technique for energizing seals is chemical swelling. The swelling occurs when the elastomeric material comes into contact with swelling agents such as oil, brine, and surfactant. The swelling increases the elastomer volume causing the annular gap between liner-casing/formation to be closed and contact pressure generated (Akhtar et al. 2018). The swelling technique is commonly used in the activation of packers. Swelling elastomer packers become common field applications. They have been used to; completing multilateral wells, closing water or gas-bearing formations, isolating production zones, sectioning multi-fracturing zones, and straddling corroded casing or tubing (Evers et al. 2013).

3.1.5 Failure Mechanisms of Liner Hangers Seal Assembly

In deep and complex offshore drilling, deploying liner strings have become more demanding. Running a liner string can result in major challenges in the installation tools and cementing technologies. These tools often operate in some of the most critical wellbore temperatures, pressures, borehole solids, and deviations (Nida 2005). Despite the significant advantages of liners, the failure of liner-top is still a challenging issue. In the conventional system that utilizes the cone and slip technique, the failure rate of the top packers exceeds 40% (Nida, 2005; Walvekar and Jackson 2006). In mechanical liner hanger, a leak is the dominant failure mechanism, particularly in the cones and slips connections (Figure 3.4 (a)) (Walvekar and Jackson 2006; Jackson and Smith 2006; Williford and Smith 2007). Liners are also vulnerable to fail under high burst and collapse pressures as shown in Figure 3.4 (b) (API 65-2 2010; Payne et al. 2016). Corrosion is also a common failure mechanism in geothermal wells liner hangers (Figure 3.4 (c)) (Thorbjornsson

2016; Kruszewski and Wittig 2018). The outcomes of an informal survey conducted in 1999 over several GoM operators revealed that 30% to 50% of pressure seals in overlaps failed (Moore et al. 2002). Nida (2005); Walvekar and Jackson (2006) state that liner top and liner installations fail because of a variety of reasons that can be attributed to liner top cement integrity failure, inability to run the liner to the predefined depth, and tool failures such as darts, plugs, and running/setting tools.

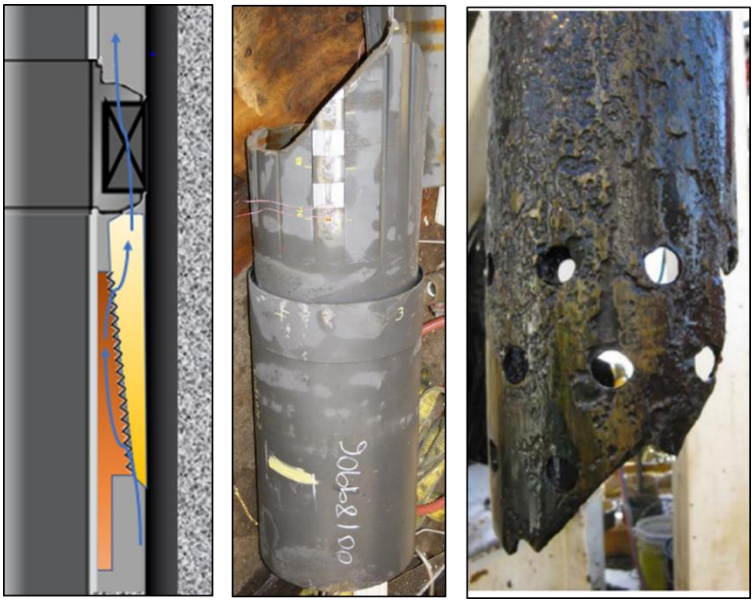

(a) **(b)** **(c)**

Figure 3.4: Failure mechanisms in liner hanger (a) leak in top liner, (b) burst (Payne et al. 2016), and (c) corrosion (Thorbjornsson 2016)

3.1.6 Failure Mechanisms of Elastomeric Materials

Elastomer is a very important element for several of the barriers of the wellbores such as liner hanger seal assembly, packers, casing hanger seal assembly, valves, and tubular connections. Elastomers usually energize to expand and provide specific contact pressure technically called sealability. The system sealability can be lost in case the elastomer integrity is compromised by one or more of the failure mechanisms that will be discussed in this section. According to Walker (2017), elastomer failure can be diagnosed by excessive fluid leakage caused by loss of contact

pressure (stress) at the mating surfaces interfaces or loss of seal integrity due to physical damage. Some failure causes are superficially obvious (e.g. gross swelling, compression set, and thermal degradation) (Brown, 2002).

Key factors that have a significant impact on the failure of the elastomeric materials include but are not limited to; material specifications, manufacturing processes, seal design, seal configuration, transportation, handling, storage, inspection and testing procedure, installation procedure, operating conditions, and human error (Flitney 2014; Walker 2017). The mechanisms of elastomers failure can be classified into the following categories (shown in Figure 3.5) (Brown 2002; Mackenzie and Garfield 2007; Walker 2017; PPE 2019; Ahmed et al. 2020b):

1) Chemical
    - Degradation/attack
    - Swelling
    - Gasification or rapid gas decompression (RGD)
2) Physical
    - Manufacturing fault
    - Mechanical damage (incorrect installation, wear, shear)
    - Compression loads
    - Abrasion effects while handling and storage
3) Thermal degradation
4) Fatigue under pressure and temperature cycles

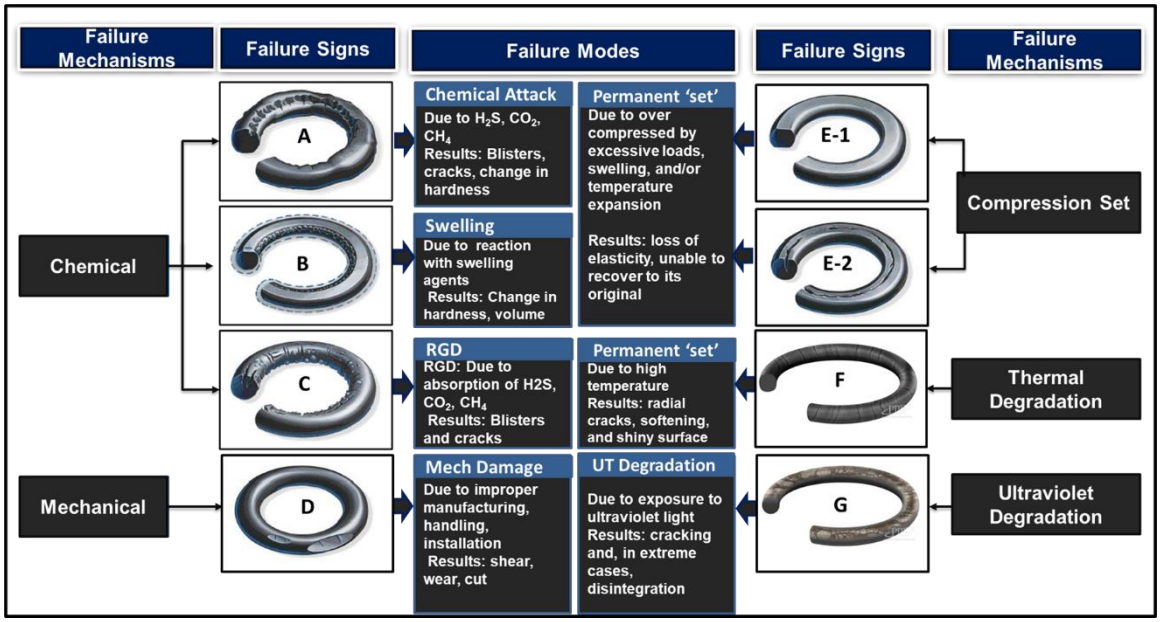

Figure 3.5: Elastomer common failure mechanisms (images source: Marco Rubber Inc. 2019; PPE 2019)

3.1.6.1 Chemical Failure Mechanisms

Chemical failure usually occurs through the interaction of elastomer with its environments which may include corrosive substances such as water, brine (particularly heavy brine), acids, bases, sour gases (H_2S, CO_2, CH_4), mercaptans, oxygen, ozone, defoamers, emulsifiers, amines, inhibitors, peroxides, and surfactants (Brown 2002; Walker 2017). Three mechanisms cause the elastomer chemical failure such as degradation, swelling and rapid gas decompression (RGD). In degradation, also known as chemical attack, corrosive fluids such as H_2S, CO_2, and CH_4 react with elastomer and break its cross-link. In this case, some of the damage signs such as cracks, blisters, and voids, can be observed as shown in Figure 3.5 (A) (Marco 2019).

The second chemical failure mechanism is volumetric swelling. Some fluids can be absorbed by elastomers and result in their swelling as shown in Figure 3.5 (B) (Brown 2002). Volumetric swelling is a combination of chemical and physical interactions. In this process, change in elastomer key properties such as dimensions, hardness, tensile strength, and tear strength always

occurs (Walker 2017). NORSOK standard M-710 (2014) specifies +25/-5% as a swelling acceptance range. In static applications, volume swelling up to 20 % is acceptable and can be beneficial because it is enhancing the seal interference in the extrusion gap. However, higher swelling may damage the elastomer because it leads to gap fit issues, extrusion, fracture, and loss of tensile strength (Walker 2017; PPE 2019).

The third chemical failure mechanism is called rapid gas decompression (RGD) or explosive decompression (ED) as shown in Figure 3.5 (C). RGD is also known as a structural failure. In this process, the elastomer is exposed to high-pressure gas at elevated temperatures for a certain period. The gas is absorbed into the elastomer's molecular structure forming voids or air pockets. When the external pressure suddenly drops at a rate higher than the limit specified in NORSOK M-710 (2014), the trapped gas released out of the elastomer and forms certain signs of failures on the elastomer surface. Common signs are blisters, cracks, pits, deep splits, ruptures. Elastomer is prone to RDG failure, especially when operating at a pressure above 725 psi in dissolved gas or gas systems with decompression rates above145 psi/h (Walker 2017). Mackenzie and Garfield (2007) claim that elastomers are more prone to fail by RGD according to their relatively low elastic strength. Therefore, elastomers intended to serve in wellbores with high pressure/temperature cycling should have a higher elastic modulus/hardness. RDG failure can also be avoided by increasing the system decompression rate (gradual depressurization) and minimizing the temperature if applicable (Marco 2019; PPE 2019).

3.1.6.2 Physical Failure Mechanisms

The second failure mechanism is physical, which may occur during manufacturing, transportation, storage, installation, and retrieval. Brown (2002) states that material damages may happen in the early stage of the elastomer manufacturing process due to inappropriate material selection,

incorrect material compositions, defects during material processing (forming), insufficient testing, and qualification procedure. The author claims that perfectly manufactured elastomer can be damaged if installation procedures are not followed. There are many factors to be considered in order to maintain the elastomer integrity during installation such as adequate energization load, even distribution of the load, correct elastomer size, contamination, and sharp edges (Marco 2019; PPE 2019; Ahmed et al. 2020a; Ahmed et al. 2020b). Damage can be in the forms of wear and tear, cuts, notches, scratches, nicks as shown in Figure 3.5 (D).

Elastomer permanent set means it is unable to recover to its original configuration after removal of deforming loads/stresses because it lost elasticity (PPE 2019). Elastomer may suffer from compression fracture when it is over-compressed by excessive loads, swelling, and/or temperature expansion (Marco 2019). The failure can be inferred by the fracture (s) that occur in the plane parallel to the applied load as shown in Figure 3.5 (E-2) (Walker 2017).

3.1.6.3 Thermal Failure Mechanisms

Elastomers thermal degradation is one of the most detrimental factors that limit their use in high-temperature reservoirs. Conventional elastomers usually break at temperatures ranging from 150°F to 200°F (Garfield and Mackenzie 2007). Blizzard (1990) highlights that the integrity of many elastomers can be compromised at a temperature greater than 400°F. Thermal failure can be diagnosed by radial cracks, softening, and shiny surface (shown in Figure 3.5 (f)), and usually accompanied by compression set (Marco 2019; PPE 2019). Special types of elastomers have recently been developed to withstand high-temperature downhole conditions. For example, Y267 EPDM and FFKM work at temperatures up to 500°F and 617°F respectively (Hirasuna et al. 1983; PPE 2019).

3.1.6.4 Pressure Cyclic Loads Failure Mechanisms

Well barriers have a higher potential to fail under pressure cycling conditions. Repeated pressure cycles induce continuous stresses in the barrier elastomeric materials. Elastomers can lose their strength, sealability, and eventually can be physically damaged. Blizzard (1990) demonstrates that the design and materials of many elastomers do not consider excessive pressure fluctuations. Pressure cycling is a common phenomenon during production, stimulation, and injection operations (Dusseault et al. 2014). Wells, where the sealant may be exposed to high pressure and/or temperature cycling, include geothermal, HPHT, deep water, injection, and gas storage (Bosma et al. 1999).

3.2 Cement in Liner Hanger Dual Barrier System

3.2.1 Liner Cementing

In liner-casing overlap, cement is used as a zonal isolation sheath. The cement sheath acts as a barrier element in a system called a dual barrier system because it also comprises another barrier element known as seal assembly. In this dual barrier system, the cement builds a continuous, permanent, and impermeable hydraulic seal binding that is supposed to plug the influx of uncontrolled fluids into the wellbore. The cement also carries the mechanical loads of the wellbore structural components such as tubular, valves, tools, and equipment. Moreover, the cement creates a binder layer that protects the casing strings against the formation corrosive fluids (ISO 16530-1, 2017; Teodoriu et al. 2018). From a technical viewpoint, cementing casing-liner overlap is one of the most challenging tasks at the downhole because of the small annular clearance between liner and host casing or open hole. The liner cementing becomes more challenging when deploying a long liner string. Verbakel and Salazar (2016); Muncrief et al. (1984) claimed that cementing a

liner string with a length exceeding 1000 m (3280.84 ft) requires specific procedures, equipment, and techniques to assure a high-quality cement job.

Technically, there are two techniques for liner cementing. The first technique is known as modified circulation, which looks like squeeze cement. In this technique, the liner and its respective equipment are run using the drill pipe. Then, the base of the liner is squeezed, usually to a position slightly above the shoe of the previous casing. This distance/length is called the overlap. API Bulletin E3 (2018), suggests a length of cement column in the range of 50 to 500 ft to fill the liner-casing overlap. However, it has become a common industry practice to keep at least 300 ft of overlap cement from the casing seat to the top of the liner (Agnew and Klein, 1984). Using a modified circulation technique for cementing deep liners is a complicated operation because the liner is usually isolated from the rest of the completion string by close clearance and packer. In this process, the pressure is often trapped behind the liner. The liner may experience a collapse failure if the pressure is not carefully controlled (API 65-2 2010; Payne et al. 2016). The second technique used for liner cementing is called puddle (Simpson, 2017). This technique is commonly used for cementing short liner strings. In this technique, the drill pipe utilized to spot the cement slurry along the section in which the liner is planned to deploy (Simpson, 2017).

3.2.2 Key Properties Influencing the Performance of Anti-Gas Cement Slurry

Key cement properties that have a substantial influence on the performance of the anti-gas cement slurry are; gas transition time (static gel strength development), density to preserve hydrostatic pressure control, rheological (flow) properties to ensure good displacement, thickening time, fluid loss, slurry stability (sedimentation and free fluid), shrinkage/expansion, and strength development (compressive and sonic strength) (API RP 65-1 2018). A brief discussion is made here of how these properties affect the cement performance.

3.2.2.1 Gas Transition Time

To maintain the well integrity in the short term during the well construction stage, slurry cement is usually designed and placed at the liner-casing overlap to prevent uncontrolled fluids flow (Williford and Smith, 2007). However, the cement hydraulic integrity can be lost according to the gas migration. The migration of gases during the transition of cement slurry from a liquid to a solid is an industry-wide issue that still needs further research. The transition period of cement is called the "Gas Transition Time." Gas transition time is an important cement property that needs to be controlled, especially while cementing the wellbore shallow gas zone(s). The gas transition time can be defined in terms of the evolution of the static gel strength (SGS). This concept was proposed by Sabins et al. (1982). The authors were the first to claim that the transition time of a cement slurry ends once the slurry develops SGS beyond 522 lbf/100ft^2. Rogers et al. (2004) defined the transition time as the time needed for a cement slurry to build an SGS from 100 to 500 lbf/100 ft^2. The authors asserted that it has become a common filed practice that when a cement slurry reaches an SGS of 500 lbf/100 ft^2, it is an indication that the cement develops sufficient solid mass capable of preventing formation gas percolation. According to API STD 65-2 (2010), when potential gas flow is deemed to be severe, the cement slurry should be designed to attain a critical SGS in a period less or equal to 45 minutes as shown in Figure 3.6 (A). The standard recommends this period to eliminate the risk associated with gas migration. Technically, cement column hydrostatic pressure is a function of SGS development and hydration of kinetics of the cement (Al-Buraik et al. 1998; API STD 65-2 2010). API STD 65-2 (2010) demonstrated that during SGS development, cement hydrostatic pressure decay occurs (see Figure 3.6 (A→C)), and the gelled fluid progressively loses its ability to transmit hydrostatic pressure to the formation as the case in Figure 3.6 (C). Therefore, an underbalanced condition similar to a situation happens sometimes during

the drilling process may be occurred. In this context, the principal difference between well control during drilling and cementing operations is the free fall or U-tubing phenomenon. This phenomenon is most likely to happen during the cement placement due to the instant decay of the cement slurry hydrostatic pressure (Beirute, 1984). Whereas hydrostatic pressure decay most likely occurred during drilling according to insufficient density or cutting settlement resulting from poor wellbore conditioning.

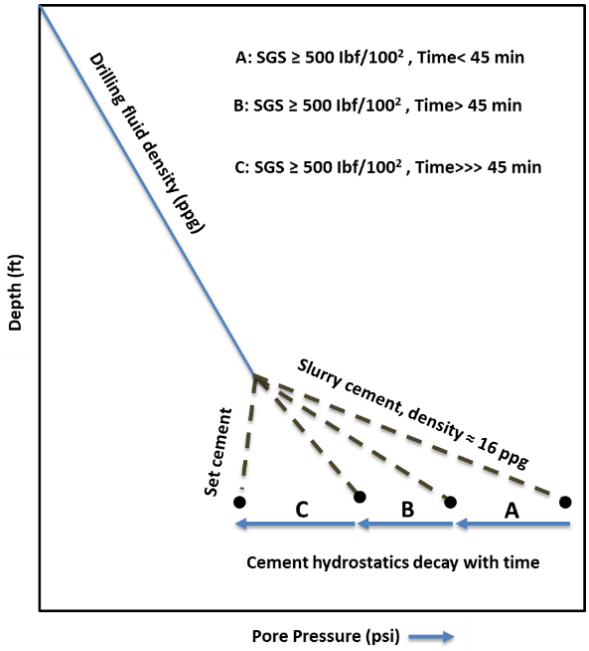

Figure 3.6: Cement hydrostatic pressure decay during its transition from liquid to solid phase

3.2.2.2 Others Key Properties

Besides SGS, other key properties critical to the performance of the anti-gas cement slurry include density, fluid loss, rheological and thixotropic behaviors, thickening time, and slurry stability. Density plays a critical role in the design of cement formulations. As a general notion, the effective pressure of cement density exerted at any depth of the well should be greater than the formation pore pressure and less than the fracture pressure. Therefore, density is important to maintain overbalanced conditions necessary to prevent kick and lost circulation and to prevent losses to the

formation (API STD 65-2 2010). The overbalanced conditions can be disrupted due to loss of fluids from the cement slurry caused by a mechanism called “Fluid loss”. In this phenomenon, a filtration process occurs and the aqueous phase of the slurry seeps into the formation. Fluid loss rate can also significantly be impacted by formation permeability, the magnitude of overbalance pressure, and removal of drilling fluid cake. API 10B-2 (2013) recommends a fluid loss rate of less than 50mL/30 min to maintain acceptable slurry performance. It is advised to incorporate fluid loss materials (viscosifiers) in cement slurries that are expected to traverse gas-charged zones and pay zones as well as when the annular gas is tight. The rate of fluid loss can be lowered by adding materials called “fluid-loss control agents.” Such agents include but are not limited to; bentonite, liquid latex (e.g. styrene butadiene, vinylidene chloride, polyvinyl acetate), copolymers, synthetic and natural polymer (e.g. cellulose, polyvinyl alcohol, polyalkanolamines, hydroxyethylcellulose (HEC)), and blends (Nelson 1990; API RP 65-1 2018).

API RP 65-1 (2018) stated that as the loss of water from cement slurry increases (by physical separation as cement harden), the solids settlement and concentration also increase. This process may lead to uncontrolled gelation (thixotropy) and other changes to the cement properties (e.g. inability to apply hydrostatic pressure, low strength, and high permeability). In deviated wells, free water can coalesce and may create voids and continuous channels that promoting the migrated gas percolation (Al-Buraik et al. 1998). Therefore, it is extremely recommended to consider additives to control free water to a zero level or traces particularly in highly deviated wells or horizontal wellbores, as well as formations with high-pressure gas-bearing. Fluid loss additives that recommended to enhance the performance of the cement slurry include but are not limited to; bentonite, hydrosolube polymers, silicates, and metallic salts (Nelson et al. 1990).

Rheology (flow) is an important property that can significantly impact the slurry placement and the friction pressure generated during the cement placement if it is not well-controlled. The cement rheology is very sensitive to the bottom hole temperature and a lesser pressure. Cement slurry with flat rheology at expected downhole temperatures is extremely important to maintain hydraulic wellbore integrity. The increase in the viscosity of the slurry according to the lowering temperature can adversely affect the thickening time which makes the slurry un-pumpable and can lead to severe damage to the wellbore (Ahmed et al. 2018). Cement pumpability is commonly characterized in terms of consistency and thickening time. API STD 65-2 (2010) defines the thickening time as the time frame at which the slurry will remain pumpable under conditions similar to the downhole during cement placement. According to API RP 10B-2 (2013), the fluid will not be pumpable at a consistency of 100 Bc (Bearden consistency). The time cement slurry takes to attain 100 Bc is the called "thickening time". The length of the thickening time mainly depends on the slurry viscosity and flowability. Al-Buraik et al. (1998); Pour and Moghadasi (2007); Ahmed et al. (2018) underlined that adjusting the thickening time during slurry placement is very crucial for preventing any potential release of uncontrolled gas and for complying with designed pumping schedules (rates) specified by API. In this context, current API schedules are inappropriate for deepwater wells cementing applications. For these applications, API RP 65-1 (2018), recommends operators establish special schedules using simulators. Developed schedules should be followed during the cement placement. In addition, a recent study has shown that water impurities can impact cement properties such as thickening time and compressive strength (Saleh et al. 2018).

The compressive strength developed by a specific cement system is of secondary importance compared to the properties of the liquid slurry. This notion is due to the fact that most of the cement

systems have the ability to attain compressive strength exceeds the minimum limits established by the relevant standards and regulators (Nelson 1990). Among the various properties of the hardened cement, compressive and tensile strength are by far the most important properties that need further consideration. Compressive strength should be adequate to support the wellbore load-bearing capacity and to create an impermeable sealed annular barrier. To achieve these functions, cement requires to develop a compressive or sonic strength of a minimum of 50 psi (API RP 65-1 2018). Compressive strength also significantly affects the WOC time that should be respected before drilling out and perforate the production casing. It is common industry practice to wait for the cement to attain compressive strength of 500 psi and 2000 psi prior to drilling out and perforating respectively (Nelson 1990). From technical and safety viewpoints, CFR (2016) recommends eight hours of waiting time to resume drilling after cementing the conductor casing. Whereas, the code recommends 12 hours for surface, intermediate, or production casing (or liners). In addition to using accelerators to increase the rate of cement compressive strength developments, strengthening agents are also necessary to increase the cement tensile strength. Carter et al. (1968) stated that incorporating fibrous materials (e.g. Nylon fibers) to well cement in concentrations between 0. 15% and 0.5% BWOC, enhance the cement's resistance to stresses resulting from drill collars, and perforation. The cement resistance can also be enhanced by the addition of particualted rubber and latex (Hook 1971).

3.2.3 Gas Migration Additives

Gas migration can be prevented by controlling the decay of the hydrostatic pressure of the cement slurry that occurs during the critical liquid-to-solid transition time (Nelson 1990; Dusseault et al. 2014). The hydrostatic pressure decay technically may be controlled using gas migration control additives (GMCA) that are usually added to reduce the permeability of the cement matrix. The

additives provide no protection from the migrated gas influx as soon as the cement develops sufficient SGS and set (Hopkins 2016). Dusseault et al. (2014) stated that the well operator is exclusively responsible for the decision to add GMCA, hence, most current regulations do not recommend the addition of the GMCA.

In response to the gas migration issues encountered in many oil and gas fields in1960s, the evolution of the GMCA progressed rapidly (Talabani and Hareland 1995). Many researchers have suggested conventional (normal size) and unconventional (nanoscale) GMCA to overcome gas migration issues. With regard to conventional additives, silica fume (high fineness amorphous silica) was introduced in the1980s, in the North Sea offshore wells as materials to control the shallow gas flow normally confronted in these wells (Coker et al. 1992). Drecq and Parcevaux (1988) claimed that latex was used in cement field application in 1982 to generate a homogeneous impermeable membrane above the cement matrix to inhibit the gas propagation in the porous cement matrix. Further study to investigate the influence of latex upon cement was conducted by Tavares et al. (2013). The authors used a gas migration simulator to simulate the downhole environment. The results indicated that slurries contain a high percentage of latex proved to block the migrated gas compared to the slurries without latex additives. Grinrod et al. (1988) demonstrated that Statoil developed microsilica as GMCD to avert the gas migration while drilling the uppermost shallow formations in the Gullfaks field located on the Norwegian North Sea shelf. Gas migration in South Texas fields has been reported as one of the most incidents contributors. To overcome this problem, Bour and East (1988) designed a cement slurry comprising of fly ash as GMCD. The authors claimed that according to laboratory results, fly ash accelerated the SGS development, and thereby the gas transition time was significantly reduced. Calloni et al. (1995) tested three cement recipes include silica fume, polymer latex, and carbon black to optimize best

for service formulation. The authors concluded that carbon black exhibits superior performance upon silica fume and latex in terms of efficient sealability and cost. In this context, carbon black is commonly used for cementing gas zones drilled in the Adriatic Sea. Dao et al. (2004) awarded United States Patent (US 6,936,574 B2) for the invention of copolymer as GMCA. Coploymer is a gel-like liquid that dispersed to inhibit the migrated gas that originated from gas-bearing zones. In attempts to solve the gas migration issues encountered in some HTHP deep wells in Saudi Arabia, Al-Yami et al. (2009) evaluated thirty cement recipes to select a suitable GMCA. The authors disclosed that the formulation containing silica sand, silica flour, hematite, manganese tetraoxide, and expansive additives is the best candidate. Abbas et al. (2013) claimed that the gas migration could be reduced when mixing the cement with Hydroxypropylmethylcellulose (HPMC) polymer as a multifunctional cement additive to improve oil well zonal isolations. Pilots tests conducted by the authors using a cement hydration analyzer. HPMC polymer established an impermeable barrier that successfully rendered the migrated gas percolation through the cement.

Nanomaterials have recently been studied by researchers to modify main properties of cement, such as compressive strength, static gel strength and gas transition time that play key roles in controlling the gas migration. Graphite nanoplatelet (GNP) was used by Peyvandi et al. (2017) to examine its effect on cement performance. The results of the authors' experimental work showed that GNP is beneficial for the wellbore zonal isolation because it minimized the inception of microcracks and microannulus into the cement bulk. These types of defects are always representing channels for the migrated gases. Nanosynthetic graphite (NSG) was evaluated by Ahmed et al. (2018) ; Kimanzi et al. (2019) to study its effect on cement gas transition time (SGS development). The outcomes of the laboratory pilot tests revealed that the addition of only 0.5%

by weight of cement (BWOC) of NSG, the modified slurry reached a critical SGS of 345 Ibf/100 ft^2 after 45 minutes. Meanwhile, neat Class H cement reached a critical SGS of 132 lbf/100 ft^2.

Although the conventional and unconventional GMCA described have been used and proposed to control and mitigate gas migration problems, the industry is still considering further research in this area. This contention is supported by the fact that each well has a unique situation. Therefore, designing a GMCA that can be compatible with every single well maybe a non-viable concept.

3.2.4 Failure Mechanisms of Set Cement

The hydraulic and mechanical integrity of set cement can be jeopardized in case it exposed to the excessive inducement of the mechanical principal stresses, namely radial, hoop/tangential/circumferential, and shear/axial. Profound review from previous studies conducted by several researchers disclosed that excessive radial stress that localized on the annular cement is most likely resulting in crushing as well as in severe debonding at outer casing- cement-inner casing/rock interferences as shown in Figure 3.7. Whereas the over inducement of hoop stress is most likely creating radial cracks as shown in Figure 3.7. Ahmed et al. (2020a); Zeng et al. (2019) demonstrated that high-temperature wells and hydraulic fracturing wells are the most common down holes suffering from cement failure according to the growth of radial cracks (microcracks).

On the other hand, the excessive concentration of the shear/axial stress that normally acts over the cement axis results in shear stress (deformation) that occurs in bulk cement and/or in the cement- casing /formation interfaces as shown in Figure 3.7. Shear stress is commonly initiated due to cement contraction/ shrinkage and the movement of the wellbore structural loads. Overall, the majority of studies available in the literature reveal that cement is most prone to fail in tension

(Mueller and Eid 2006; Nath et al. 2018). Based on the conclusions drawn from previous studies, the criteria for cement failure are organized as shown in Figure 3.8 to show how stresses relate to the mechanical properties of cement and to show the prospective cement failure scenarios. Figure 3.8 shows that the tensile strength is the most mechanical property that needs strengthening. This notion arises from the fact that cement is intuitively brittle and has a tensile strength less than of compressive strength by around an order of magnitude.

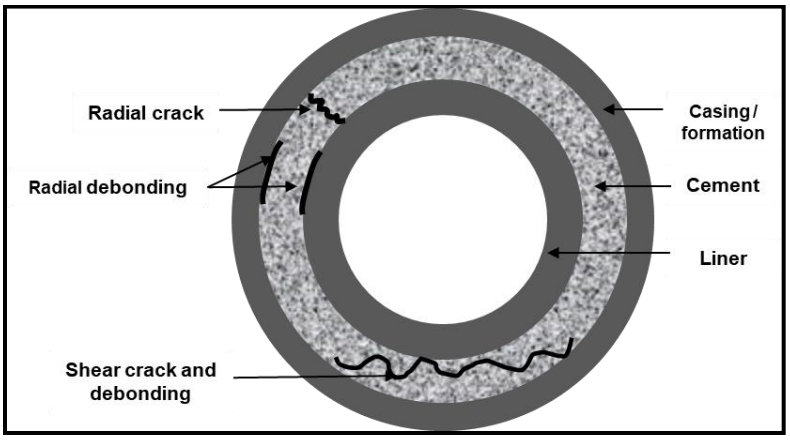

Figure 3.7: Common failure modes in set cement

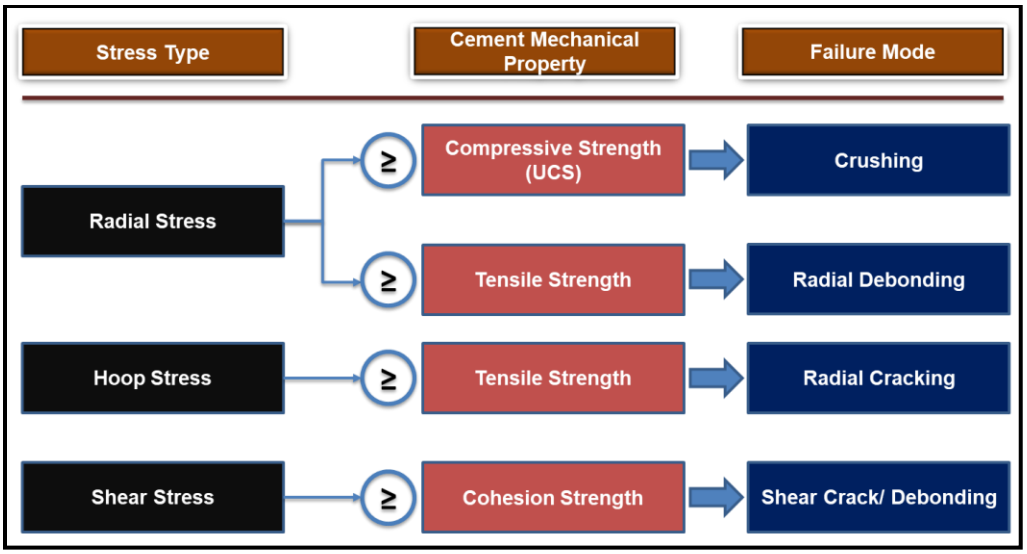

Figure 3.8: Stresses influencing set cement failure modes

3.2.5 Cement Pressure Integrity Test (PIT)

According to ISO 16530-1 (2017), the integrity of the well barrier (s) can be verified by applying a differential pressure that may be either positive or negative. In this context, the standard defines the pressure test as a process of applying pressure from a known source to verify the mechanical and hydraulic sealing capacity of the component. The testing medium could be the fluids that exist in the wellbore at the time of the barrier installation and testing (e.g. drilling mud, completion brine or water) (API RP 96 2013).

3.2.5.1 Pressure Test

NORSOK D-010 (2013), recommends conducting a pressure test for well barriers under, but not limited to the following conditions:

1. Before exposure to pressure difference that can be encountered in its operating phase
2. In case there is a suspicion or observation of a leak
3. In case the barrier element has been accidentally subjected to differential pressure higher than original design limits of the well
4. Periodically, (depends on barrier type and regulations requirements)

In the positive pressure test procedure, the pressure is applied against the direction of the reservoir fluid flow (Figure 3.9 (a)), assuming that the well barrier is constructed to act in bidirectional ways to prevent the reservoir uncontrolled fluids influx (API 96 2013; NORSOK D-010 2013; ISO 16530-1 2017). During the pressure test, fluids (e.g. sulfate-reducing bacteria) that may be injected into the wellbore should not impact the barrier elements (ISO 16530-1 2017). In addition, the effect of the temperature variations with the depth and climate should be considered, especially in the arctic and offshore reservoirs (API RP 96 2013). The pressure test is commonly performed in two stages, low and high (NORSOK D-010 2103). The low-pressure test stage conventionally carried

out first. In this stage, low-pressure values in the range of 217.56 to 435.11 psi are normally applied and kept on hold for at least 5 minutes. After a successful low-pressure test, the second stage includes a high-pressure test proceeds. In this stage, the applied pressure values must be equal to or exceed the maximum differential pressure the barrier can encounter during its life cycle. CFR (2016) recommends 10 minutes as a minimum holding period. The code comprises guidelines for the pressure test of the wellbore main barriers such as casing strings, cement, BOP, diverter, sub-mudline hangers, wellhead hangers, and seal assembly. A summary of pressure test requirements for some of these barriers is given in Table A. 1, Appendix A.

3.2.5.2 Negative Pressure Test

The negative pressure test (also known as flow/inflow test) has recently been introduced in the oilfields to test some of the barrier systems to improve the quality level and to enable the testing of some of the barriers that cannot be tested using the positive pressure test method. From a qualification point of view, the highest level of mechanical barrier verification can be achieved by conducting a negative test because it is performed in actual downhole conditions. According to the Bureau of Ocean Energy Management, Regulation and Enforcement BOEMRE (2011), the negative pressure test is a useful technique because operators can directly determine the potential leak pathways, assess the barrier performance, and evaluate the well control integrity. Per API RP 96 (2013) the barrier verified using a negative pressure test is called "tested barrier." Whereas, the barrier called "confirmed barrier" when it is verified using a positive pressure test. CRF (2016) recommends performing a negative pressure test for the wells that used mudline suspension system, the wells that used subsea BOP stack, any barrier that is expected to expose for a negative differential pressure that is created with the disconnection of the BOP, and the final casing or liner (see Figure 3.9 (b)). In addition to improving the barrier qualification level, the negative test is the

only procedure available for testing some of the downhole barriers, namely subsurface safety valve (SSSV) (ISO 16530-1, 2017) as shown in Figure 3.9 (c). In the negative test, the reservoir or formation pressures are used as a pressurization source (see Figure 3.9 (b) and (c)). Unlike the positive pressure test, the maximum differential pressure is applied in the direction of the potential production fluids flow.

The objective of the negative pressure test is to confirm that the well barrier component(s) can retain the maximum differential pressure that is likely to occur when the wellbore falls in an underbalanced condition. The underbalanced condition is often encountered during the preparation for subsequent operations, such as drill out a cement plug below a permeable pressurized formation, completion activities (e.g. after well conditioning and prior cement placement), well testing, and riser disconnection (NORSOK D-010 2103). During the negative test, the underbalanced well condition can be created by replacing or pumping some of the kill-weight fluid out of the well and injecting lower density fluid above the mechanical barrier which is required to be tested (API RP 96 2013). The pressure holding time for the negative test is 30 minutes (NORSOK D-010 2013). The negative test requires a rigorous procedure, precaution, and contingency plan because the test is performed at underbalanced conditions (API RP 96 2013). This fact is supported by the information from the incident investigation report issued by BOEMRE (2011) after a catastrophic blowout that occurred at Deepwater Horizon (Macondo). The report linked the causes of the incident to the negligence of the rig crew to restore the defects in the cement sheath detected during the negative pressure test. In addition, the interpretation of the test results is erroneous (negative pressure test was accepted although the integrity of the well was not verified).

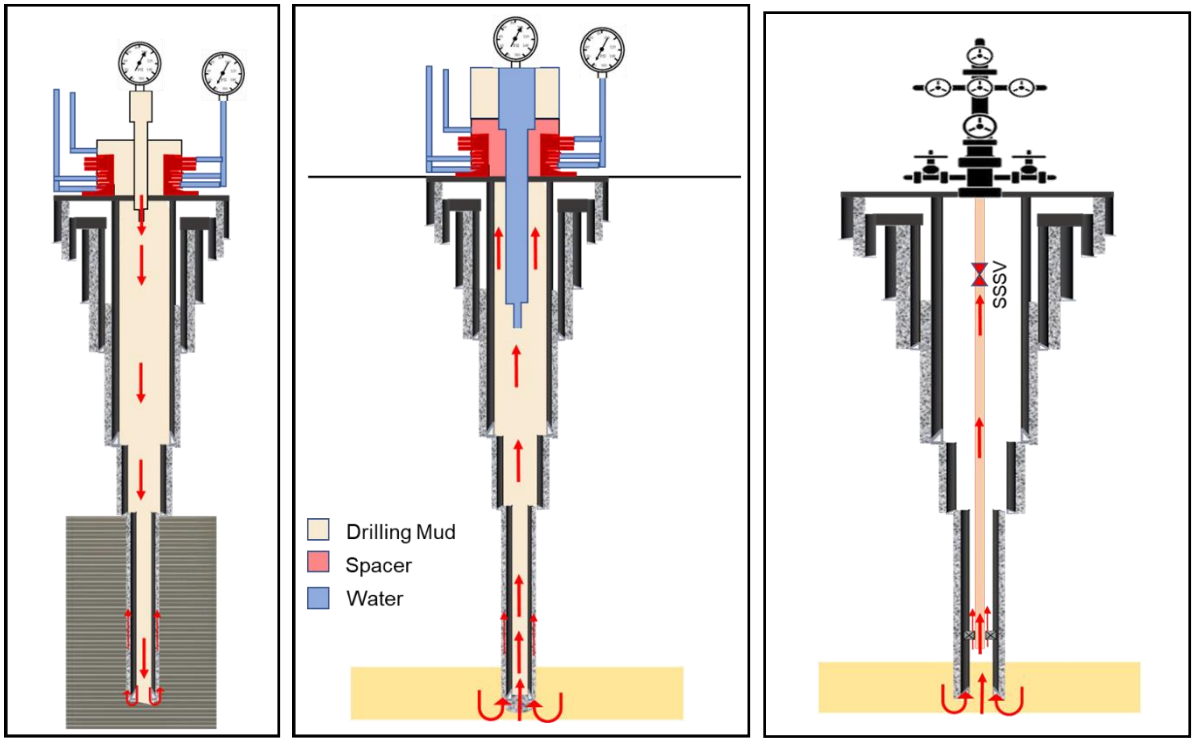

(a) **(b)** **(c)**

Figure 3.9: General representation of pressure test (a), negative pressure test for production liner cement (b), and SSSV (c)

3.3 Gap Analysis in Current Regulations and Standards for Dual Barrier Testing

3.3.1 Relevant Regulations

The USA Code of Federal Regulation

CFR (2016), Sec 250.425 states that it is mandatory to conduct a pressure test for each string of the well casing program as specified in Table A. 1, Appendix A. The code also recommends testing the barrier elements of deployed casing/liner, specifically the seal assembly to ensure successful installation of the casing/liner. Drilling or other downhole operations must not be resumed unless satisfactory pressure test requirements are met. The pressure test holding time must be a minimum

for 30 minutes. The test is considered to be failed if a decline more than 10 % of the test pressure is observed. Given the description of the liner hanger dual barrier system (seal and cement), pressure test arrangement (shown in Figure 1.2), it is difficult to differentiate which of the barriers passes the test. In addition, a good elastomer seal in the liner hanger may be masking a poor cement job. A good cement job may also be masking a faulty elastomer seal in the liner hanger. This was one of the concerns raised by a regulatory agency.

Gap Analysis

Although the full description provided by CFR (2016) for the liner hanger pressure test, the installation sequence of the seal assembly and the cement does not allow each barrier to be tested independently. The code does not mention any procedure for individual evaluation of these barrier elements, leaving a big challenging gap. Hopkins (2016) also emphasized identifying the primary barrier in the liner hanger dual barrier system is a challenging task since there is no testing procedure available in current regulatory guidelines or industry standards to independently test the barrier elements without any degree of uncertainty or misinterpretation. The author believes that according to the API STD 65-2 (2010) definition for the barrier as : "A component or practice that contributes to the total system reliability by preventing liquid or gas flow if properly installed." The seal assembly in the dual barrier system can be identified as a primary barrier if it passed the gas-test qualification (Figure 3.10) and is properly installed. Cement can be identified as a primary barrier if it is properly designed and dispatched in a well. Furthermore, the author believes that a qualified seal assembly and a verified cement sheath can act as two independent well barrier components unless their operation envelopes are overridden.

The concerns mentioned were also raised by the U.S. Department of the Interior (DOI 2016). DOI (2016) disclosed that current standards do not contain sufficient guidelines to ensure

that liner hanger seal assemblies are designed, tested, and qualified in accordance with standardized protocols. Based on the abovementioned concerns, the U.S., DOI strongly recommended establishing new methods of performance evaluation for individual cement test and seal assembly so that the debatable interpretation of the results could be eliminated, thus the seal would not restrict independent testing of the cement sheath.

To verify the cement integrity, CFR, (2016), Section 250.425 recommends performing a pressure test with a holding time of 30 minutes as mentioned before in this section. However, results from the experimental and analytical studies performed by Al Ramadan et al. (2019) revealed that a 30-minute holding time is not enough to detect a leak when it invades a cement column of 300 ft at the liner-casing overlap. Based on this claim, further researches are required to identify the appropriate holding period that should be considered while conducting the cement pressure test.

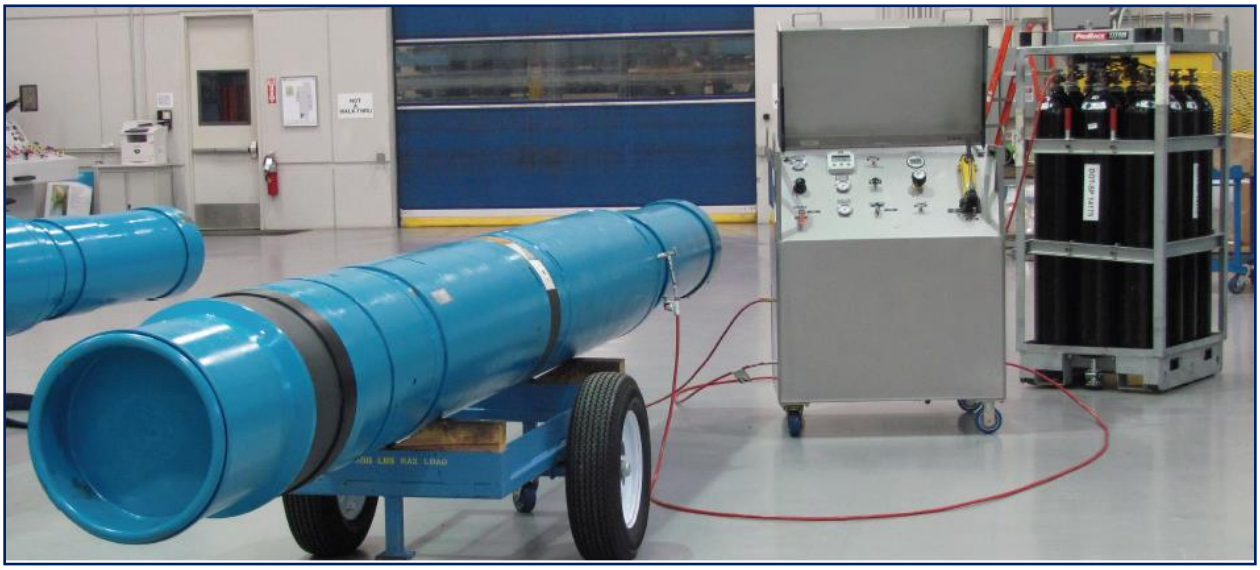

Figure 3.10: Assembled shallow liner hanger packer with nitrogen charging unit (Pleasants et al. 2014)

3.3.2 Relevant Standards

In this section, deeper search has been conducted on industry-recognized standards that are commonly used for well barrier systems to study their scopes and limitations with respect to the testing and verification of the dual barrier system. The applicable industry standards reviewed in this study included API, NORSOK, ASTM, ASME, ANSI, and NACE.

3.3.2.1 API Standards

API standards relevant to the performance evaluation of dual barrier system are listed in Table 3:1.

Table 3:1: List of reviewed standards

Standards	Title
API RP 19LH (2019)	Liner hanger Equipment
API STD 96 (2013)	Deepwater well design and construction
API STD 65-2 (2010)	Isolating potential flow zones during well construction
API STD 65 (2018)	Cementing shallow water flow zones in deepwater wells

API RP 19LH (2019); Liner hanger Equipment:

In response to the liner hanger issues and concerns raised by BESS (2014), QC-FIT report and DOI (2016), API was called to draft a new standard for liner hanger equipment "API RP 19LH" (Morris et al. 2015). The first edition of this specification standard (API 19LH 2019) has been issued in June 2019. However, the scope of the standard covers neither sub-mudline suspension equipment /shallow liner hangers nor testing and verification procedure for dual barrier system. The scope is tailored to cover the production liner hangers, specifically conventional and expandable liner systems including major components, such as liner hangers, liner packers, tie back/ polished bore receptacles, seal assemblies, and running/setting tools. The scope does not cover installation and field maintenance. Although the standard does not cover the shallow liner

hanger system, an in-depth review has been made to find out any gaps regarding the production liner hanger system performance evaluation, hence it is an element of the well dual barrier system. The review also aims in realizing to what extent this standard could be adapted to a shallow liner hanger system.

The standard states that the specification requirements should be established and confirmed in two stages, the design and manufacturing as shown in Table 3:2. During these stages, the user/purchaser is solely responsible for choosing the validation grade; meanwhile, the supplier is responsible for complying with the user's requirements. In the design stages, validation grades for the product and the system must be specified by the end-user. In this standard, the system is defined as a single tubular device that combines the functions of two or more products (e.g. conventional hydraulic/mechanical set liner hanger system). The product requires to be validated according to three design validation grades designated as V3, V2, and V1. V3 represents the minimum level of testing and inspection; the product will be validated according to manufacturer/supplier appropriate procedure. V2 is higher than V3. In this grade, the product (e.g. liner hanger, packer, and seal assembly) must be validated with water under axial loads and temperature cycling. V1 represents the higher and stringent level because the product must be validated with gas (nitrogen) under axial loads and temperature cycling. The liner system validated following the same rules set for product design validation. The grades in the system validation are designated as VS3, VS2, and VS1. To validate the liner system design, a performance envelope shall be generated. The envelope used to determine the maximum allowable operations boundaries for burst pressure, collapse pressure, tensile-hanging capacity, and compressive-upward lifting resistance.

The quality must be controlled and validated during and after the product/system manufacturing process to confirm that the user requirements are fulfilled. The standards classified

the quality validation into three grades designated as QL3, QL2, and QL1. QL3 represents the minimum validation level, however, it complies with the manufacturer predefined validation policies. QL2 is a higher grade than QL3; it implies that a certain number of samples should subject to verification in order to ensure the quality is met. QL1 represents the highest grade in which a rigorous qualification method usually applied to validate the product/ liner system.

Table 3:2: Liner hanger testing and qualifications stages

Specification requirements								
Design Validation Stages Requirements						**Manufacturing Validation Stages Requirements**		
Product Design Validation Grades			**Liner System Design Validation Grades**			**Quality Control Grades**		
V1	V2	V3	VS1	VS2	VS3	QL1	QL2	QL3

As per API 65-2 (2010), the expandable liner hanger system has reduced pressure rating capacities for burst and collapse, which needs to be carefully considered in the well design criteria. API 19 LH (2019) introduces new methods for design analysis and verification which are not considered in current standards. The standard defines design verification as a procedure or process of examining the result of specific design to determine its conformance with the specified requirements. The methods recommended for design verification are distortion energy theory (commonly known as von Mises yield criteria), supplier defined analysis, triaxial yield and collapse equations (analytical approach), and finite element analysis (numerical approach). The combination of these methods to verify liner system design will fill the gap in the determination of burst and collapse rating capacities.

Gap Analysis

As mentioned earlier in this section, API 19LH (2019) provides guidelines for the production liner hanger systems evaluations in systemic testing, verification, and validation structure at the factory-

level. However, this standard does not encompass sub-mudline liner hanger that is recognized as the most critical barrier for isolating the shallow gas zones.

For the production liner, the standard is limited for design and product/systems quality control. The liner running and setting are not included. The standard states that design requirements shall include, but not to be limited to, criteria for, performance ratings, sizes, materials, environment compatibility, operating temperature limit, temperature cycle range, and other. However, it is observed that the pressure cycling range is not incorporated in the mentioned criteria. Failure of seals according to pressure cycling is one of the most critical failure mechanisms that can lead to the creation of fluid migration pathways (Dusseault et al. 2014; Wu et al. 2016; Ahmed et.al 2019b). The results of a recent study by Ahmed et al. (2019b) revealed that the pressure cycling test is important to evaluate sealing performance.

API RP 96 (2013)

API RP 96 (2013) "Deepwater Well Design and Construction" is a reference standard that provides the well engineers with a thorough understanding of deepwater well design considerations and identifies the appropriate barriers required to maintain the well. The scope of this standard also provides a more detailed description of the philosophy and functions of barriers, planning, verification, integrity, installation, and maintenance. The standard also introduces the concept of barrier verification, which can be accomplished either through the negative pressure test or other confirmation processes (e.g. pressure test, other physical tests, and inference from observations).

Gap Analysis

The standard discusses risk considerations for shallow zones, particularly the risk of shallow water and gas. However, special design criteria and testing procedures for the shallow liner hanger that incorporates a dual barrier system are not included. Only discussion on the classification of

production liner hanger systems is included. For dual barrier systems, the standard states that dual barriers (barriers in series) require pressure testing. However, the standard discloses that if the first barrier is successfully pressure tested, it will limit the pressure verification of the second barrier. It follows from this statement that the standard does not contain sufficient procedures to independently test the barrier elements in the dual barrier system.

API RP 65 (2018) and API RP 65-2 (2010)

After the well barriers, design-related standards were overlooked. API STD 65 (2018) "Cementing Shallow-water Flow Zones in Deepwater Wells" and API STD 65-2 (2010) "Isolating Potential Flow Zones During Well Construction" were thoroughly reviewed since the barrier used in well construction should be identified according to these standards. The standards focus on preventing uncontrolled fluids through barrier element(s) that are placed during the well construction phase. The standards set two broad levels of classification for the well barrier systems: physical and operational. The physical barrier system is subdivided into hydrostatic, mechanical, or solidified chemical material (namely, set cement). Technically, there are two types of the mechanical barrier elements, annular and wellbore. The mechanical wellbore barrier elements include cased hole retrieval tools (e.g. packers, retrievable bridge plugs), drillable bridge plugs, retainers, and cementing heads. LOWC prevention annular mechanical barrier elements include set cement, liner top packers, expandable tubular, multiple seals in a single high-pressure wellhead housing, sub-wellhead liner hanger profiles, inflatable external casing packers, and hydraulic set external casing packers.

Gap Analysis

It is obvious from the comprehensive review conducted herein that the standards do not explicitly address the liner hanger dual barrier system. However, it indirectly refers to the dual barrier system as stated in the following paragraphs.

The standards mentioned that "When both cement and mechanical barriers are used in series, it is not possible to physically test them independently to know which is holding pressure. Consequently, both should be designed to be effective and withstand the maximum anticipated load." Based on this quote, it is obvious that the standards lack a testing and verification procedure for a dual barrier system.

The standards specify that when the cement is used during the well construction phase to seal off a mechanical barrier(s), it must be properly designed and placed. In this case, cement may be considered a barrier. There is however no distinction in cement being a barrier or a "primary" barrier (Hopkins 2016). It is clear from the discussion made on this point that the identification of the primary barrier (cement or mechanical barrier) is not given by the standards.

3.3.2.2 NORSOK and ISO

NORSOK D-010 (2013)

NORSOK Standard D-010 (2013) "Well Integrity in Drilling Well Operations" defines requirements and guidelines to the well integrity with more focus on well barriers acceptance criteria. The standard scope covers the minimum functional and performance requirements for each barrier element as well as barrier schematic elements for each phase of the well life cycle. The well equipment specifications are not part of the standard scope.

Gap Analysis

The standard addresses the risk of drilling into shallow gas formations and sets certain measures to prevent, control, and mitigate the risk. The standard recommends special consideration to be taken for the design, installation, testing, and verification of casing strings and cement that are placed to isolate the shallow gas risky zone(s). However, specific recommendations for deploying a shallow liner hanger and sealing it with a cement sheath to form a dual barrier system are not discussed. The standard does not contain acceptance testing criteria for the liner hanger and the liner hanger and cement as a dual barrier system. The standard only mentions testing acceptance criteria for casing cement as an independent barrier.

ISO 16530-1 (2017)

ISO 16530-1 (2017) "Petroleum and Natural Gas Industries-Well Integrity. Part 1: Life Cycle Governance " was developed to address the well integrity during each of the well life cycle phases: basis of design, detailed design, construction, operation, work-over, and abandonment. The standard includes barriers plan classifications, performance standards, verifications, and emergency shutdown safety systems. Considerations for corrosion and erosion mechanisms as well as operating limits are also given. In addition, risk assessment techniques to identify risks that should be prevented, controlled, and mitigated with the appropriate barrier(s).

Gap Analysis

The standard lists the main well barrier elements (WBEs), with a description of their functions and failure characteristics, that are relevant to the operational phase. However, the description of dual barrier systems is not considered. Liner top packer and cement are discussed as independent barriers. It is clear that the standard lacks identification of liner hanger and cement as an integrated dual barrier system.

3.3.2.3 ASTM, ASME,ISO, NORSOK, ANSI, NACE

These standards are not used to test the dual barriers system (seal assembly and cement sheath) as an integrated barrier. However, they are intensively used for testing and qualifications of the elastomeric materials and metallic components of the liner hanger systems.

ASTM and ISO are commonly used individually or collectively to evaluate key properties of elastomeric materials at a lab-scale. Elastomers tests that significantly influence the total reliability of dual barrier systems include but are not limited to: Hardness (ASTM D1415 2018/ISO 48 2018), tensile strength/modulus/elongation (ASTM D412 2012; ISO 37 2017), stress relaxation (ASTM D1646 2019; ISO 3384 2019), compression set (ASTM D395 2018; ISO 815-1/2 2018), and fluid aging (ASTM D471 2016; ISO 37 2015). The downhole conditions that may influence the barrier elements materials reviewed in this section are CO_2 decompression environment (NACE TM0192 2012; NACE TM0297 2017), and elastomer resistance to sour gas (NACE TM0187 2011).

NORSOK M-710 (2014) is the most well-known standard that is used as a reference for performing rapid gas decompression (RGD) test also known as explosive decompression (ED) at lab scale. In addition to that, the standard is used as a reference for performing aging tests at different conditions. The parameters varied in these conditions are type and concentrations of aging gas (H_2S, CO_2, CH_4 or a mixture), temperatures, and test durations. NORSOK M-710 (2014) sets acceptance criteria to evaluate elastomers' quality.

Gap Analysis

Based on the review conducted herein, the following gaps and limitations were identified:

A pressure cycling test is not part of the reviewed standards requirements. The test is not recommended despite many researchers disclosed that some of the wellbore barrier elements

deteriorate according to high-pressure variation. Under pressure cycling, the barrier is most likely to fail (Bosma et al. 1999; Dusseault et al. 2014). The results of the experimental work performed by Ahmed et.al (2019a) revealed that the sealing integrity of some elastomers can be lost due to sudden shocks resulted from repetitive pressure cycling.

NORSOK, ISO, and NACE do not consider the extreme conditions of the downhole temperature in deepwater wells during the rating and qualification of the elastomeric materials. For example, ISO 23936-2 (2011) and NORSOK M-710 (2014) set 2175 psi and 212 °F as maximum pressure and temperature respectively in material compatibility tests. These limits are far from the boundaries stated in the API definition for HPHT (15000 psi and 350 °F). Elhard et al. (2017) proposed developing new standards and/or revising the current guidelines so that elastomeric material testing can be in line with HPHT requirements. The author claimed that current standards recommend the use of elastomers for downhole pressure up to 5000 psi.

For elastomers RDG test, the current acceptance criteria determined by NORSOK M-710 (2014) does not reflect the actual downhole conditions in which phenomena of RGD happened for two reasons. First, the dimensions of the standardized seal/specimen (O-ring with a cross-section of 5, 33 mm, ID: 37,47 mm) is small compared with the actual dimensions of elastomers used in the field. Secondly, the standard acceptance criteria are based on a crack rating system to accept or reject the test. The criteria are very subjective hence the test results depend on the inspector visual judgment (Patel et al. 2019a).

3.4 Summary and Findings from Literature Review

This chapter reviewed wellbore barrier systems, specifically the liner dual barrier system hanger (seal assembly and cement sheath). The following summaries and conclusions are drawn:

1. Leak mechanisms are still not well-defined. In addition, currently, there is no agreed-upon accepted definition of the term "zero leakage" which is a very important barrier performance acceptance criterion.
2. Shallow gas kick is being cited as the major cause of the blowouts globally. More studies are needed to develop leakage models that consider the complex behavior and the unsteady nature of the gas under actual downhole conditions.
3. Currently, there are no adequate specific standards and guidelines for assessing seal assembly in liner hanger elastomeric materials. For testing and evaluation of liner hanger seals, the industry relies on standards developed for packer equipment.
4. Incompatibility of the elastomeric materials with the downhole chemical environment is one of the severe issues that resulted in elastomers' failure. The most damaging effect occurs when elastomers expose to CO_2, H_2S, CH_4.
5. Pressure cycling test does not recommend in current standards and regulations although some studies revealed that elastomers are prone to failure under pressure cycling conditions.
6. There are many anti-gas migration additives formulated to control migrated gas, however, the problem of gas migration is still a challenge for the oil and gas industry due to the uniqueness of each well.
7. There is a lack of procedures, guidelines, and standards that deal with testing and qualification of dual barrier elements (seal and cement) independently in order to identify which of the elements can act as a primary barrier.

Chapter 4: Experimental Work for Evaluation Liner Dual Barrier System

4.1 Scope of the Experimental Work

The experimental scope in this study was divided into two main stages: the first stage aims to test the elastomers independently, whereas the second stage aims to test the elastomer seals and the cement as a dual barrier system. The scope of the first stage of the experimental work is to investigate the performance of the liner hanger seal assembly under normal and irregular conditions. In this context, normal conditions imply that the elastomers did not expose to any form of chemical or physical damage, perfectly manufactured (flawless), and perfectly installed. The irregular conditions investigated herein include physical damage, chemical degradation, and pressure cycling. EPDM and NBR were chosen as samples for the experiments because they are commonly used in most field applications. Elastomers sealability was investigated by conducting pressure tests. The pressure was decided to be 40 psig based on the FEA simulation results as well as safety considerations. The pressure holding time determined to be 30 minutes as per CFR (2016), Sec 250.423 (a) requirements. In some of the tests, the holding time was extended to 60 minutes to assess its influence on the elastomers sealability. The scope of the second stage of the experimental work is to investigate the performance of the seal and cement as a dual barrier system. The tests were conducted at conditions almost similar to those applied during the elastomers' independent tests. All tests were conducted at room temperature of 68 °F.

4.2 Experimental Setup Design and Description

The setup was fabricated from outer and inner acrylic pipes that have diameters of 10 in. and 8 in. respectively. The length of each pipe is 3 ft. The top and bottom of the pipes were closed with

acrylic plates and connected with four outer threaded roads to prevent gas leakage during the elastomers pressure test. Two elastomer samples with cord thickness of 0.75 in **(**Figure 4.1) were placed in the annular space between the outer and inner pipes. The elastomers were inserted between two aluminum rings and separated by a third ring in the middle (Figure 4.2 (b)). Six threaded roads passed from the setup upper cap until they touched the upper aluminum rings. The roads shown in Figure 4.2 (a) were used to energize the elastomers by applying torque using an adjustable wrench. The elastomers' compression (displacement) was measured by using the paper scales attached to the outer pipes as shown in Figure 4.2 (c). Elastomers displacement was used as input for the FEA model to determine the contact pressure (stress). The displacement values were changed significantly based on the elastomer type and the torque applied.

Figure 4.1 : O-ring elastomers to seal the annulus between the inner and outer pipes

Figure 4.2: Seal energization using six rods (a) O-ring elastomers separated with aluminum rings (b) ; and seals compression (displacement) measurement (c)

A port was tapped on the setup upper cap to inject the nitrogen into the inner pipe that was perforated at the bottom to direct the gas flow underneath the bottom of the lower elastomer. The leak through elastomers was monitored by filling the annulus above the top elastomer with a water column. In addition, a set of cameras was distributed around the setup. Schematic and actual components of the setup are illustrated in Figure 4.3 (a) and (b).

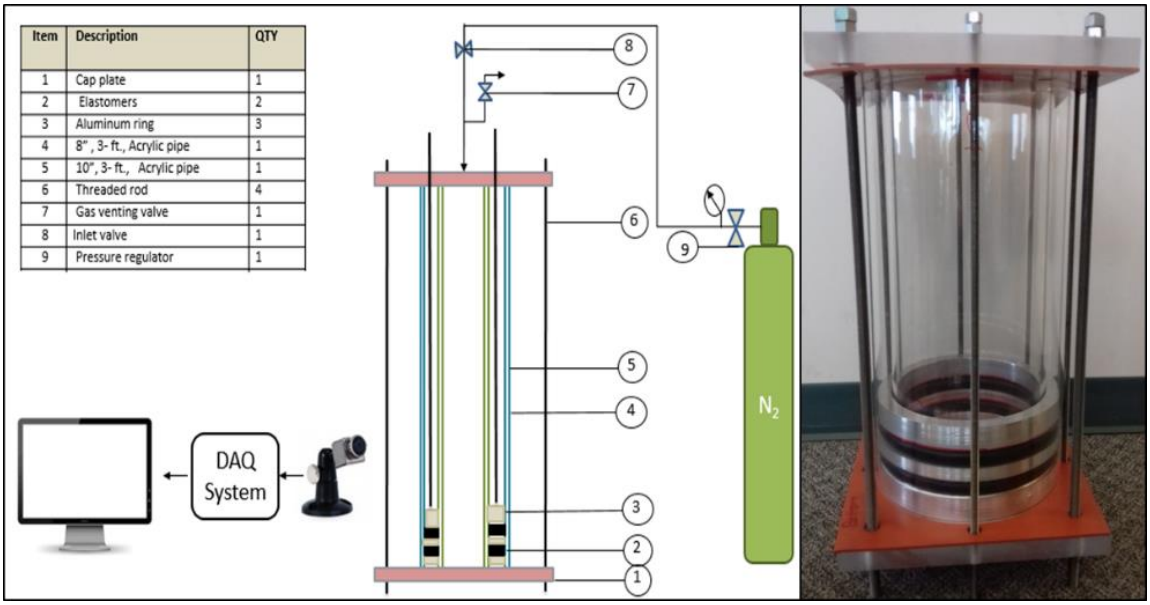

(a) **(b)**

Figure 4.3: A Representation that describes the arrangements of the setup components (a) and the actual setup (b)

4.3 Test Description

4.3.1 Elastomers Tests as Independent Barrier

In this stage, three types of experiments were conducted to assess the performance of EPDM and NBR as shown in Figure 4.4. In the first experiment, the elastomers were tested under normal conditions. Whereas in the second and third experiments, the elastomers were tested after chemical degradation and physical damage, respectively. The chemical degradation was achieved by immersion of elastomers in the surfactant as well as the aging of elastomers with CO_2 in the autoclave cell. Elastomers were physically damaged by creating seam on their surface. Figure 4.5 shows the elastomers sealability test.

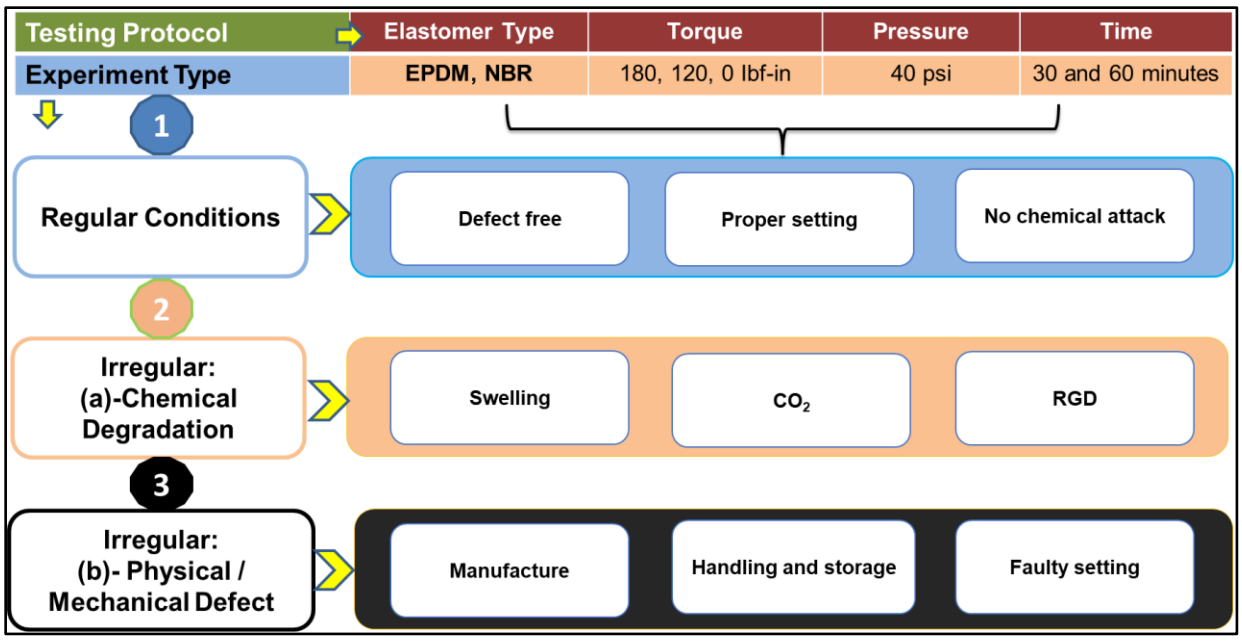

Figure 4.4:Experiments testing protocols for elastomers

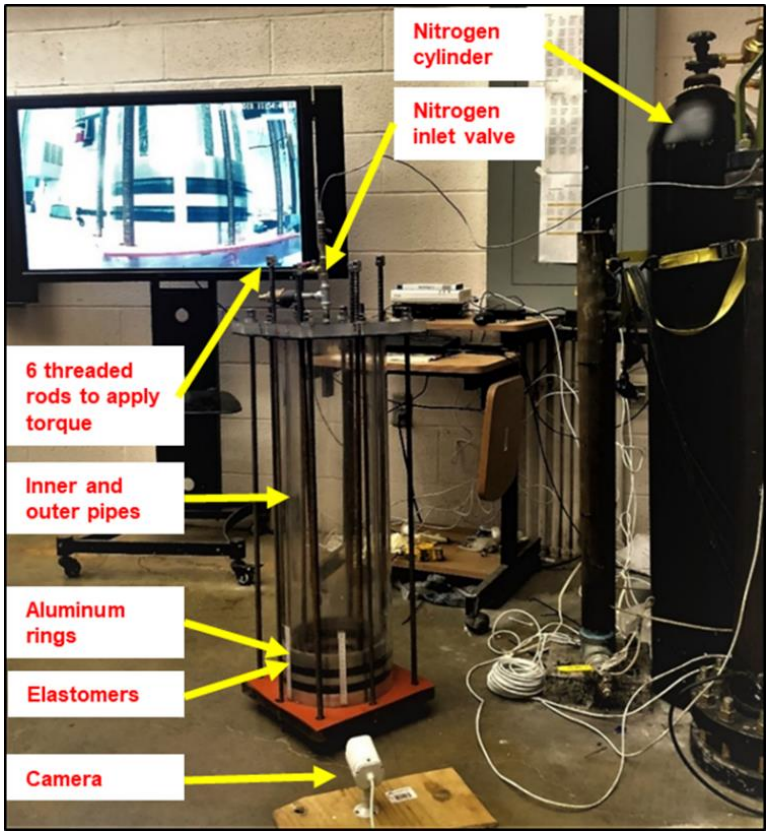

Figure 4.5: Elastomers sealability test

4.3.1.1 First Experiment: Elastomers Test Under Normal Condition

After the elastomers were placed in the annulus, they were energized by applying a torque of 180 in-Ibf and subjected to pressure test as shown in Figure 4.5. The pressure test was conducted at three different stages as depicted in Figure 4.6. The first stage is the setup pressurization. In this stage, the nitrogen was injected into the setup, and the pressure was raised gradually from point (1) to point (2) at which the nitrogen flow automatically stopped when the pressure reached 40 psig. The amount of uncertainty for injection pressures is ± 1 psi. It was inferred from this stage that the inner pipe can be filled with 40 psi in 5 min. The second stage is the pressure holding time (point (2) to point (3)). In this stage, the nitrogen cylinder valve, as well as the nitrogen inlet valve (Figure 4.6), were closed. The pressure inside the setup was held constant for 30 min as recommended by CFR (2016), Sec 250.425. Over each holding time, the pressure gauge was observed to monitor any pressure drop. The third stage is the setup depressurization (point (3) to point (4)). After 30 min, the setup was completely evacuated in a few seconds when the venting valve was opened. The test was repeated after the torque was reduced to 120 in-lbf and 0 in-lbf to assess the effect of energization on the elastomers' performance. The amount of uncertainty for measured torques is ± 2 in-lbf.

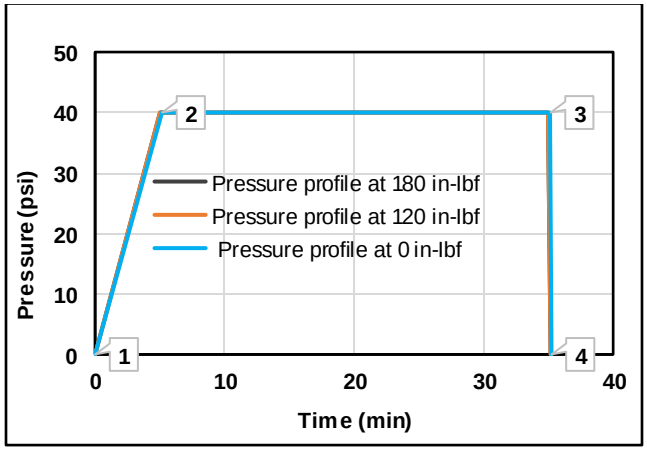

Figure 4.6: Sequence of the pressure test stages

A third test was conducted under pressure cycling conditions. In this test, a series of ten pressure cycles were performed under different energization steps (180 in-lbf, 120 in-Ibf, 0 in-Ibf, and one-week relaxation with 0 in-lbf). The objective of this test is to examine the elastomers' sealability under pressure cycling conditions that frequently encountered at the field operations. The cyclic process achieved by raising the pressure up to 40 psig within 5 minutes, shut-off the injection valves, and maintain the sealing system (elastomers) under pressure for 10 minutes. At the end of the holding time, the vent valve was opened quickly to decrease the pressure to 10 psig, then the valve was closed within one second. After closing the vent valve, the injection valve was opened very quickly to re-fill the setup to 40 psig.

4.3.1.2 Second Experiment: After Chemical Degradation

Under the chemical degradation condition, the elastomers were tested following the same procedure of the normal condition tests. In this test, EPDM and NBR samples were immersed in a surfactant for a week as shown in Figure 4.8. The surfactant selected for the experimental work is Capstone™ FS-22 because it is one of the most aggressive surfactants that deteriorates the elastomers' integrity massively. Capstone™ FS-22 is a non-ionic partially fluorinated acrylic copolymer composite of 30% solids in methyl isobutyl ketone (MIBK). It is believed that other surfactants will have some form of degradation on elastomers. However, the effect of other types of surfactants was not investigated in this study. Generally, the degradation process can change elastomers key properties such as volume, elongation, hardness, tear strength, and tensile strength. These changes in elastomers properties can result in significant failure.

Following elastomers' degradation in the surfactant, volumetric swelling was observed in both samples. Figure 4.7 shows EPDM elastomer configuration before and after it was immersed in a surfactant. The swelling effect was more obvious on the NBR samples. The massive

volumetric swelling showed in Figure 4.9 (a) made the elastomers installation in the setup very difficult. The elastomer experienced a significant deformation after they were inserted in the setup as shown in Figure 4.9 (b). The swelling generated a high contact pressure according to enormous friction between the pipes wall and the surface of elastomers. Therefore, the elastomers were not torqued during the pressure tests because the swelling expanded the elastomers' dimensions and afforded more friction that raised the pre-compression force at the elastomers-pipes interfaces.

Figure 4.7: EPDM samples before (left) and after (right) surfactant degradation

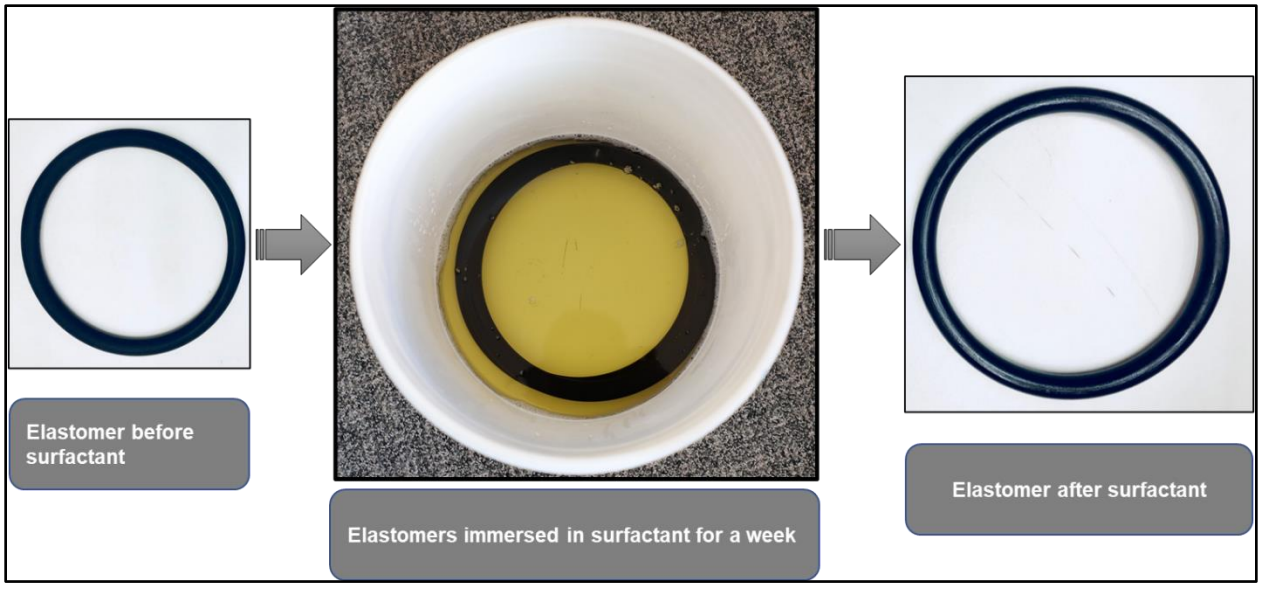

Figure 4.8: NBR degradation with surfactant for a week at ambient conditions

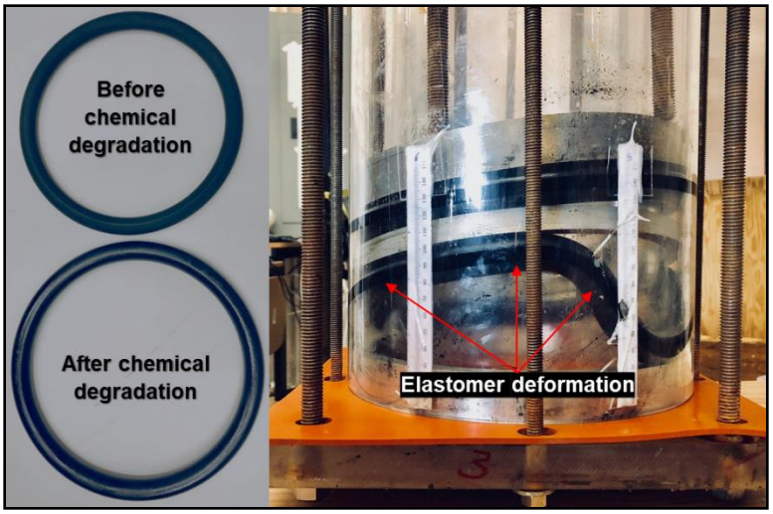

(a) **(b)**

Figure 4.9: NBR samples before and after surfactant degradation (a) and samples structural deformation in the annulus after they were installed in the setup (b)

EPDM samples were exposed to a second chemical degradation using CO_2 to examine their sealing integrity under corrosive downhole conditions. The samples were locked for three days in pressurized autoclave cell (600 psig) filled with CO_2 at room temperature as shown in Figure 4.10. This aging condition was selected to replicate the shallow section conditions of the well drilled on the MP 295, GoM. The incident occurred in this well at the shallow liner hanger that has a relatively low temperature and pressure (around 600 psig). At the end of the aging periods, the cell pressure (600 psig) was suddenly released in less than one minute which is above the upper limit of RGD rate specified in Norsok M-710 (2014). After the samples were removed from the cell, blisters and cracks emerged as shown in Figure 4.11. One of the reasons for the cracks and blisters is because of the high decompression rate used in this study, which is slightly more than the decompression rate used in an RGD test. It is worthy to note that a standard RGD test was not conducted in this study. The is because the elastomer size and exposure conditions (described in this section and section 4.2) are different from those specified for a standard RGD test. However,

according to Norsok M-710 2014, for a decompression to be considered as RGD, one of the conditions is that the decompression rate should be between 290 psi to 580 psi per minute. In this study, the pressure 600 psig was released in less than one minute which is above the upper limit of RGD rate. Thus, the blisters and cracks emerged. Another reason for the formation of cracks and blisters is because of the molecular structure of CO_2 which allows it to react with the elastomer molecular chains and deteriorate the elastomer chemically. This reason is supported by the outcomes of the experimental study performed by Salehi et al. (2019) to evaluate the performance of common elastomeric materials of the well barrier systems in corrosive environments. In the experiments, the authors inserted NBR, EPDM, FKM, and PTFE samples in an autoclave for seven days at a different temperatures and pressures to age the samples. Corrosive gases were injected at various concentrations such as 100% CO_2, 0.05% H_2S in CH_4 carrier, 100% CH_4, and a mixture of all gases to interact with the samples. The results showed that the order of corrosive gas that adversely impacted the elastomer hardness and compression from high to low is CO_2>All gases>H_2S>CH_4. The results showed that H_2S and CH_4 had the least effect on elastomers' volumetric swelling. Meanwhile, the mixture of CO_2, H_2S, and CH_4 has been observed to be the most damaging effect on elastomers' swelling. In general, among other corrosive gases, CO_2 has been reported as the most severe gas that compromises the elastomers' integrity.

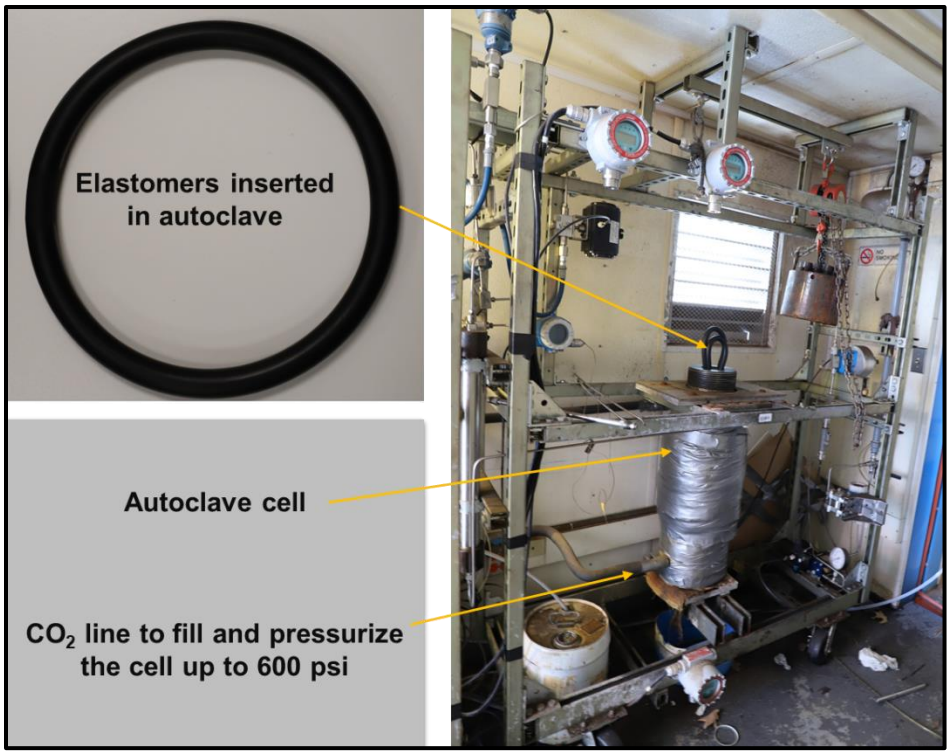

Figure 4.10: Elastomers degradation in an autoclave cell

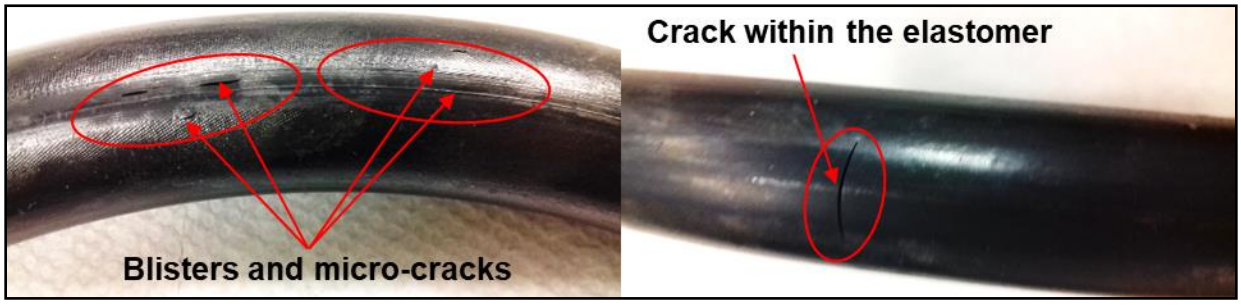

Figure 4.11: Defects in forms of blisters and cracks on surface of the elastomers after CO_2 chemical degradation

4.3.1.3 Third Experiment: After Physical (Mechanical) Defect

The elastomers in this experiment were intentionally defected as shown in Figure 4.12 by creating seam on their surface. The objective of this test is to evaluate the effect of the surface imperfection on the elastomers' sealability. Defective elastomers were subjected to pressure tests using the same procedure as in previous experiments.

Figure 4.12: Elastomer after creating a seam as an intentional physical defect.

4.3.2 Elastomers and Cement Tests as Dual Barrier System

The second stage of the experimental work is to test the elastomers and cement sheath as a dual barrier system to demonstrate whether the cement can act as a primary barrier element in a dual barrier (elastomer seal or cement sheath), in case the elastomer seals in a failure mode. Three experiment scenarios were established as illustrated in Figure 4.13. In the first experiment, faulty EPDM samples and neat Class H cement were tested collectively. The test was performed first because the neat cement was expected to leak (fail). In the second experiment, the cement was mixed with a commercial gas migration control additive to assess the effect of the anti-gas additives on the cement sealing behavior. The commercial gas migration additive used to design the cement slurry in this study is a proprietary product of a well-known oil and gas service company. The company offered the additive to the University of Oklahoma to perform the experimental work to evaluate its ability to improve the cement zonal isolation, especially in combatting gas migration in shallow formations. The author does not have the right to disclose any information about this product. In the third experiment, the inner acrylic pipe was replaced with a steel pipe while the acrylic pipe was used as the outer pipe to monitor the leaks in order to assess the effect of surface roughness on the cement hydraulic bonding integrity.

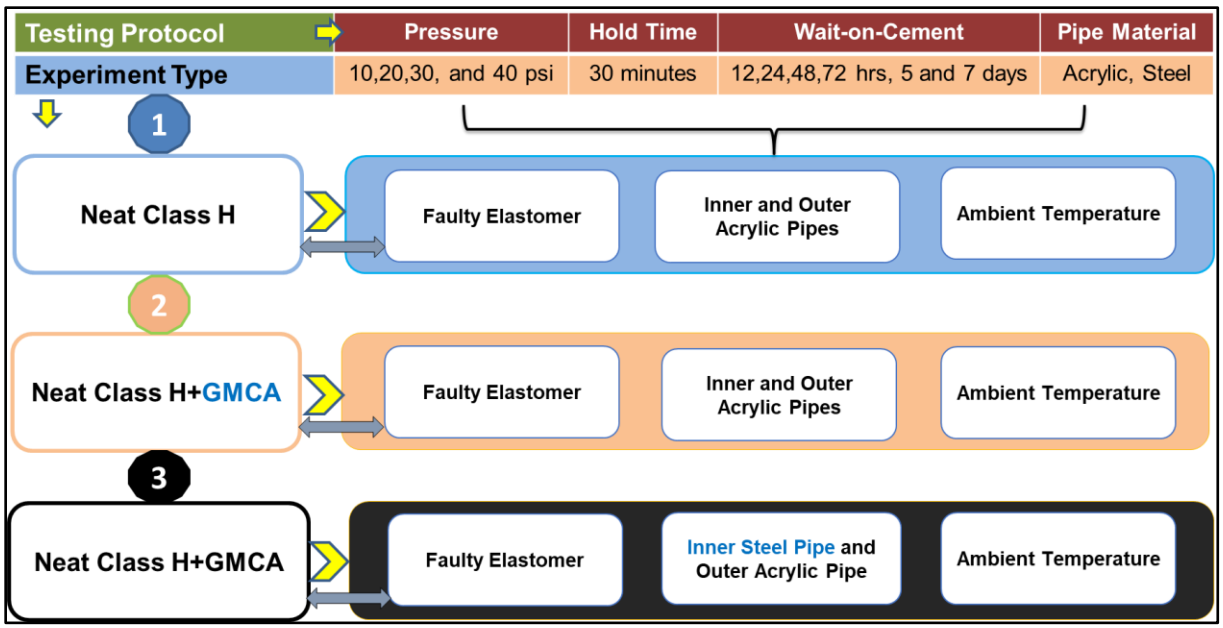

Figure 4.13: Experiments and testing protocols for elastomers and cement as a dual barrier system.

The pressure tests conducted in the abovementioned experiments (scenarios) according to the following steps:

1. The faulty EPDM elastomers were tested independently before pouring the cement slurry in order to observe the leak intensity.
2. Then the setup was dried, and the cement slurry was poured immediately above elastomers as shown in Figure 4.14 (a) and (b). The height of the cement column was decided to be 1 ft (12-in), to avoid the end effect in the FEA model.
3. After 12 hours WOC a pressure test was conducted as recommended by CFR (2016), Sec 250.422. In this test, the gas inlet valve (item 3 in Figure 4.14(b)) was opened to inject 10 psi for 30 minutes, during which gas bubbles, if any, were monitored.
4. After 30 minutes, the gas inlet valve was closed and leak (gas bubbles) was monitored for another 30-minutes (holding period). This period was specified based on CFR (2016), Sec 250.425 which recommends 30 minutes duration for the pressure test of the liner hanger.

5. The third and fourth steps were repeated for 20 psi, 30 psi, and 40 psi. The amount of uncertainty for injection pressures is ± 1 psi.
6. In addition to 12 hours WOC, additional pressure tests were conducted after 24 hours, 48 hours, 72 hours, 5 days, and 7 days WOC for each scenario. In fact, a total of 72 tests were conducted during the second stage of the experimental work.

Pressure profiles over the holding time (30 minutes) were plotted for each test because they provide indications on the cement sheath sealability. In addition, they can be used to compare the sealability of various cement formulations.

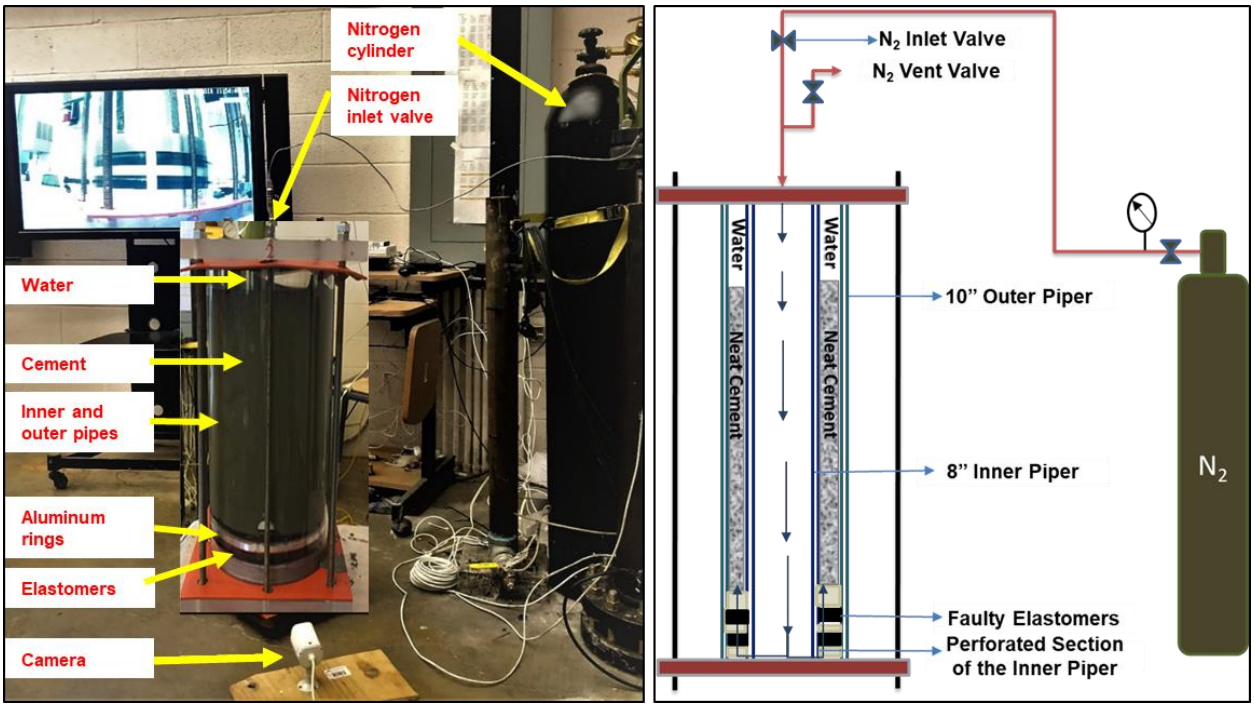

(a) **(b)**

Figure 4.14: Cement placement above the elastomers (a) and setup schematic for cement and elastomer test (b)

4.4 Experimental Work Limitations and Assumptions

In this section, the assumptions of the experimental tests, and the limitations of the setups used are presented. Based on the FEA preliminary simulations results, the length of setup fabricated for

elastomers independents tests was decided to be 3 ft to avoid end-effect. End effect in this context is defined as the length that does not affect the simulation accuracy and the experimental tests results. The end effect is also an indication of whether the boundary conditions and the length might generate odd results at the end of the model components or not. One of the setup limitations is that it is prone to break at very low values of internal pressure and torque. The setup is made from acrylic pipes that cannot withstand burst pressure of 100 psi. The setup cap plates are also made of brittle acrylic materials. It was observed that the upper cap plate started breaking when the torque exceeded the 180 in-lbf. Therefore, the maximum torque in the experiments was limited to 180 in-lbf. The availability of rubber formulations and physico -mechanical properties are very important to compare and justify the final results as well as to provide a broader understanding of the elastomers' sealing behavior. However, some of these properties such as tensile strength, percent of elongation at break, tear strength, and compression set were not available from the supplier. These properties and the compound formulation are supplier's confidential data, and the measurement of these properties would significantly exceed the scope of this research.

The assumptions considered in the elastomers tests are amount of the torque applied to energize EPMD and NBR seals are same; the friction coefficient between the pipes and seals (EPDM and NBR) is constant; the upper elastomer properties are not affect by the water poured on the top to detect the gas leakage, and the elastomers do not interact with the testing medium (nitrogen). It is worthy to mention that while the volumetric swelling of the elastomers may appear to be good as it provided adequate contact between the sealing interfaces that prevented leaks, it should be noted that the pressure tests were performed at room temperature. In addition, the elastomers were exposed to the surfactant at ambient temperature and pressure. Chemical attacks on elastomers can accelerate at temperatures beyond ambient. These attacks and alteration of

molecular structure can be exacerbated at elevated temperatures, thus reducing the elastomers sealing performance. In addition, the inert nature of N_2 may have also masked the impact of surfactant degradation at room temperature.

In the dual barrier setup, the length of the setup and the cement column were limited to 18-in and 12-in, respectively. To avoid and eliminate the end effects on the experiments and FEA results, the length of each pipe (18-in) has been selected to be approximately 2 times greater than the inner pipe diameter (8-in). The height of the cement column has been chosen to be 12-in. This height represents 1.5 the average diameter of the cement sheath to mitigate the influence of the end effects upon the experiments results. In addition, the tests were also conducted at a relatively low testing pressure (40 psig) because applying a pressure beyond this value could risk damaging the setup. As mentioned earlier, the setup cannot withstand burst pressure of 100 psi, so it was decided to perform the tests at 40 psig, keeping a safety factor of 2.5. In the experiments, it was assumed that defects observed in the cement matrix and at the inner pipe-cement-outer pipe interfaces were independent from the length of the cement column. In addition, it was assumed that the inert nature of the testing medium (N_2) eliminated its interaction with the cement sheath.

Chapter 5: Results and Discussion of the Experimental Work

In this chapter, the results obtained from the experiments were analyzed to evaluate the performance of EPDM and NBR samples. Pressure tests were performed to determine the elastomer's sealing capacity independently under various operating conditions, such as normal, after a chemical failure, and after a mechanical failure. Test results from experiments conducted to evaluate the performance of cement and elastomers as an integrated dual barrier system were also presented.

5.1 Elastomers Test Results

5.1.1 Pressure Test Under Normal Conditions

In this scenario, normal conditions mean that the elastomers are in sound quality, and their integrity is not compromised due to chemical degradation or mechanical damage, such as manufacturing defects, cracks, and /or field installation permanent structural deformation. After inserting the elastomers in the setup and energized, a preliminary test was performed. The aim of the test is to ensure that the applied torque is transmitted omnidirectionally on the aluminum rings that compress the elastomers to seal the testing medium (nitrogen) tightly. Preliminary test results for EPDM and NBR were plotted in Figure 5.1(a) and (b). For safety precautions, the pressure was gradually increased to 40 psig. During these tests, no leaks were observed. From these tests, it was concluded that 40 psi was the maximum test pressure the setup could withstand.

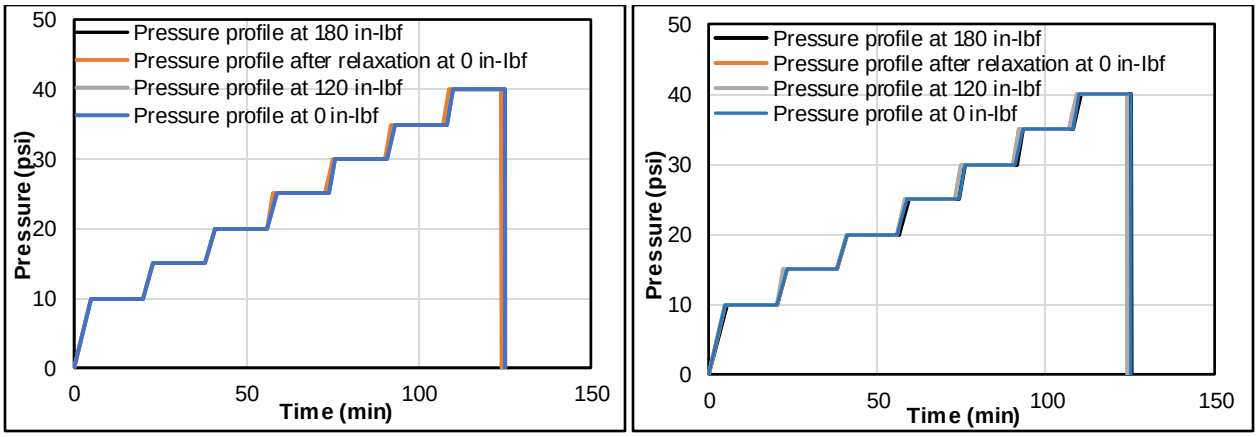

(a) **(b)**

Figure 5.1: EPDM preliminary pressure test at different torques (a). NBR preliminary pressure test at different torques (b).

5.1.1.1 EPDM Pressure Tests for 30 and 60 minutes Holding Times

Succeeding the preliminary pressure tests, the EPDM elastomers were energized by applying a torque of 180 in-Ibf. The nitrogen was injected until the pressure reached 40 psig and held for 30 minutes. No leak and pressure drop were reported. The test was repeated after the torque was reduced to 120 in-lbf and 0 in-Ibf. The torque was lowered to assess the effect of the energization force on the elastomers' performance. Then, the test was repeated after the elastomers relaxed for a week, and no torque was applied. The purpose of relaxation for one-week was to investigate the effect of the pre-compression force that deformed (energized) the elastomers according to the friction force resulted from the elastomers squeezing against the walls of the pipes. Figure 5.2 (a) shows that for all the energization scenarios and under normal conditions, no leaks were observed within 30 minutes holding period. The observations indicated that elastomers offered tight sealability up to 40 psig pressure test.

The tests were repeated following the same procedure mentioned; however, the 30- minutes holding period was extended to 60-minutes to assess the effect of the holding time on the leak appearance. Figure 5.2 (b) shows that for all energization scenarios and under normal conditions,

no leak was reported within 60 minutes of holding period. The elastomers proved tight sealability up to 40 psig pressure test. The test results confirmed the notion claimed by Hopkins (2016). The author stated that increasing the test holding time to 60 minutes was most likely not improve the leak detection and safety in the filed applications because leakage can be detected very quickly during the pressure test in case tested barrier in a faulty mode.

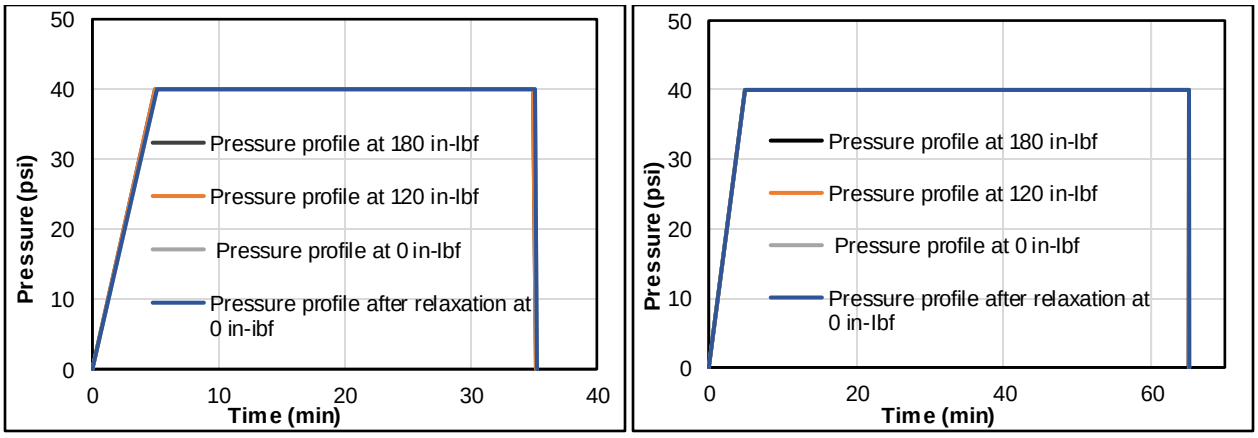

(a) **(b)**

Figure 5.2: EPDM pressure test at different torques and 30 minutes (a), 60 minutes (b).

EPDM Pressure Cycling Test

The objective of exposing the elastomers to a pressure cycling test was to assess their sealing capacity and failure modes when they encounter high pressure shifts and cycles in field applications. Four pressure cycling tests were conducted after the following torque/energization: 180 in-lbf, 120 in-Ibf, 0 in-Ibf, and one-week relaxation with 0 in-lbf. In each test, the cycle was repeated 10 times, and the pressure profiles are shown in Figure 5.3. No leak was observed during these tests as shown from the stability of the pressure profiles over the holding periods (10 minutes), which implies proper sealing.

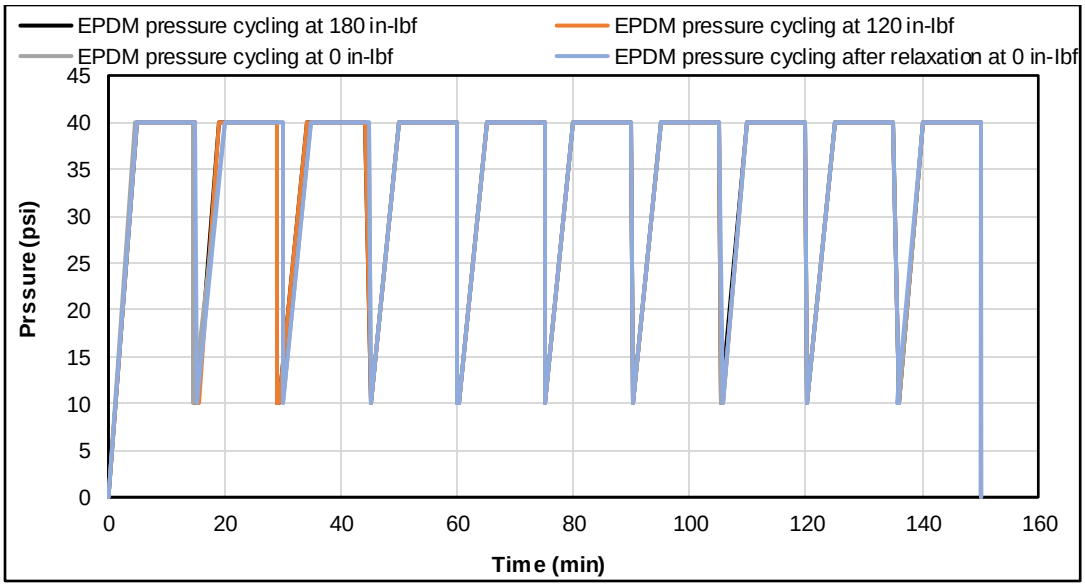

Figure 5.3: EPDM pressure cycling test at different torques

5.1.1.2 NBR Pressure Test for 30 and 60 Minutes Holding Times

NBR samples were exposed to 30 and 60 minutes pressure test following the same energization procedure applied during the EPDM pressure tests. As shown in Figure 5.4 (a), during the pressure holding time (from 5 minutes to 35 minutes), there was no pressure variation nor drop. This result was valid for all the energization steps (180 in-lbf, 120 in-Ibf, 0 in-Ibf, and one-week relaxation with 0 in-lbf). Additionally, a leak was not reported during all the tests performed, which implies that the NBR samples can provide an intact sealing up to 40 psig. After that, the tests were repeated following the same sequence, however, the holding period was prolonged for 60 minutes. As shown in Figure 5.4 (b) the pressure profiles have a plateau trend during the holding time. In all tests, a leak was not observed indicating that the NBR samples provided tight sealing for the test conditions.

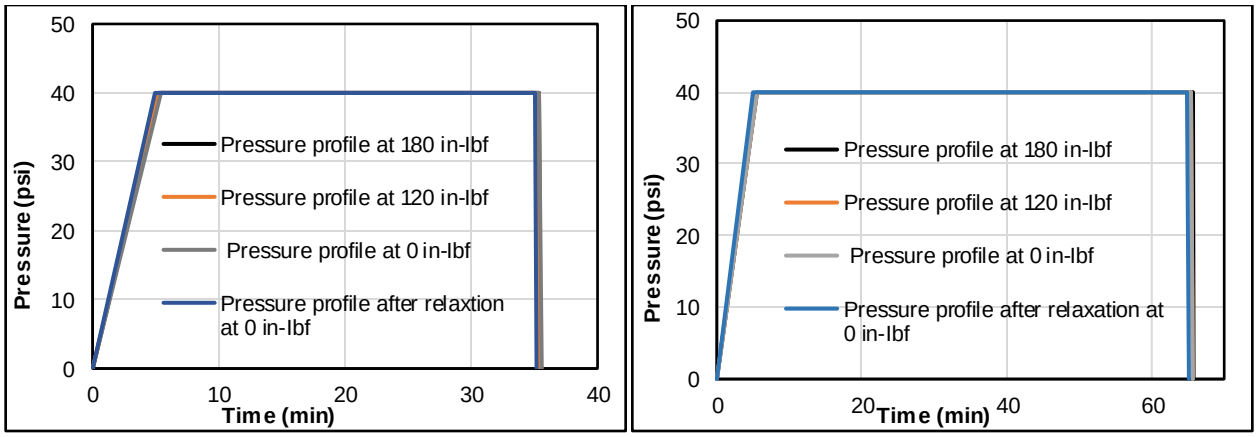

(a) **(b)**

Figure 5.4: NBR pressure test at different torques and 30 minutes (a), 60 minutes (b)

NBR Pressure Cycling Test

Figure 5.5 shows the pressure profile of the NBR samples when they were exposed to pressure cycling tests. It is obvious that a leak was not seen during the first and second tests in which torques of 180 in-lbf and 120 in-Ibf were applied. The minor deviations that occurred at the 8th and 9th cycles were from the variations of nitrogen filling time (setup pressuring up) and variations of pressure release during setup evacuation. These deviations had no effect on the elastomers sealing performance. It is worth noting that, when the torque was reduced to zero, a leak appeared in the form of a blowout as shown in Figure 5.6 (b). The sealing of elastomers was initially lost at the end of the 3rd cycle (first leak) and continued losing at the end of the next four successive cycles as shown in Figure 5.7. However, in the last three cycles, the elastomers exhibited better contact pressure, which was reflected by the stable pressure profile over the holding periods.

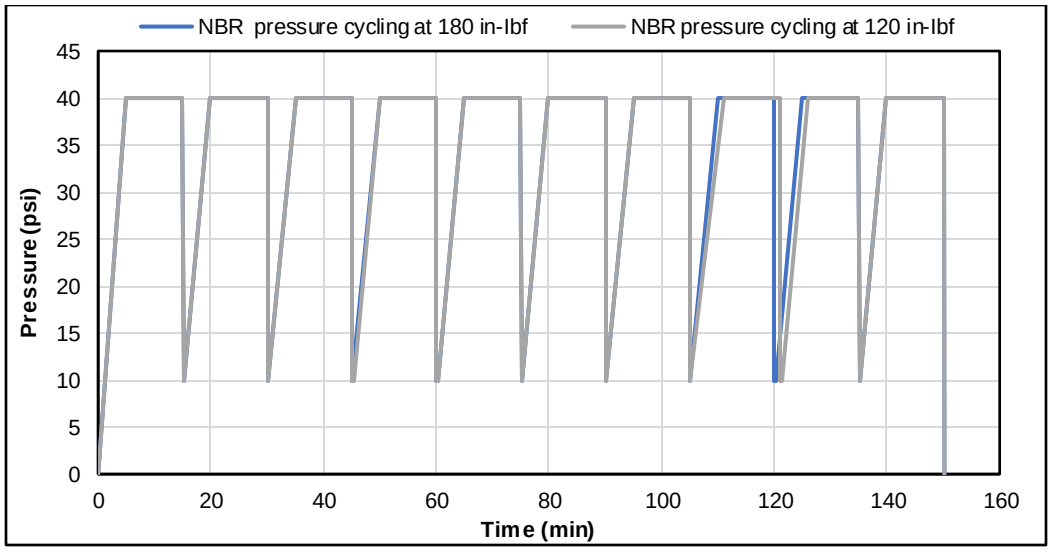

Figure 5.5: NBR pressure cycling test at 180 in-lbf and 120 in-lbf (successful tests)

(a) **(b)**

Figure 5.6: NBR before pressure cycling (a) and failure during pressure cycling (b)

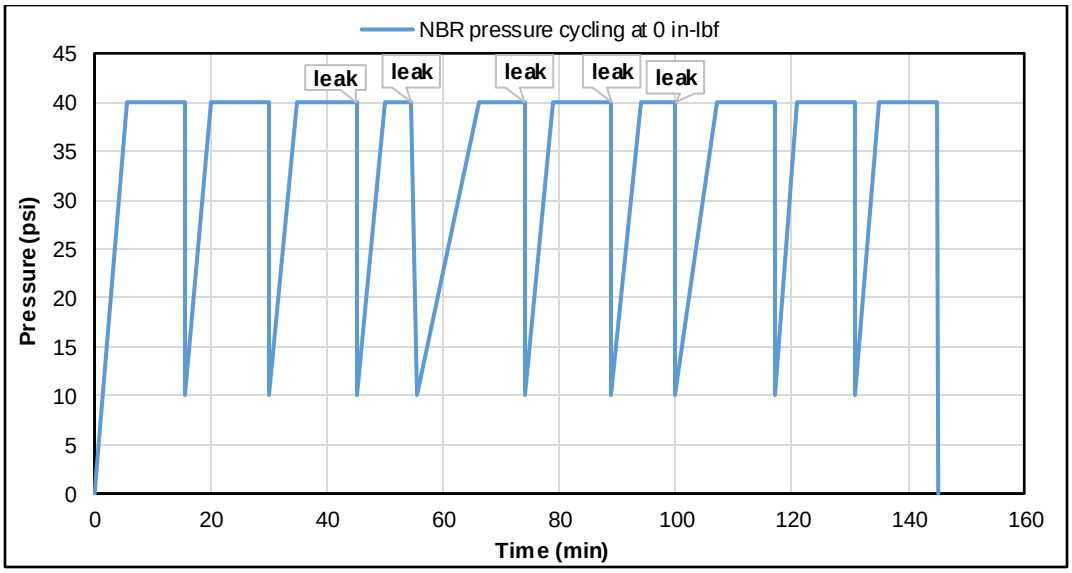

Figure 5.7: NBR pressure cycling test at zero torque (failed test)

The pressure cycling test was repeated one week after elastomers relaxation (supposed recovered from stress) without applying torque. The results revealed that NBR's sealing performance showed much deterioration as depicted in Figure 5.8. The elastomers lost their sealability within 2.5 minutes of the 2nd cycle. Due to sealability deterioration, the planned holding time (10 minutes) was incomplete in the successive cycles because leaks led to a sudden drop in the pressure. As the number of cycles increases, the elastomers sealing integrity deteriorates drastically until it is totally lost at the end of the pressure cycling test (10th cycle). From this test, it can be concluded that in field applications, the seal assemblies of the liner hangers are likely to lose their contact pressure from pressure cycling operations in the absence of sufficient energization force. A lack of contact pressure at a liner-casing interface can favor formation fluid influx into the wellbore. To support this conclusion, the torque was increased to 60 in-lbf to provide sufficient energization force. After the test was repeated, the number of failed cycles decreased. Then, the torque was raised up to 120 in-Ibf to provide more sufficient force. As a result, the leak was completely eliminated, which implies that the elastomers provided intact sealability capable to resist the leak flow.

Comparing the performance of EPDM and NBR under no torque condition, it is clear that, the performance of EPDM was not impacted by the number of pressure load cycles. However, the performance of NBR deteriorated as the number of cycles increased. Generally, the EPDM samples exhibited a better sealing behavior than the NBR samples, and the influence of energization was more evident in the NBR performance based on the conditions of the tests considered in this study. It is worth mentioning that, the evaluation of the elastomers' performance based on limited parameters may limit a fair comparison between seals behavior. For example, a comparison between EPDM and NBR samples under the cyclic pressure tests described herein would be more detailed in case the other physico-mechanical properties of the samples such as tensile strength, percent of elongation at break, tear strength, and compression set are available. Therefore, the rubber sealing performance should be investigated holistically by evaluating a variety of physico -mechanical-properties, chemical compounding, and frictional values between elastomers and pipes.

Overall, the following conclusions can be drawn from the pressure cycling tests:

- The elastomer's integrity can be adversely impacted as the cycling number increase; hence cycles repetition imposes more stress on elastomers. Consequently, the stress inducement can reduce the contact pressure at the casing-elastomer-liner interface.
- The seal performance under pressure cycling conditions depends on the type of elastomer, energization force, and the number of pressure cycles.

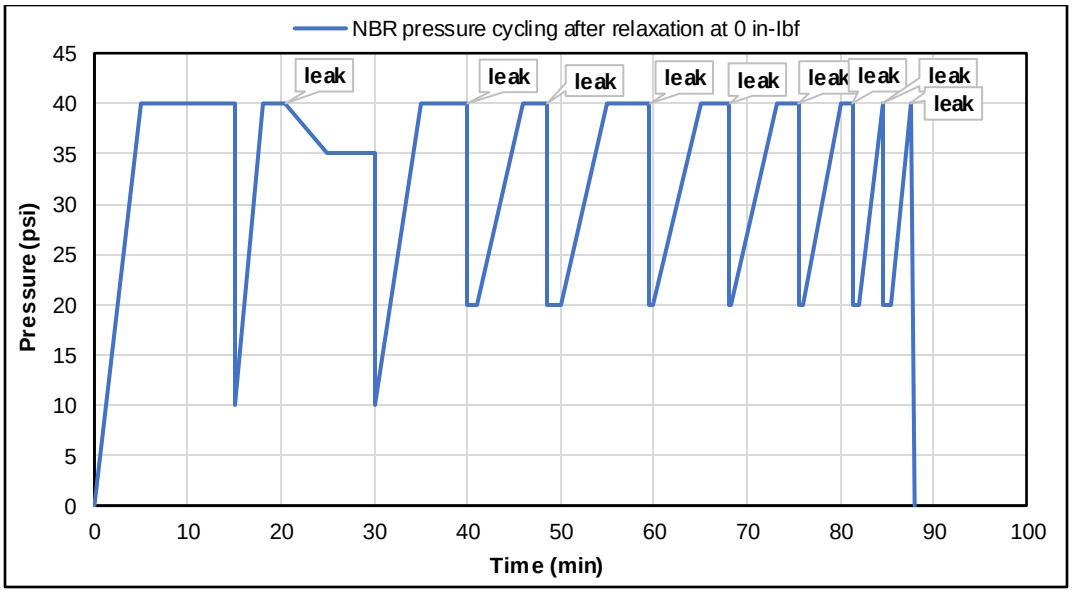

Figure 5.8: NBR pressure cycling test after one-week relaxation (failed test)

5.1.2 Pressure Test After Chemical Degradation

In this scenario, EPDM and NBR samples were immersed in a surfactant that is normally used in some non-aqueous drilling fluids. The elastomers were immersed for a week at atmospheric temperature and pressure to assess the effect of chemical degradation on the elastomers sealing performance. The samples were then inserted into the setup, and no torque was applied to energize the seals. In addition, other EPDM samples were also degraded with CO_2 using an autoclave cell.

5.1.2.1 Pressure Test After Chemical Degradation with Surfactant

EPDM Tests for 30 and 60 Minutes Holding Times

After EPDM chemical degradation with a surfactant, they were immediately tested at 40 psig and 30 minutes holding time. The test was repeated for two consecutive days to evaluate the effect of time (recovery) on the elastomers' sealability. The pressure profiles were plotted in Figure 5.10 (a). The results showed that no leak or pressure drop was reported. In all mentioned tests, an additional test in which the holding time increased to 60 minutes was performed as shown in Figure 5.10 (b), and no leak was observed. It was observed that the elastomers' hardness was decreased

from 75 to 63.75 shore A (shown in Figure 5.9), that their diameters increased from 8.74 to 8.82 in, that their thickness increased from 0.75 to 0.78 in. Norsok standard M-710 (2014) specifies 20 units as a maximum allowable reduction limit for elastomer hardness. Based on this criterion, the reduction in the samples' hardness is within the standard acceptance range. One valid explanation for the reason elastomers retained their sealing integrity under this adverse condition is the substantial increase in the contact pressure generated at elastomer and pipe walls interfaces because of the excessive volumetric swelling.

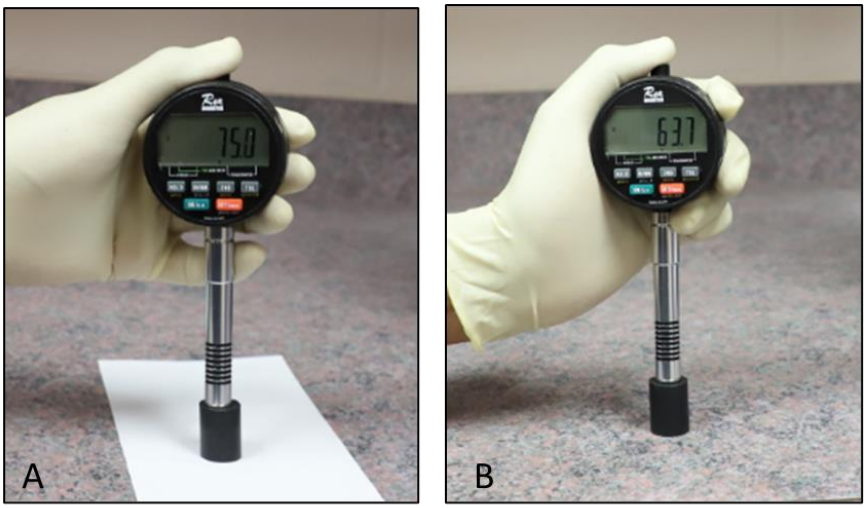

Figure 5.9: EPDM hardness in Shore A before and after surfactant degradation

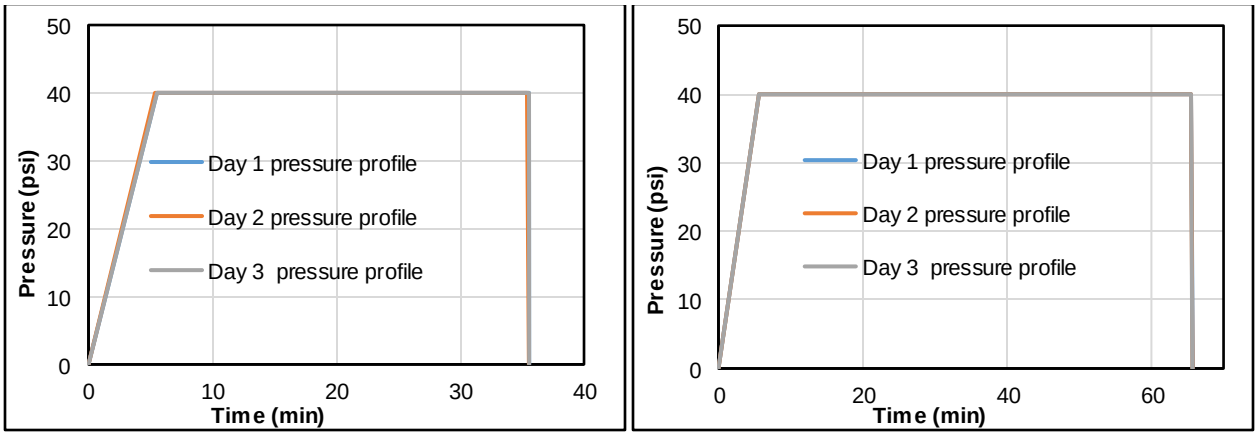

Figure 5.10: EPDM pressure test at Day 1, Day 2 and Day 3 after exposure to a surfactant and 30 minutes(a), 60 minutes (b)

EPDM Pressure Cycling Test

The pressure cycling test was conducted on day 1, day 2, and day 3 to assess its effect on EPDM performance. The results shown in Figure 5.11 revealed that over 10 pressure cycles, EPDM showed stable pressure profiles at their respective holding periods. This trend infers that the samples have maintained a firm seal bonding.

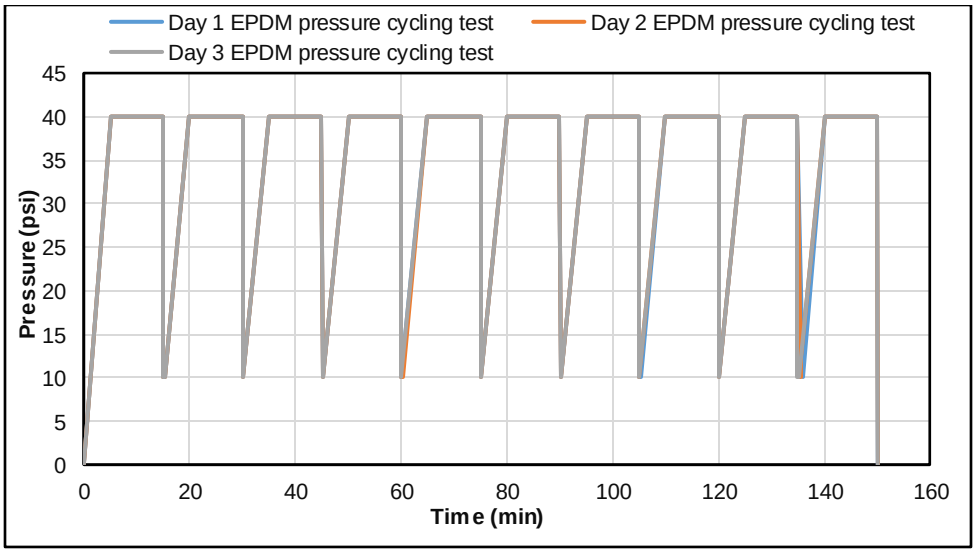

Figure 5.11: EPDM pressure cycling test at Day 1, Day 2, and Day 3 after exposure to surfactant

NBR Pressure Tests for 30 and 60 Minutes Holding Times

After removed from a surfactant, the diameter of the NBR samples increased from 8.74 to 8.94 in, and their thickness also increased from 0.75 to 0.87 in. Whereas their hardness decreased from 66 to 44 shore A (21 units reduction) as shown in Figure 5.12. In accordance with Norsok M-710 (2014) criteria, NBR samples were considered failed under the test conditions specified in this study. Despite the failure of the samples in hardness, pressure tests were performed on NBR samples for 30 minutes and 60 minutes holding times, following the same procedure and successive intervals (days) for EPDM. No torque was used because of the massive volumetric swelling. Figure 5.13 (a) and (b) show the pressure profiles for 30 minutes and 60 minutes pressure

tests, respectively. A leak was not seen, and the extension of the holding time did not have any effect on NBR's sealing performance.

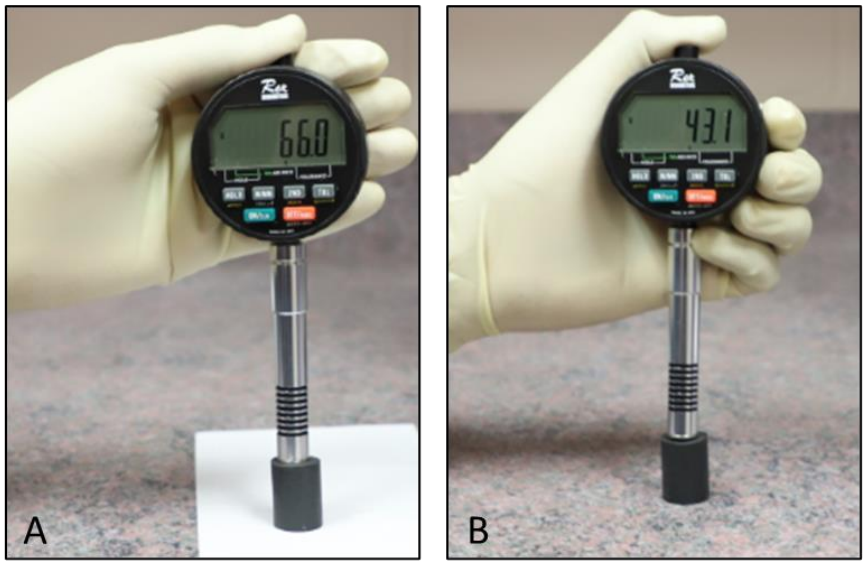

Figure 5.12: NBR hardness in Shore A before and after surfactant degradation

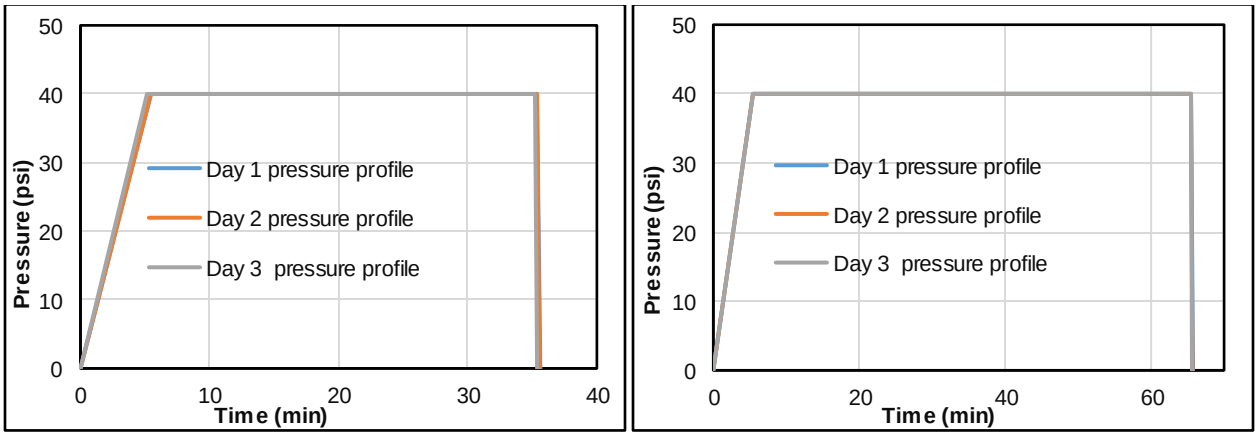

(a) **(b)**

Figure 5.13 : NBR pressure test on Day 1, Day 2, and Day 3 exposure to surfactant and 30 minutes(a), 60 minutes (b)

NBR Pressure Cycling Test

Pressure cycling tests were performed on day 1, day 2, and day 3 to evaluate the elastomers' performance after they were exposed to surfactant. Figure 5.14 indicates that no leak was observed during the pressure cycling test.

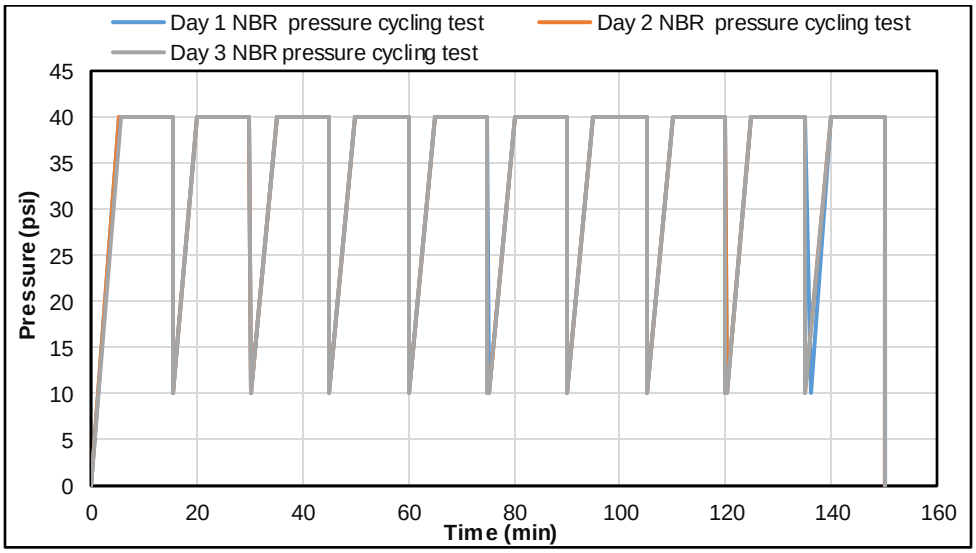

Figure 5.14: NBR pressure cycling test on Day 1, Day 2 and Day 3 after exposure to a surfactant

It can be concluded from the swelling tests conducted in this study that volumetric swelling may be beneficial in terms of providing sufficient contact stress that assists in maintaining intact bonding at seals-pipes interfaces. However, the tests evaluated herein were conducted at ambient temperature. In addition, the elastomer samples were degraded by the surfactant at ambient temperature and pressure. Certainly, these conditions did not simulate the actual downhole environment. In reality, the elastomers' chemical degradation can be tremendously accelerated as temperature increases. The alteration of elastomers' molecular structure due to the chemical degradation can be exacerbated at elevated temperatures, thus, compromising the elastomers sealing integrity. In addition, the inert behavior of N_2 used as a test medium may have also masked the impact of surfactant degradation at room temperature. Therefore, these factors need to be

compensated for at the stage of the seals testing and qualification, especially if the seals are intended to serve in environments containing surfactants.

5.1.2.2 Pressure Test After EPDM Degradation with CO_2

This scenario was suggested to present an in-depth investigation of the elastomers sealing behavior when they are attacked by corrosive gases, such as CO_2. In this scenario, EPDM samples were degraded for three days with CO_2 in an autoclave cell that pressurized up to 600 psig at room temperature as shown in Figure 4.10. After degradation, superficial mini-blisters and micro-cracks were observed as shown in Figure 4.11. Under these aging conditions, the defective samples were installed in the setup, and two pressure tests were conducted. The first test conducted without applying any torque. Whereas in the second test, a torque of 180 in-lbf was applied to assess the effect of the energization compression on the cracks closure. The results from both tests showed that the elastomers lost their sealing integrity, and a leak was propagated intensively within a few seconds after the setup pressurization. Figure 5.15 (a) and (b) demonstrate the EPDM failed the pressure tests after CO_2 degradation. After 5 minutes of the setup pressurization, Figure 5.15 (a) shows an almost instantaneous pressure decline at the rates of 8 psig/second for the 40 psig test, 6 psig/second for the 30 psig test, 4 psig/second for the 20 psig test, and 2 psig/second for 10 psig test. It is evident that, as the injection pressure increases, the decline rate also increases. This trend is reflected and supported by Figure 5.15 (b) which shows that as pressure increases, the first bubble leak time decreases. In this context, the first bubble time was determined from the start of the gas injection until the first bubble seen on the water column placed on top of the upper elastomer. Figure 5.16 (a) and (b) show that increasing the torque had minor to no effect on averting the leak pathways. The same instantaneous pressure decline rates were reported for all the tests conducted at 180 in-lbf. The effect of torque may have been slightly observed as the first

bubble time of 10 psig pressure test, shown in Figure 5.16 (b), was later than the first bubble of 10 psig pressure test, shown in Figure 5.16 (b). However, variation (0.017 seconds) is very small, in addition to the small pressure at which this variation was reported. Overall, the results from these pressure tests confirm the detrimental effect of CO_2 degradation on elastomers' performance, which many researchers have concluded.

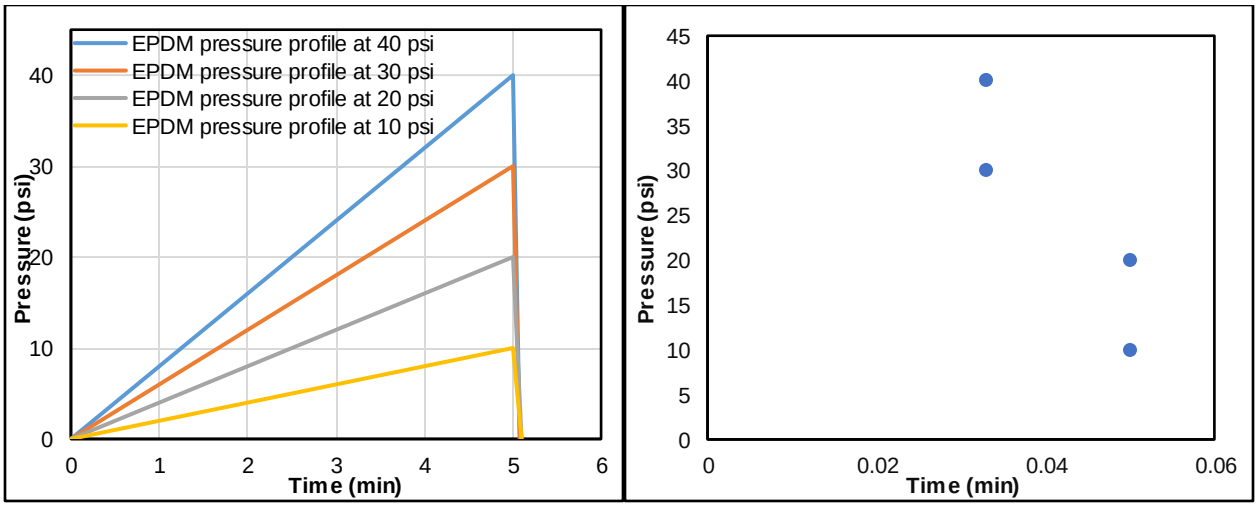

(a) **(b)**

Figure 5.15: EPDM pressure tests (a) and first bubble times (b) after CO_2 degradation with no torque

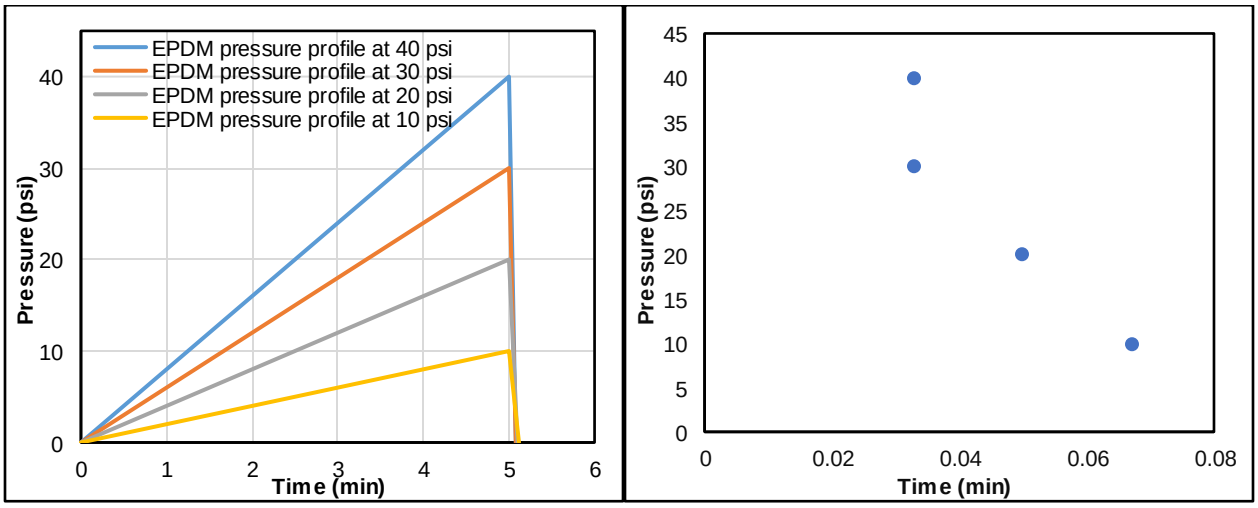

(a) **(b)**

Figure 5.16: EPDM pressure tests (a) and first bubble times (b) after CO2 degradation with 180 in-lbf

5.1.3 Pressure Test After Physical (Mechanical Defect)

Seal integrity is most likely compromising according to the physical/mechanical defects or surface imperfections that may arise from manufacturing, handling, and/or installation. To replicate seals mechanical failure, in this scenario, seams/grooves were intentionally created on the surface of the elastomers (shown in Figure 4.12) to assess their performance.

5.1.3.1 EPDM Pressure Test for 30 Minutes

In this scenario, the elastomers were torqued up to 180 in-lbf, and the pressure tests were performed at 10, 20, 30, and 40 psig to show the relationship between pressure and the leak intensity at a constant energization. The first test was conducted at a low pressure (10 psig), and the pressure profile was plotted in Figure 5.17 (a). The pressure decline implies that the seals failed to hold the pressure because the artificial seams compromised their sealing integrity. The test was repeated at 20, 30, and 40 psig as shown in Figure 5.17. The figure reveals that the pressure decline is more obvious as pressure increases. Reported pressure decline rates were 0.018 psig/sec for the 40 psig test, 0.014 psig/sec for the 30 psig test, 0.0094 psig/sec for the 20 psig test, and 0.0005 psig/sec for 10 psig test. Figure 5.17 (b) shows the time of the first bubble leak which was approximately 12 seconds into the 40-psig test. This figure also validates the evident pressure decline with an increase in pressure (Figure 5.17 a), because the first bubble leak time (Figure 5.17 b) increases as pressure decreases. From these tests, it could be concluded that a kick can breach the defective liner hanger seal assembly very quickly, and in a few seconds, can reach the wellhead.

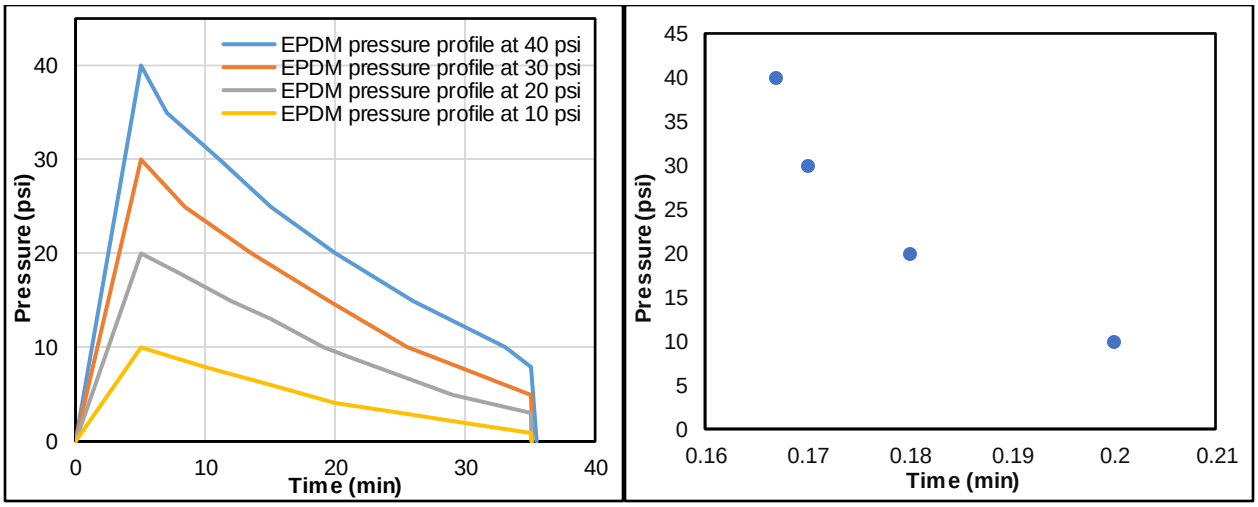

(a) **(b)**

Figure 5.17: EPDM pressure tests (a) and first bubble leak times (b) after physical defects

5.2 Results from Elastomers and Cement (Dual Barrier System) Tests

In this section, the results of three experimental scenarios are presented to describe the performance of a dual barrier system consisting of faulty EPDM elastomers and Class H cement. The aim was to determine whether the cement sheath can act as a primary barrier, in the event that elastomeric element of the liner hanger in a defective mode. The tests were performed at different pressures (10, 20, 30, and 40 psi) and different WOC/curing intervals (12 hours, 24 hours, 48 hours, 72 hours, 5 days, and 7 days). Details of the results of each test scenario are discussed in the following subsections.

5.2.1 Faulty Elastomer and Neat Class H Cement

The dual barrier system was established after faulty elastomers were inserted at the bottom of the annulus in the setup and neat Class H cement with a density of 16.5 ppg (pound per gallon) was placed above the elastomers. The faulty elastomers were intentionally installed to allow the nitrogen flowing to across them and then permeate the cement column.

Pressure Tests After 12 Hours WOC

12 hours after cement placement (WOC), a 10 psi pressure test was performed. The test revealed that the interfacial bonding strength at the cement-acrylic pipe walls (inner and outer) was insufficient. This conclusion was inferred by the intensive leaks seen at several points on the bonded interfaces. Only three leak points were seen inside the bulk cement, which appeared in forms of micro-channels. At the end of the test period (30 minutes), a pressure drop of 5 psi was recorded. Then the test was repeated for 20, 30, and 40 psi. The results of these tests demonstrated that the higher the pressure, the more pressure decreases were reported as shown in Figure 5.18 (a). A notable event that occurred during the 40-psi test was the upward movement of the cement column (see Figure 5.19). The movement happened during the first five minutes of the test. The cement movement reflected a weak bonding strength. Figure 5.18 (a) shows that the pressure drop at 30 and 40 psi was almost instantaneous with an approximately 100% pressure decline within 5 to 6 minutes. In fact, the debonding at casing-cement-formation interfaces can create micro-annulus which significantly amplifies the stresses magnitudes. As a result, the cement may be damaged mechanically in response to the stresses over inducement.

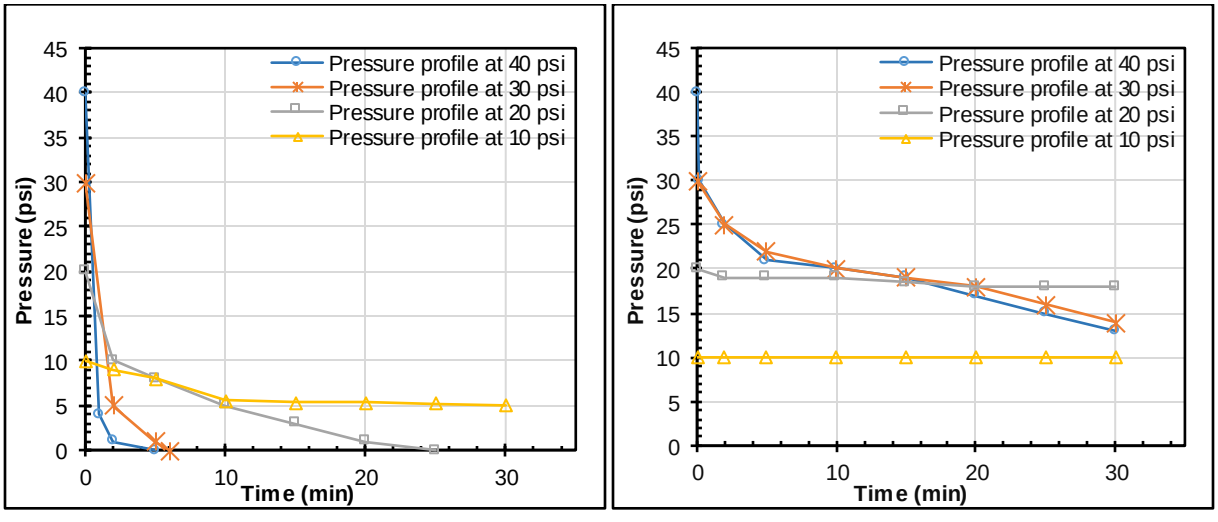

(a) **(b)**

Figure 5.18: Faulty EPDM and neat Class H cement pressure decline after 12 hours WOC (a) and after 24 hours WOC (b)

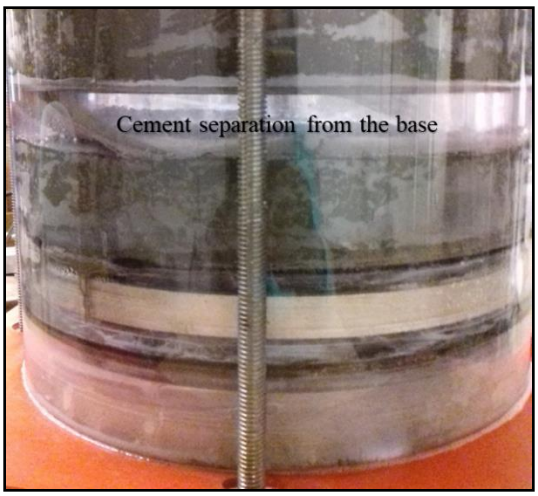

Figure 5.19: Cement separation during the 40-psi pressure test

Pressure Tests After 24 Hours WOC

Figure 5.18 (b) shows the pressure decline curves of the pressure tests performed after 24 hours of WOC. Obviously, at 10 psi test, the cement prevented the gas migration, and there was no leak observed. In the 20-psi test, no leak was observed, however, two stages of 1-psi decline each were reported at 2 minutes and 18 minutes, respectively. The cement held 18 psi to the end of the test. In 30 and 40 psi tests, the pressure decline was obvious, revealing the reduced performance of the dual barrier system. Over the test duration, the 30-psi test showed a 53.3% decrease in pressure while the 40-psi test showed a 67.5% decrease in pressure. It is important to point out that increasing the WOC time is important for improving the cement sealability.

Pressure Tests After 48 Hours and 72 Hours WOC

Pressure tests were repeated after 48 and 72 hours WOC. Figure 5.20 (a) shows pressure profiles after 48 hours of WOC. The 10 psi test had no leaks, while 20 psi test had 1 psi pressure drop. In the tests of the 30 and 40 psi, a significant decrease in the pressure was observed during the first five minutes. After that, a transient pressure drop was observed until the end of the test period. The improvement in the cement sealability was verified by the pressure reduction in the 30 and 40 psi

pressure tests. The 30-psi test had a 36.7% pressure decline while the 40-psi test had a 52.5% pressure decline over 30 minutes.

Figure 5.20 (b) shows the results of 72 hours of WOC tests. The 10 and 20 psi tests showed no leaks, confirming the system's sealability at these pressures. A sharp decrease within 5 minutes was observed with a transient drop between 5 and 20 minutes, and no pressure drop between 20 and 30 minutes in the 30 and 40 psi tests. The total pressure decreases were 33.3% and 50% for 30 and 40 psi tests, respectively. The pressure drop was improved, which means the sealability of the dual barrier (cement in particular) was enhanced with increased WOC intervals. Despite this improvement, cement cannot be identified as a primary barrier according to leaks and pressure declines at these relatively high pressures (30 and 40 psi).

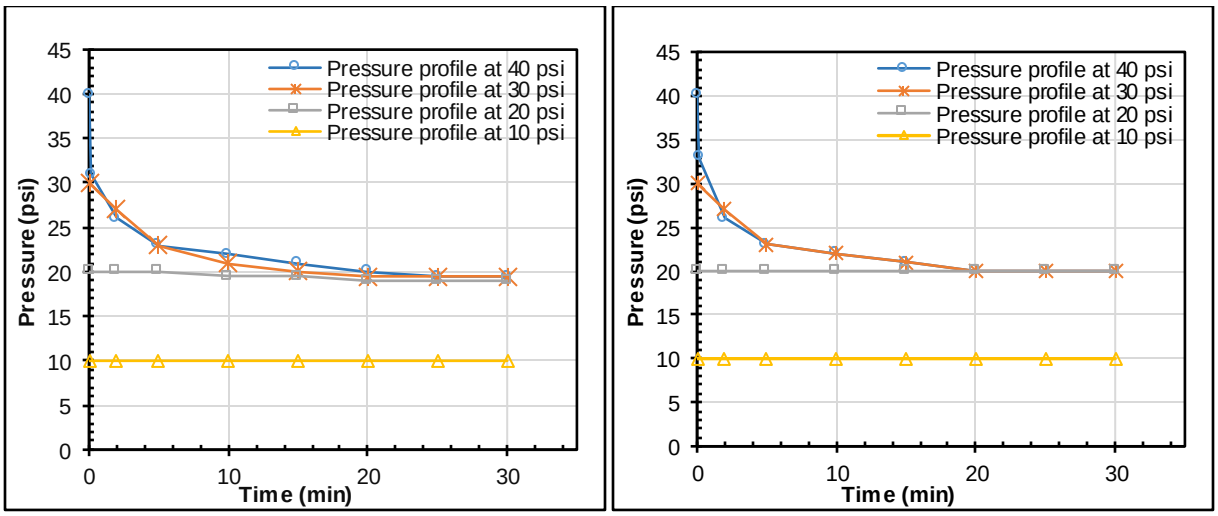

(a) (b)

Figure 5.20: Faulty EPDM and neat Class H cement pressure decline after 48 hours WOC(a) and after 72 hours WOC (b)

Pressure Tests After 5 and 7 Days WOC

Additional pressure tests were performed after 5 and 7 days WOC. After 5 days, the cement sheath is tightly sealed during the pressure tests of 10 and 20 psi, and no leakage was observed. However, gas bubbles were seen within 5 minutes, and a gradual decrease in pressure after this time was observed in the 30 and 40 psi tests as shown in Figure 5.21 (a). The last set of tests was performed

7 days after WOC. The test results are depicted in Figure 5.21 (b). Obviously, a pressure decline was not recorded in the 10 and 20 psi tests. However, pressure drops of 16.67 % and 40 % were recorded during the 30 and 40 psi tests, respectively. The conclusions from these tests showed that as the WOC time increases, the cement sealability improves. However, neat Class H cement cannot function as a primary barrier under the test conditions mentioned herein.

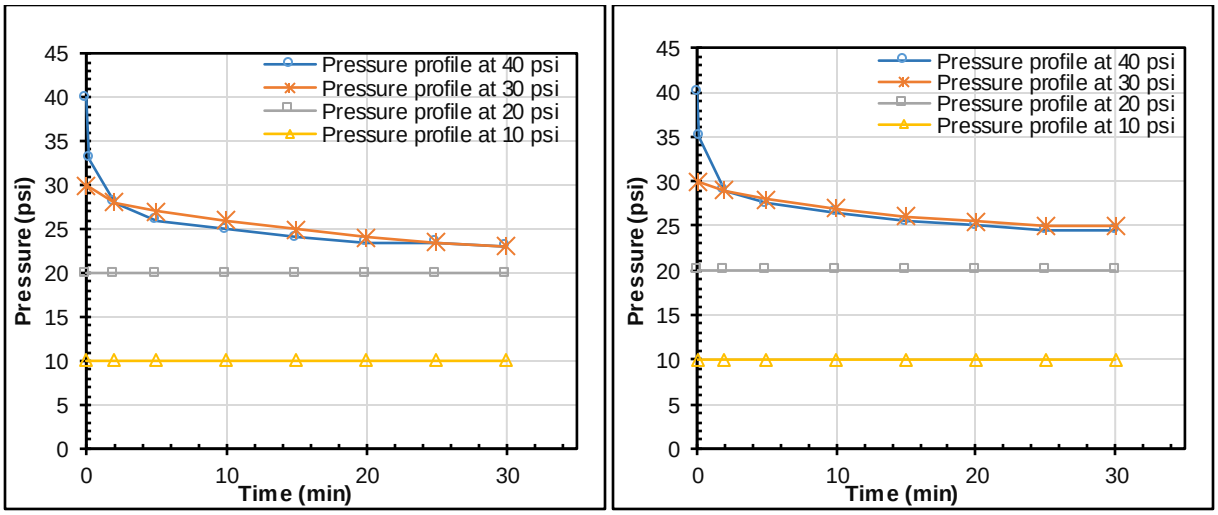

(a) **(b)**

Figure 5.21: Faulty EPDM and neat Class H cement pressure decline after 5 days WOC (a) and after 7 days WOC (b)

5.2.2 Faulty Elastomer and Commercial Gas Migration Additive

This experiment mainly focuses on assessing the effect of the anti-gas migration additives on the cement performance. To create this scenario, faulty EPDM elastomers, and Class H cement mixed with a commercial gas migration additive (slurry density 16.6 ppg) were tested as a dual barrier system. Several pressure tests were conducted after 12 hours, 24 hours, 48 hours, 72 hours, 5 days, and 7 days WOC to study the cement behavior during its transition from a slurry to early gelation and to a hardened cement. During this critical transition, cement sealability is most likely to be kicked by migrated gases.

Pressure Tests After 12 Hours WOC

A pressure test was performed at 10 psi after 12 hours (WOC). Just 55 seconds after the start of the test, a high-intensity leak was observed at the inner acrylic piper-cement-outer acrylic pipe interfaces. The leak is more intensive at the inner pipe-cement interface. The leak was attributed to the severe de-bonding caused by the smooth surface of the acrylic pipe, lacking sufficient roughness required to bond the cement with the pipes. Following the first 30 minutes injection time, the gas supply valve was shut-in, and a gradual pressure decline was observed during the next 30 minutes holding time. It was noted that no leak was seen within the cement matrix. Then, the test was repeated after the pressure was raised to 20 psi. After about 5 minutes from the beginning of the test, the cement sheath moved (separated) in a manner similar to the separation shown in Figure 5.19. As a result of this separation, the leak intensity was increased significantly because the bonding of cement and pipes became weaker. After this test, two tests were conducted at 30 and 40 psi. The leak intensity increased considerably, particularly at the inner pipe-cement interface. The pressure profiles from these three tests were shown in Figure 5.22 (a). It is obvious that the pressure dropped significantly over the holding period. In these tests, cement defects (cracks, fractures, voids) were not seen, and leak channels through the cement sheath were not reported.

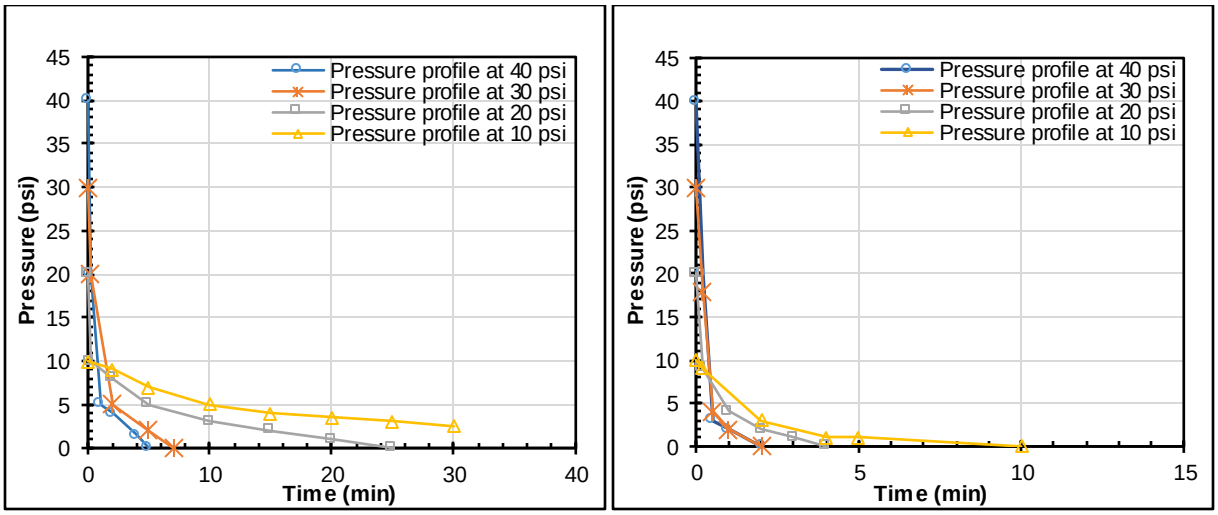

Figure 5.22: Faulty EPDM and Class H cement with gas migration additive pressure decline after 12 hours WOC (a) and after 24 hours WOC (b)

Pressure Tests After 24 Hours WOC

Pressure tests at 10, 20, 30, and 40 psi were repeated after 24 hours of WOC. The leak intensity was increased because of the cement separation and movement that occurred after 12 hours of WOC and during the 20-psi pressure test. The cement separation and movement worsened the bonding at the cement-pipes interface. The bond at the cement-inner pipe was more impacted by the separation than the cement-outer pipe. This observation was supported by many leak locations that appeared at the cement- inner pipe interface. However, fewer locations were observed at the cement-outer pipe interface as illustrated in Figure 5.23. In all the tests, the pressures dropped suddenly within the first minute of holding times by 50%, 80%, 94%, and 95% for 10, 20, 30 and 40 psi respective pressure tests (Figure 5.22 (b)). It is important to note that increasing the WOC time improved the bonding strength between the outer pipe and the cement sheath, especially for the 10 and 20 psi tests. However, it did not improve the bonding strength at of cement- inner pipe interface.

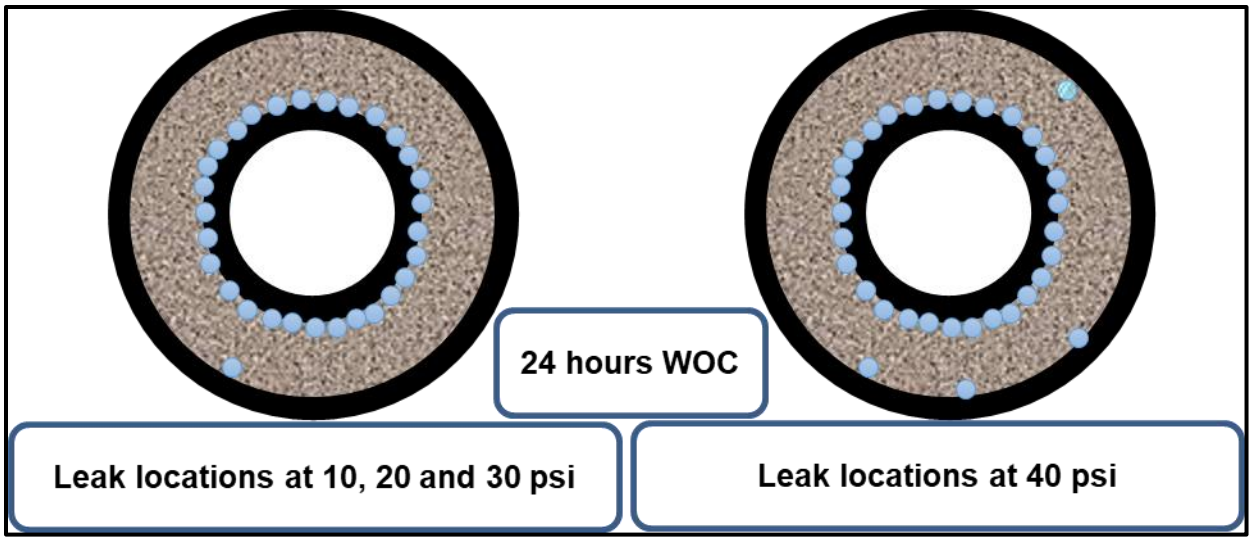

Figure 5.23: Leak locations during pressure tests after 24 hours WOC

Pressure Tests After 48 Hours and 72 Hours WOC

The pressure tests were performed after 48 and 72 hours WOC. The leak intensity between the inner pipe and cement sheath was almost the same as in the pressure tests after 24 hours WOC, except for an increase in the size of the bubbles. No leak between the outer pipe and cement was observed during the 10 and 20 psi tests. However, one leak position was seen during the 30-psi test, and four positions appeared during the 40-psi test (same positions during the test after 24 hours WOC).

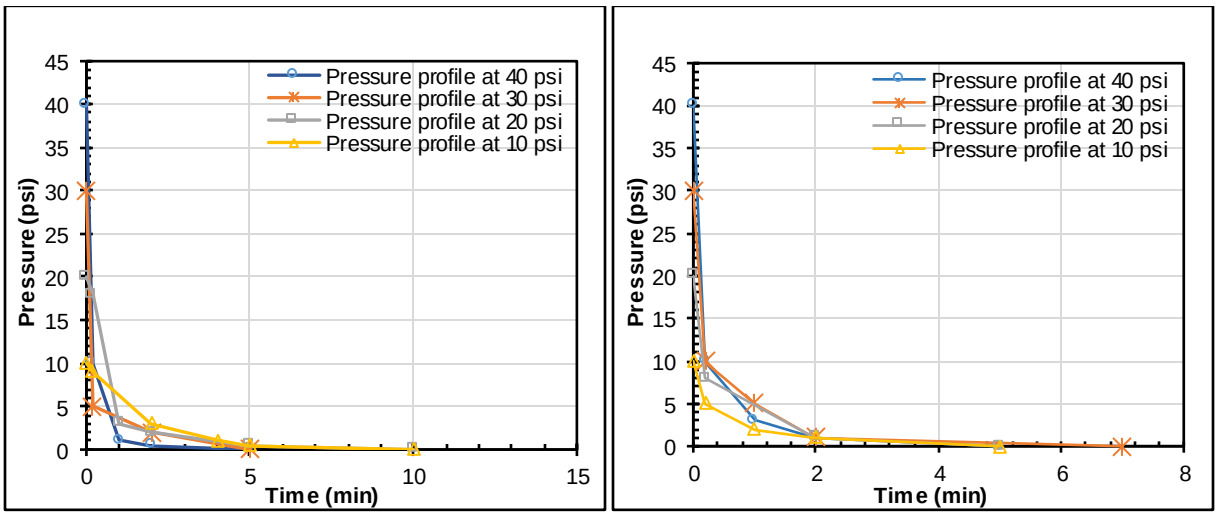

(a) **(b)**

Figure 5.24: Faulty EPDM and Class H cement with the commercial gas migration additive pressure decline after 48 hours WOC (a) and after 72 hours WOC (b)

After 48 hours of WOC, the pressure declined abruptly after one minute of the holding time by 50%, 85%, 90%, and 97.5% for the pressure tests of 10, 20, 30 and 40 psi respectively (Figure 5.24 (a)). It was noted that the pressure decline rates were higher compared to the rates after 24 hours of WOC. This could be attributed to more de-bonding issues that occurred at the inner pipe-cement interface as WOC progressed.

The tests were repeated after 72 hours of WOC. The pressure decline profiles were observed to be similar to those reported after 48 hours WOC as shown in Figure 5.24(b). In all the tests, the leak pathways were created at the inner pipe-cement interface. Leak pathways at the outer pipe-cement were not seen during the 10 and 20 psi tests. However, new leak positions appeared during the 30 and 40 psi tests as shown in Figure 5.25.

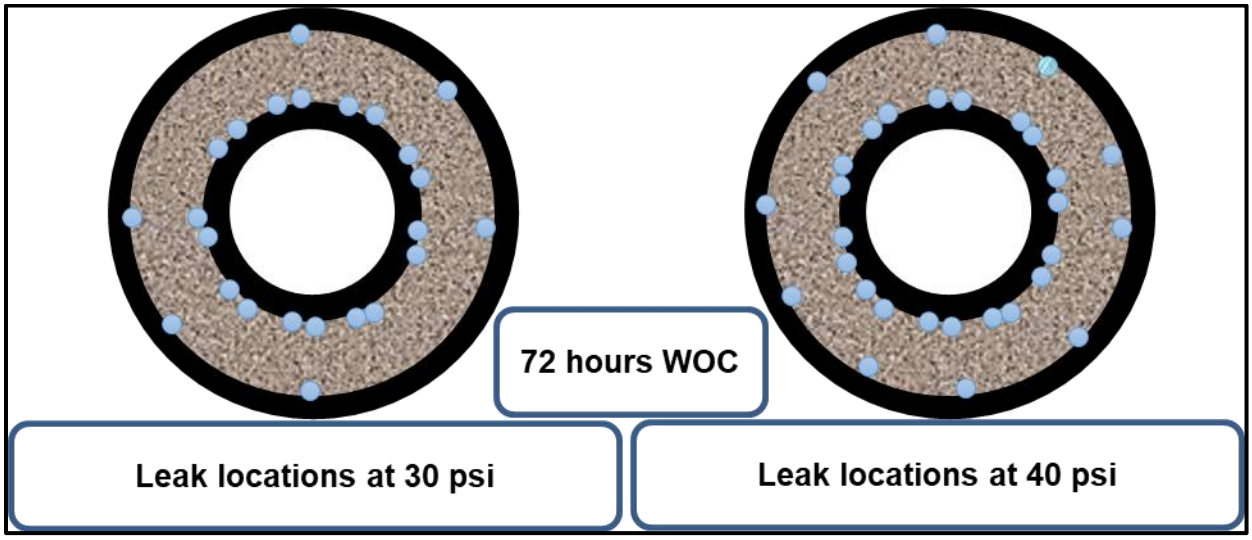

Figure 5.25: Leak locations during pressure tests after 72 hours WOC

Pressure Tests After 5 and 7 Days WOC

After 5 and 7 days of WOC, pressure tests were performed to assess the cement sheath performance. During the tests after both WOC days, the leak rates at the inner pipe-cement

interface increased slightly compared to 72 hours WOC. However, during the 30 and 40 psi tests, the leak rates at the outer pipe-cement decreased slightly compared to the tests after 72 WOC. A leak was not reported at 10 and 20 psi. The pressure-decline curves after 5 and 7 days WOC were shown in Figure 5.26 (a) and (b). For the two WOC intervals, the pressure declines were sudden, almost within the first minute of the holding time. The pressure declines were 85%, 92.5 %, 94%, and 95% for the respective pressure tests of 10, 20, 30 and 40 psi.

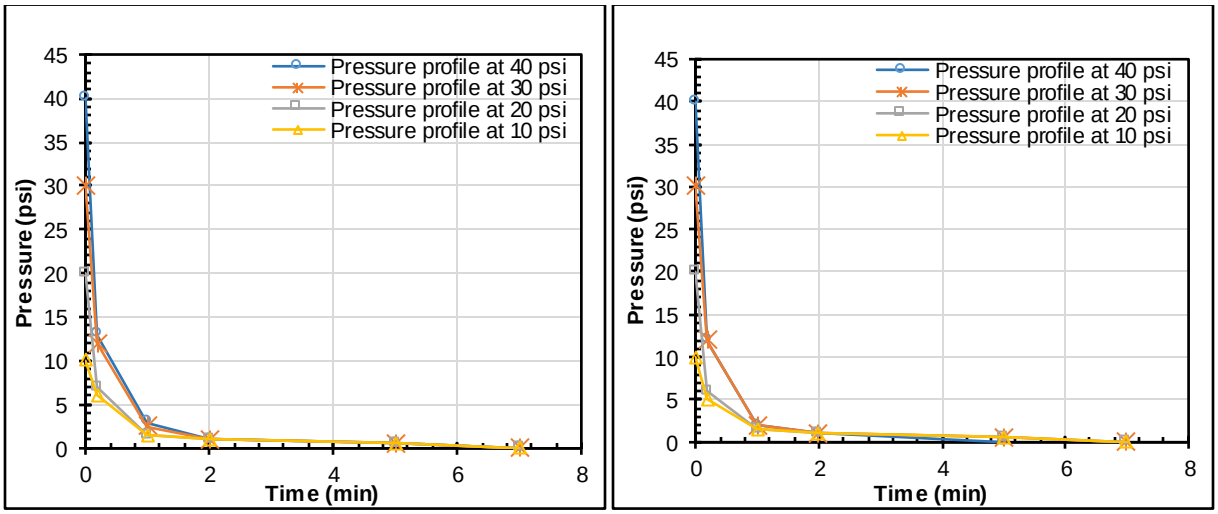

(a) **(b)**

Figure 5.26: Faulty EPDM and Class H cement with gas migration additive pressure decline after 5 days WOC (a) and after 7 days WOC (b)

5.2.3 Faulty Elastomer and Commercial Gas Additive Cement (Setup with Inner Steel Pipe and Outer Acrylic Pipe)

Pressure Tests After 12 hours WOC

In this scenario, the inner acrylic pipe was replaced with a steel pipe to investigate the effect of the pipe material on the cement sealability. Then, a pressure test at 10 psi was conducted after 12 hours of WOC. After 15 seconds from the start of the test, a high-intensity leak was seen at the cement-outer acrylic pipe interface. However, a leak did not exist within the cement matrix, and at the cement-inner steel pipe interface as shown in Figure 5.27. It can be inferred that there was severe

de-bonding between the cement sheath and outer acrylic pipe walls. The leak appears at the cement-acrylic pipe interface that occurred due to the de-bonding resulted from the smooth surface of the acrylic pipe. To support the bond strength between the cement and the outer pipe, four band clamps were tightened firmly around the outer pipe to prevent the pipe expansion during the cement pouring. However, this process did not strengthen the bond as proved by the gas leak at the cement-pipe interface. Then the test was repeated at 20 psi, and the leak was not seen at the inner steel pipe-cement interface. The leak absence was also recorded at 30 and 40 psi pressure test. This observation indicates the bonding strength improvement at the cement-inner steel pipe. The profiles of the four tests were shown, in Figure 5.28 (a). The pressures significant decline was linked to the sever de-bonding at the cement- outer acrylic pipe de-bonding, hence cement defects were not observed.

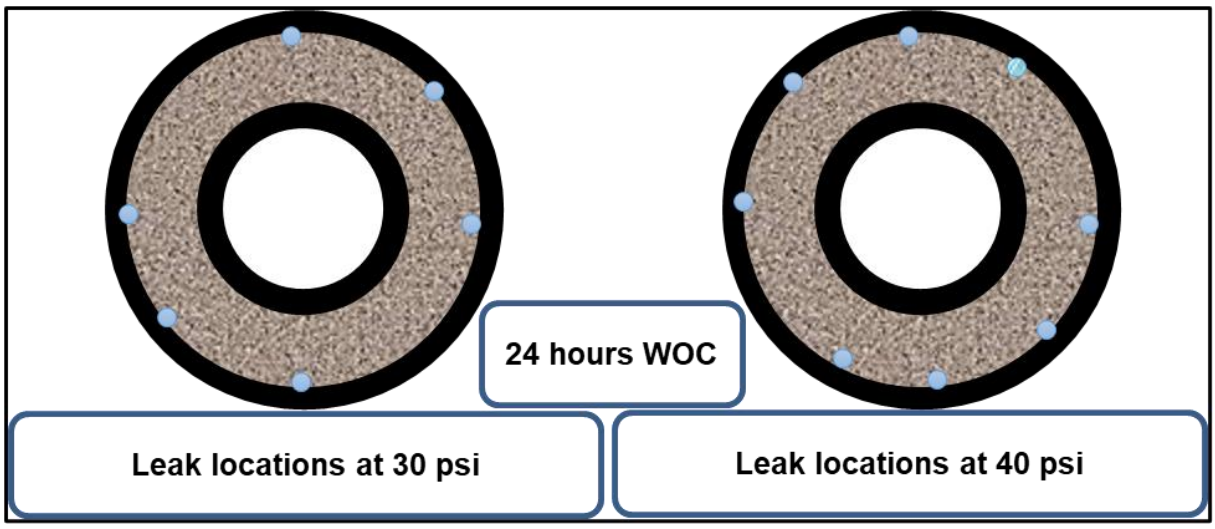

Figure 5.27: Leak locations during pressure tests after 24 hours WOC

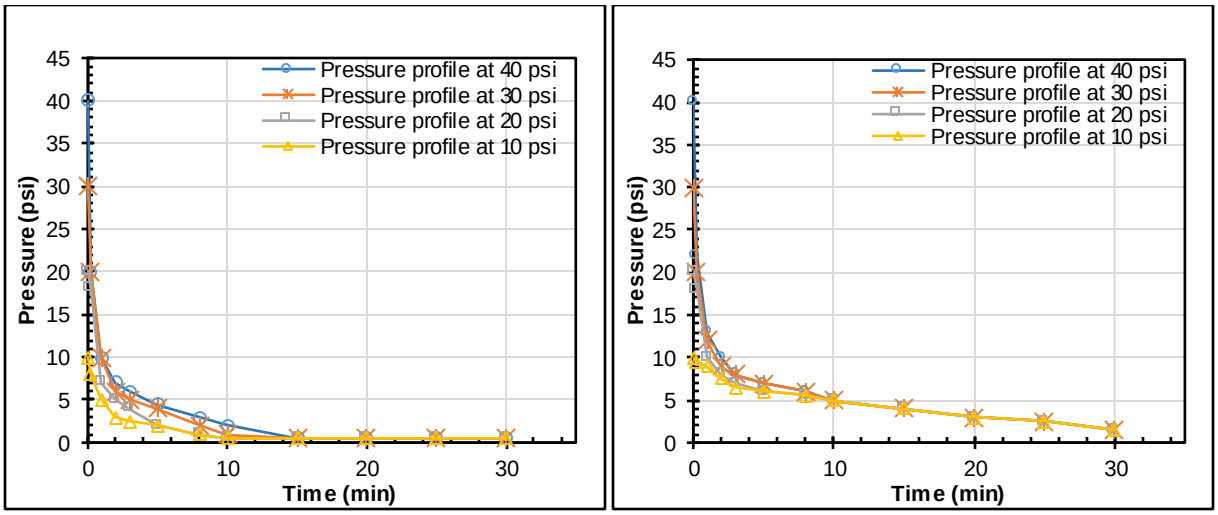

(a) **(b)**

Figure 5.28: Faulty EPDM and Class H cement with the commercial gas migration additive (setup with inner steel pipe and outer acrylic pipe). Pressure decline after 12 hours WOC (a) and after 24 hours WOC (b)

Pressure Tests After 24 Hours WOC

Pressure tests at 10, 20, 30, and 40 psi were repeated after 24 hours of WOC. Leak intensity decreased slightly compared to the intensity after 12 hours WOC. This observation was supported by the slight improvement of the pressure declines during the holding periods. In all the tests, the pressures showed a sudden drop in the first minute of the holding time by 40%, 70%, 76%, and 82% for 10, 20, 30, and 40 psi pressure tests, respectively. Then the pressures continued to gradually decrease until the end of the tests as shown in Figure 5.28 (b).

Pressure Tests After 48 Hours and 72 Hours WOC

Pressure tests were performed 48 and 72 hours after WOC. The leak intensity at the cement-outer pipe interface was almost same as in the pressure tests after 24 hours WOC. No leak between the cement-inner steel pipe interface was seen for all the tests after both WOC times. Figure 5.29 (a) shows that after 48 hours WOC, the pressure decreased rapidly after five minutes by 40%, 70%,

76%, and 82% for the pressure tests of 10, 20, 30 and 40 psi, respectively. The drop after five minutes holding time was lower, compared to the drop after 24 hours WOC. This can be related to the improvement in bonding between the pipes and cement sheath as the WOC time increases. After 72 hours WOC, the tests were repeated, and the pressure drop trends were similar to those reported at the tests after 48 hours WOC (see Figure 5.29 (b)). In all the tests, all the leak paths and positions were located at the cement-outer acrylic pipe and interface.

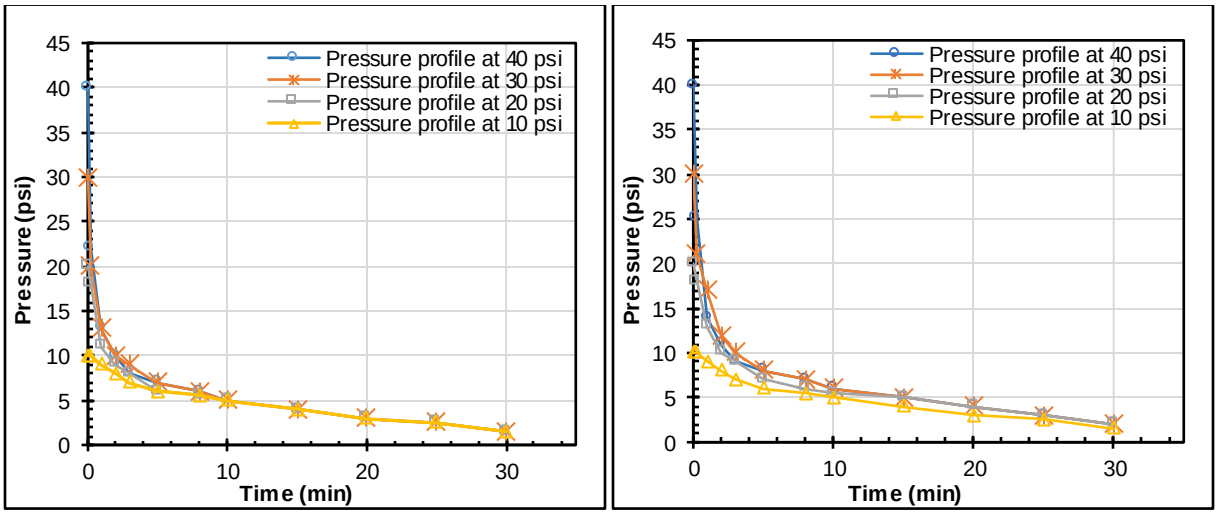

(a) **(b)**

Figure 5.29: Faulty EPDM and Class H cement with the commercial gas migration additive (setup with inner steel pipe and outer acrylic pipe). Pressure decline after 48 hours WOC (a) and after 72 hours WOC (b)

Pressure Tests After 5 and 7 Days WOC

After 5 and 7 days WOC, pressure tests were conducted to evaluate the cement sealability. During the tests after both WOC days, the leak intensity between the outer acrylic pipe and the cement appeared to have reduced slightly, compared to the test after 72 hours WOC. No leaks were observed within the cement sheath or between the inner steel pipe and cement sheath. During the tests after 5 and 7 days WOC, the pressure declines were sudden (within the first five minutes of

the holding time). After 5 days WOC, a 30%, 65%, 73%, and 80% decline for the respective pressure tests of 10, 20, 30 and 40 psi were recorded (see Figure 5.30 (a)). After 7 days WOC, a 25%, 60%, 70%, and 77.5% decline for the respective pressure tests of 10, 20, 30 and 40 psi were recorded (see Figure 5.30 (b)). The pressure declines after 7 days WOC was slight lower than the declines after 5 days WOC.

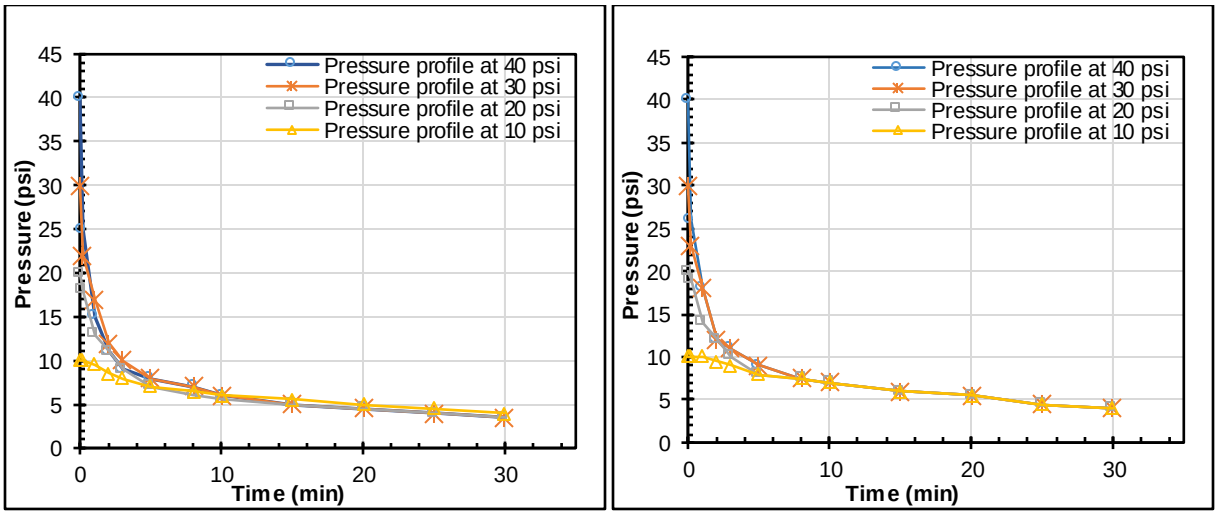

(a) **(b)**

Figure 5.30: Faulty EPDM and Class H cement with gas migration additive (setup with inner steel pipe and outer acrylic pipe). Pressure decline after 5 days WOC (a) and after 7 days WOC (b)

Chapter 6: Numerical Modeling of Liner Dual Barrier System

6.1 Numerical Modeling of Liner Hanger Elastomer Seal Assembly

6.1.1 Review of Previous Modeling Studies

There are very limited studies of numerical modeling in the current literature that have been developed exclusively to determine the contact stress (sealability) of the elastomeric materials encompassed in the seal assemblies of the liner hanger systems. Pervez et al. (2007) created a finite element model (FEM) to simulate the expansion of a horizontally solid expandable tubular that incorporates elastomer seals. This type of tubular is commonly used to isolate an open-hole in the horizontal wells. The model was developed to investigate the effect of the mandrel cone angle, tubular expansion ratio, rubber thickness, and the friction coefficient on the drawing (extrusion) force, tubular thickness, length, and surplus deformation. The simulation results were used as a guide for selecting the appropriate expansion tools and for predicting the extrusion force needed for tubular expansion to prevent any potential failure that might be encountered during the liner set.

Alzebdeh et al. (2010) presented a 2D FEA to model the elastomers' behavior when deformed to seal the open hole of a wellbore. The simulation was considered the main parameters that significantly influence the elastomers sealability. The evaluated parameters are compression ratio, seal length, seal thickness, and shear resistance at the seal-formation interface. The authors concluded that to prevent leakage from high-pressure permeable formations, a thick seal with high compression would be a viable solution for the open-hole zonal isolation. Al-Hiddabi et al. (2015) developed 2D analytical model of expandable tubular for evaluating contact stress (deformation) of elastomeric seal confined between two concentric casing strings or confined between metal tube and formation. The authors demonstrated that elastomeric seal assembly of the liner hanger can

successfully prevent fluids leakage and communication as long as its maximum internal pressure is higher than the fluid pressure acting axially at both ends of the seal boundaries.

Patel et al. (2019b) performed numerical sensitivity parametric analysis to identify the critical seal design parameters in a conventional hanger. The authors used a 3D FEA model. The study developed some guidelines to compare the performance of four most common types of elastomers used in the wellbore barrier systems. The performance of elastomers was evaluated based on the sensitivity of the contact stress (pressure) to the critical factors affecting the elastomers' sealability. The most prevalent influencing factors were found seal annular fit, amount of energization, compression ratio, elastic modulus, and Poisson's ratio. The authors claimed that the elastomers' performance was very sensitive to annular fit (i.e. radial width of seal relative to annular space), followed by Poisson's ratio and elastic modulus, respectively. Patel and Salehi (2019a) developed a 3D FEM to investigate the implications of elastomer seal energization in mechanical and expandable liner hanger assemblies using fluorocarbon (FKM/Viton) elastomer as a reference material for the study, and to compare the performance of the seal assemblies of the mechanical and expandable liner hangers. The seal performance/quality was evaluated in terms of contact stress values and profile distributed at the seal-pipe/liner interface. The authors concluded that expandable liner energization/setting is more robust to failure in the supporting components than the conventional liner.

6.1.2 Parameters Influencing Contact Pressure

Screening review on current literature (Al-Hiddabi et al. 2015, Walker 2017; Patel et al. 2019a;) showed that the elastomer contact pressure basically depends on the following parameters:

- Material properties, such as elastic modulus, Poisson's ratio, or hyper-elastic material parameters

- Amount of seal compression (compression ratio/displacement) and energization/setting procedure
- Seal, thickness, length, and configuration/shape
- Contact formulation parameters (e.g. friction coefficient, type of bonding, mesh type)
- Boundary conditions (e.g. force direction, type of support)

The most essential mechanical properties necessary for modeling and simulation are elastic (Young's) modulus and Poisson's ratio. In most solids (e.g. steel, rock), the Poisson's ratio is about a third. However, for rubbers, it is close to 0.5 (Williford et al. 1999; Lakes 1993). Seal compression is an important indicator for its expansion to fill identified gaps and can be mathematically expressed in terms of compression ratio (Alzebdeh et al. 2010; Al-Hiddabi et al. 2015) as shown in equation (1).

$$\text{compression ratio (CR)} = \frac{\text{change in seal height due to compression}}{\text{original seal height}} \times 100\% \quad \ldots\ldots (1)$$

Patel and Salehi 2019a demonstrated that the seal energization method also has a significant role in the elastomer's sealability. The authors claimed that the energization of the expandable seal yields higher contact pressure than the energization of the conventional seal at the same amount of volumetric compression. The friction coefficient between seal and pipe is most likely to influence the contact stress (Patel and Salehi 2019; Ma et al. 2014). Ma et al. (2014) claimed that reducing the frictional coefficient of the rubber can improve the working range of the maximum contact pressure, thus enhancing the rubber protection.

6.1.3 Finite Element Model of Seal Assembly

This section describes the modeling and simulation steps used to evaluate and compare the performance of EPDM and NBR elastomers incorporated in liner hanger seal assemblies. The seal performance was evaluated at various energization scenarios, friction coefficient, and chemical swelling. Finite Element Analysis (FEA) was performed using a two-dimensional model consisting of inner and outer pipes, three aluminum rings, and two elastomers seal as shown in Figure 6.1. The model was created using ANSYS software. The values of elastic modulus and Poisson's ratio of each component of the model are presented in Table 6:1. The model was developed based on a conventional liner hanger system to replicate the actual casing program of a well drilled in the Gulf of Mexico (Figure 1.3). The well shallow section was completed by an 18 5/8 in. surface liner, and a 22 in. conductor casing as shown in Figure 1.3. However, the casing and liner were downsized to 10 in. and 8 in. respectively. The length of the model was kept long enough (36 in) to avoid the end effect and convergence issues. The experimental setup used is similar to the model components and dimensions. The description of the setup is already discussed in Sec 4.2. The experimental results were used to validate the model as presented in Sec 7.1.3. Small elastomer specimen was subjected to a preliminary compression test, as shown in Figure 6.2. The goal of this test was to predict the force values and their corresponding compressions (displacements) that are need for modeling and experimental works.

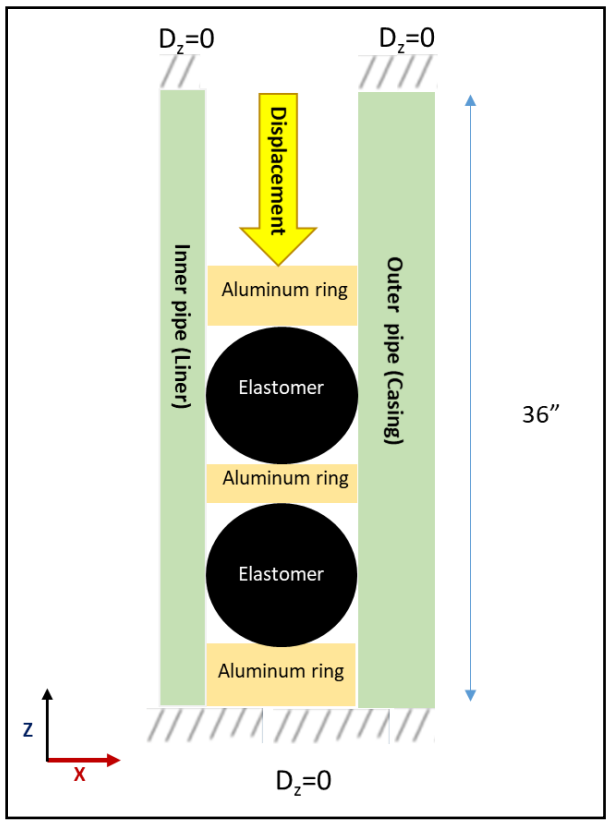

Figure 6.1: Model boundary conditions

Figure 6.2: Elastomer displacement measurement using compression machine and paper scale

In the model, the displacement function was activated to apply a vertical load in Z-direction and perpendicular to the upper support aluminum ring to energize the seals as shown in (Figure 6.1). This method simulates seal energization in actual conventional liner hanger seal assembly in which the drill pipe is used to apply an axial force to set the liner. Seal performance was determined based on the contact pressure generated at the seal-pipe interface. The contact pressure of EPDM and NBR elastomers were evaluated at different amounts of seal energization represented by varying displacements (0.5, 1, 1.5, 2, and 2.5 mm). As boundary conditions, both pipes ends are held fixed along Y-axis (Figure 6.1). Pilot simulations at different mesh sizes were run to ensure that the mesh size does not affect the simulation accuracy, and the values of the contact pressure are independent from the mesh size. The contact pressure has a consistent trend at the selected mesh size range as shown in Figure 6.3. The contact pressure predicted by the FEA model was compared with two different analytical calculations of contact pressure. The accuracy of the model used in this study ranged from 1% to 5%.

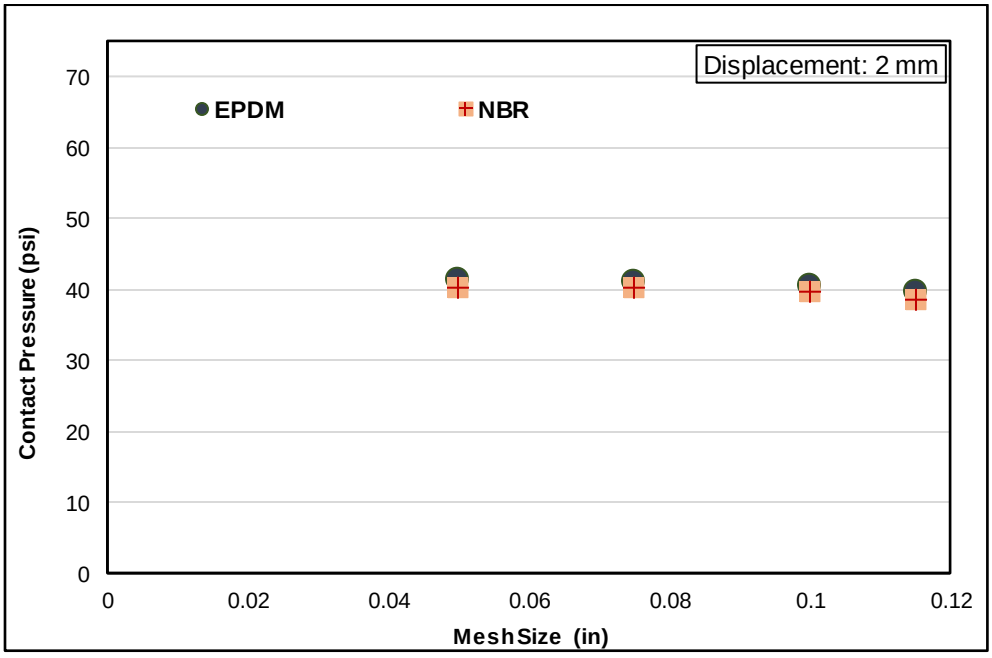

Figure 6.3: Pilot simulations to assess the effect of the mesh size on contact pressure

Table 6:1: Material properties used for the model

Elastomer	Elastic Modulus (E), psi	Poisson's Ratio (ν)
EPDM	277 psi	0.49
NBR	268 psi	0.49
Cast Acrylic Pipe	0.4×10^6 psi	0.37
Steel Pipe	29×10^6 psi	0.3
Aluminum Ring	10.29×10^6 psi	0.33

To assess the effect of chemical swelling on the contact pressure of elastomers, two EPDM and NBR specimens (shown in Figure 6.4) were immersed in a surfactant for a week. The cord diameter of elastomers before swelling is 0.75 in. The cord was increased after the swelling period, and the new cord measures were taken at three successive days in order to monitor their recovery rate as shown in Figure 7.5. The values of the cord readings after three days of recovery were used as model simulations input data to evaluate the impact of swelling on the performance of the seal assembly.

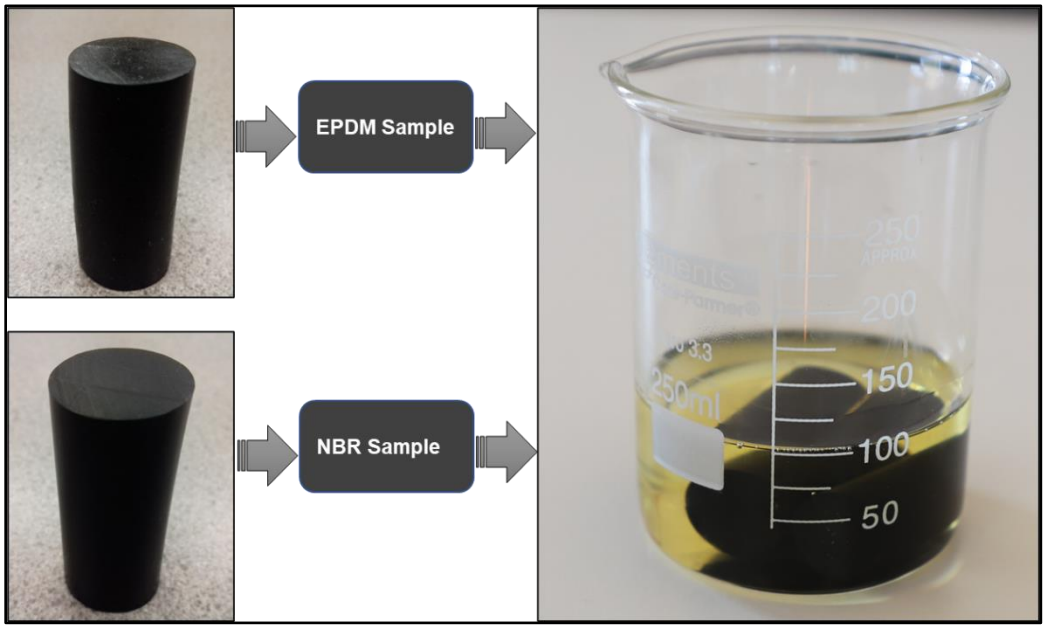

(a) (b)

Figure 6.4: EPDM and NBR elastomers specimens used for swelling study (a), surfactant degradation(b)

The following assumption are made for elastomers' FEA:

- The model elastomeric rubbers were modeled as an isotropic linear elastic material with a constant elastic modulus and Poisson's ratio listed in Table 6:1
- The FEM is an isothermal, and the effect of thermal stresses on elastomers' sealability has not been investigated since the scope of the study mainly focuses on the offshore shallow liner dual barrier system. It is worth mentioning that the effect of temperature has been included in the form of change in material properties, specifically elastic modulus and Poisson's ratio because they are the most important input data needed for the model simulation
- The elastomers were subjected to uniform energization loads
- Frictionless contact at inner pipe-elastomers-outer pipe interfaces
- Zero penetration between the rubber and the pipes

6.2 Numerical Modeling of Dual Barrier System

6.2.1 Review of Previous Cement Modeling

There are limited numerical modeling studies in the literature devoted to evaluating the set cement integrity. Bosma et al. (1999) developed FEM to predict the annular cement short-terms and long -terms integrity by modeling some critical cement failures such as cracks, debonding, and plastic deformation. The factors considered in the model are - borehole stability, cement/sealant formulation, loading scenarios, cement mechanical properties, rock mechanical properties, and thermal properties. The main simulations results revealed that the variations in stress levels in the cement were mainly due to either an increase or decrease of the downhole pressure and/or temperature. Cement failure is closely related to in-situ stress distribution and concentration. Excessive in-situ compressive stresses can lead to cement shear failure. Otherwise, tension is the

predominant failure mechanism. The author also stated that compressive strength cannot only be used to determine the cement type needed for zonal isolation. Other mechanical properties of cement, such as Young's modulus, Poisson's ratio, tensile strength, shear strength, and bonding strength, are also important to evaluate the performance of set cement.

Ravi et al. (2002) designed a procedure based on FEA to estimate the risk of cement failure. Simulated failure modes are cracking, debonding, and plastic deformation (shear). In addition, cement shrinkage and expansion. The failure was identified depending on the effect of the well loads, set cement characteristics, and formation properties. The author also demonstrated that the integrity of a set cement could be maintained by controlling its mechanical properties, the formation properties, and wellbore operating parameters.

James and Boukhelifa (2008) conducted a modeling study accompanied by a data analysis technique to determine the mechanical durability of a flexible cement system after aged for a year at a high temperature of 392°F, and for a period of six months at 482°F. The authors performed experimental and analytical work and to characterize the cement main mechanical properties/parameters, such as Young's modulus, Poisson's ratio, UCS, and tensile strength. These parameters were used as input data for modeling cement principal stresses and cement thermal stability. The authors concluded that the magnitudes of Young's modulus and Poisson's ratio did not depend on the confining stress. Gray et al. (2009) created staged numerical models to investigate cement debonding by modeling the casing-cement interface considering the complex nature at the interface of bonded materials. The considered conditions include stress state near the wellbore, e.g. triaxiality of stress, the plasticity of the rock and cement, the likelihood of bond failure, as well as the history of loading and deformation occurred over the life of the well. The

authors claimed that the wellbore integrity and failure mechanisms can be better identified in case the mentioned considerations are adopted in the numerical approaches.

De Andrade and Sangesland (2016) created a 2D numerical model to investigate the mechanisms of cement sheath failure regarding long-term of well integrity. The study focused on assessing the relevance of casing, cement, formation material properties, geometric parameters, and well-loading events, in contributing to the occurrence of cement sheath failure mechanisms. More consideration was given to assess thermal-related loading events that occurred into the wellbore casing-cement-formation interface due to the temperature variations. The authors concluded that, as wellbore temperature increases or decreases, cement sheath failures by shear and debonding become more sensitive to changes in cement Young's modulus rather than changes among the variations in the other properties evaluated. The authors also concluded that when wellbore temperature increases, the risk of cement damage by shear will also increase because the cement Poisson's ratio will decrease. Whereas the risk of inner debonding tends to decrease as the wellbore temperature decreases and cement Poisson's ratio increases. Ramos and Camus (2017) conducted a numerical simulation to evaluate the cement sheath integrity under reservoir conditions. In addition, the model also used to evaluate the effect of anisotropic stresses (creep, thermo-elasticity, and pore pressure). The authors demonstrated that creep is the dominant stress relaxation mechanism that consciously acts to stress the cement sheath mechanically during the cement solidification stage.

Patel and Salehi (2019b) created 3D FEA validated by analytical calculations to study the cement sheath structural integrity. The model utilized to identify the most critical parameters that might jeopardize the cement structural integrity. Parameters investigated are- cement mechanical properties, sheath dimensions, and wellbore pressure variations. The results of neat Class G cement

sensitivity responses to principal stresses (radial, hoop, and maximum shear) showed that wellbore pressure, cement material properties, and annulus pressure are the most parameters influencing cement mechanical stresses concentration depending on the type of stress. Among other failure modes, interfacial bond and radial cracking are the most dominant failure mechanisms. Patel et al. (2019c) performed FEA parametric analysis to investigate the possibility of a pre-stressed cement system (e.g. expanding cement) in sealing cement micro-annulus under various loading scenarios. The authors evaluated three neat Class G cement formulations ductile, moderately ductile, and brittle. Three dimensional model of casing, cement sheath and liner were created to investigate radial, hoop, and ultimate shear stresses at the liner-cement interface. The authors concluded that expanding cement can minimize the risk of failure because it elevated the tensile hoop stress over concentration. However, it generates higher radial and shear stresses than the conventional cement system.

It is evident that the scopes and objectives of most of the reviewed previous cement modeling studies focused on assessing of Class G cement integrity considering different influencing parameters. However, no study considered the effect of curing (wait-on-cement/WOC). Therefore, in this study, more emphasis was given to evaluate the performance of neat Class H cement considering critical parameters, such as the effect of WOC upon set cement mechanical properties (Young's modulus, Poisson's ratio, UCS, tensile strength, and shear bonding strength) under different pressure loading conditions. In this study, the cement performance evaluation was performed in terms of identifying potential risk of failure and identifying operation boundaries using finite element analysis (FEA) described in the following sections.

6.2.2 Finite Element Model of Liner Hanger Dual Barrier System

Assuming symmetry wellbore geometry, FEA was conducted using a two-dimensional axisymmetric model (shown in Figure 6.5(A)). The model components consist of inner and outer pipes, two aluminum rings, and one elastomer seal as shown in Figure 6.5 (B). The model components meshed in regular hexahedral shapes. Initial simulations at various mesh sizes were run to confirm that the mesh size did not affect the simulation accuracy. Normal Lagrange was selected to construct bonded contact at the interfaces of the components because it eliminates the penetration/overlapping of contacting bodies. The model components were modeled as an isotropic linear elastic material. The model was created to replicate the dual barrier system (elastomeric seal and cement sheath) of the conventional shallow surface liner hanger. Diameters of casing and liner were chosen to be 10 in. and 8 in. respectively. The length of the pipes and cement were kept long enough (18 and 12 in respectively) to avoid the end effect and simulation convergence issues. The dimensions of the experimental setup (shown in Figure 4.3) are identical to the model.

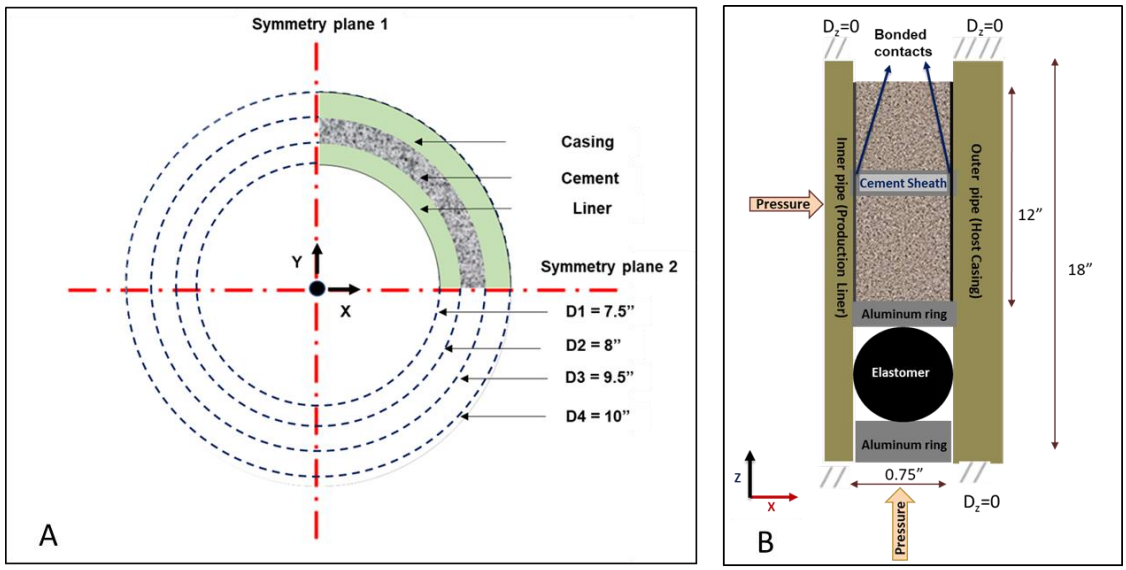

Figure 6.5: Liner dual barrier FEA model, top view (A) and side view of annular cement and seal (B)

Apart from the simulation process, the properties of the model components, such as Young's modulus and Poisson's ratio, UCS, and tensile strength were specified (shown in Table 6:2) and used as input parameters. The magnitudes of Young's modulus and Poisson's ratio, UCS of the hardened cement were obtained from the study performed by Saleh et al. (2019) because the recipe, mixing, and curing procedures were similar to those used in the experimental work of this study. Saleh et al. (2019) conducted laboratory tests for neat Class H cement cubes (2×2×2 in) cured at ambient conditions for 1, 3, 7, and 21 days. Measured ultrasonic pulse velocities (UPV) are 2272, 3014, 3415, and 3668 m/s for respective curing days. The UPV values were used in this study to calculate the magnitudes of Young's modulus and Poisson's ratio using equation (1) and (2). Jutten et al. (1989) derived these equations to represent linear elasticity and an empirical correlation between Young's modulus and Poisson's ratio.

$$E = V_P^2 \ \ \rho_c \ \frac{(1+\upsilon)\,(1-2\upsilon)}{(1-\upsilon)} \ldots\ldots\ldots\ldots\ldots\ldots\ldots\ldots\ldots\ldots\ldots\ldots (1)$$

$$\upsilon = \frac{E + 14.9}{3.9\,E + 33.2} \ldots\ldots\ldots\ldots\ldots\ldots\ldots\ldots\ldots\ldots\ldots\ldots (2)$$

E : Elastic modulus, ν : Poisson's ratio ρ_c: Cement density

Vp : Compressional wave velocity

The calculated values of Young's modulus and Poisson's ratio at 1, 3, 7, and 21 days curing time were plotted in Figure 6.6 (A) and (B) respectively. A log trend-line and linear trend-line equations from these plots were used to determine the cement's Young's modulus and Poisson's

ratio over curing times of 12 h, 24 h, 48 h, 72 h, 5 days, and 7 days as shown in Table 6:2. Similarly, the UCS values obtained from the study conducted by Saleh et al. (2019) were 5, 17.3,19.3, and 38.4 MPa on day 1, day 3, day 7, and 21 days, respectively. The UCS values were plotted in Figure 6.7, and a power trend between UCS vs. curing time was observed. From this trend (equation), the UCS values were calculated at curing intervals of 12 h, 24 h, 48 h, 72 h, 5 days, and 7 days (see Table 6:2). The tensile strength (TS) was assumed to be 10 % of the UCS, as mentioned in several studies (James and Boukhelifa 2008; Lavrov and Torsæter 2016; DeAndrade and Sangesland 2016). The values of UCS, TS, and shear bond strength (SBS) were used to describe and characterize the cement performance in terms of predicting potential failure modes. The cement performance characterization was achieved by comparing the values of UCS, TS, SBS with the induced radial, hoop, and shear stress, respectively as shown in Figure 3.8. The magnitudes of SBS were taken from the study performed by Teodoriu et al. (2018).

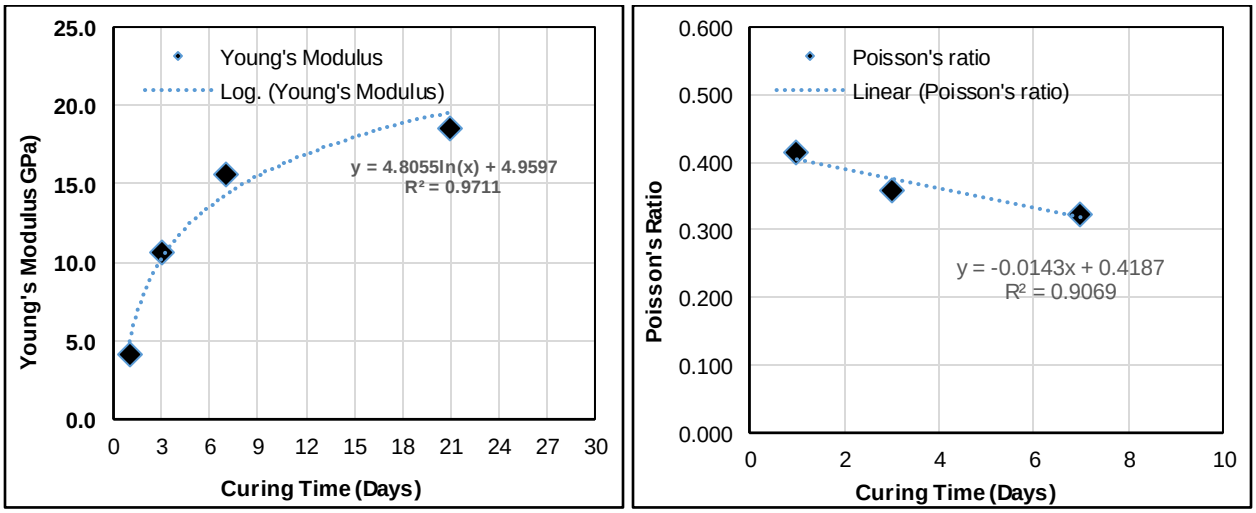

(A) **(B)**

Figure 6.6. Young's modulus (A) and Poisson's ratio (B) over curing intervals

Table 6:2: Cement properties at different curing intervals

Cement properties / Curing Intervals	Young's Modulus (E), psi	Poisson's Ratio (ν)	UCS (psi)	Tensile Strength (psi),UCS/10
Neat Class H Cement, 12 h ,WOC	0.236235×10^6 psi	0.41	585	58.5
Neat Class H Cement, 24 h ,WOC	0.719345×10^6 psi	0.40	930	93
Neat Class H Cement, 48 h ,WOC	1.202455×10^6 psi	0.39	1475	147.5
Neat Class H Cement, 72 h ,WOC	1.485056×10^6 psi	0.36	1933	193.3
Neat Class H Cement, 5 Days ,WOC	1.968166×10^6 psi	0.35	2715	271.5
Neat Class H Cement, 7 Days ,WOC	2.075606×10^6 psi	0.32	3398	339.8

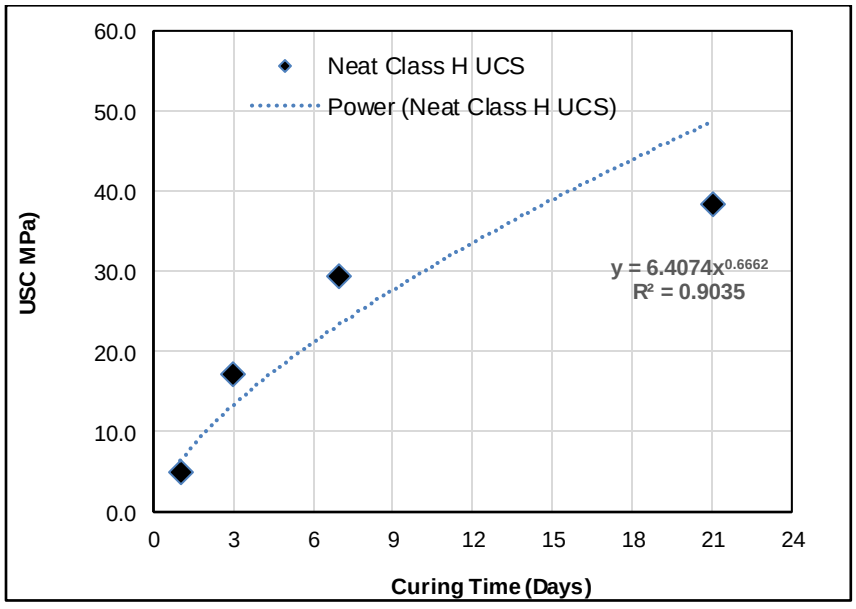

Figure 6.7. UCS increases over curing intervals

The following assumption were made for dual barrier system FEA:

- The cement was modeled as an isotropic linear elastic material
- Cement was considered as impermeable and non-porous solid material
- The values of the cement Young's modulus and Poisson's ratio which were used as input data for the FEM determined through dynamic method by measuring the ultrasonic pulse velocities (UPV) that described in this section were accurate. According to Lavrov and Torsæter (2016), the values of Young's modulus and Poisson's ratio from dynamic procedure are usually higher than values from static procedure. The cement performance considering the static procedure was not considered in this study due to limited information available in current literature on the cement's Young's modulus and Poisson's ratio at the curing intervals included in this study
- Homogeneous mixing of the cement recipe
- The cement sheath was subjected to uniform pressure loads
- Perfect bonding at inner pipe-elastomers-outer pipe interfaces

Chapter 7: Model Simulation Results and Discussions

7.1 Simulation Results of Liner Hanger Seal Assembly

FEM was created to understand the sealing behavior of the elastomeric materials of the liner hanger seal assembly as well as to compare the seals' performance. EPDM and NBR were selected for this study, and their performance was evaluated under two scenarios. The first scenario aimed at investigating the effect of seal energization/compression, pipes materials, and contact type (e.g. friction) on the seal performance. The second scenario aimed at investigating the effect of chemical swelling. Details of simulation results of each scenario are discussed in the following sub-sections.

7.1.1 Elastomers Performance Under Normal Conditions

7.1.1.1 Effect of Compression

In the model, the cord diameter of each sample was 0.75 in., which is as same as the annular space (0.75 in) between the inner pipe (liner) and the outer pipe (casing). There is no interference between elastomer, inner pipe, outer pipe as shown in Figure 7.1. The values of the contact pressure of EPDM and NBR elastomers were obtained after running 24 simulation cases (each point in the graph represents one simulation run). The friction coefficient at the elastomers-pipes interfaces is chosen 0.1 and held constant. A linear relationship between contact stress (sealability) and compression (displacement) is depicted in Figure 7.1. The graphs showed that higher compression results in higher sealing contact pressure. It is observed that EPDM exhibits a contact pressure slightly higher than NBR at the same displacements. This observation confirms that better seal performance is intuitively related to the higher elastic modulus of EPDM (277 psi) compared to NBR (268 psi).

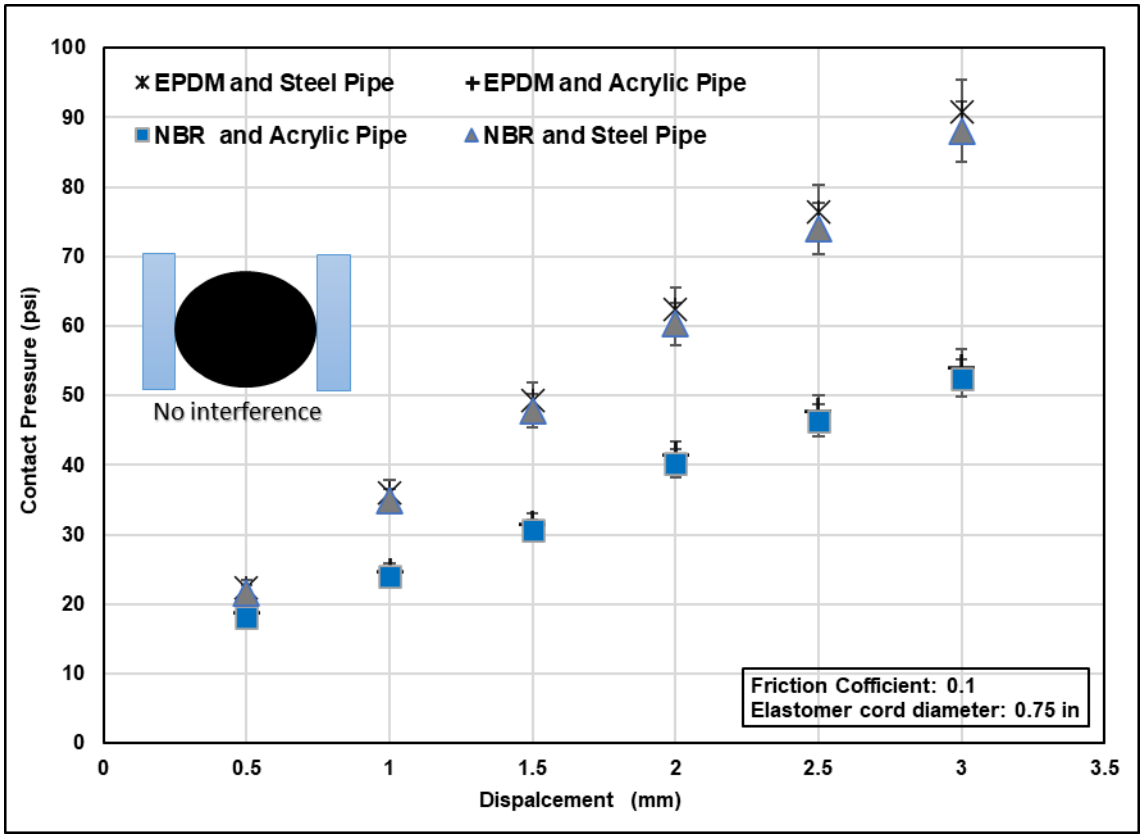

Figure 7.1: Effect of compression (displacement) and elastic modulus on contact pressure

7.1.1.2 Effect of Pipe Material

Young's modulus is the most mechanical property measures the stiffness (resistance to elastic deformation under load) of a solid material. In this scenario, to evaluate the effect of pipe material (Young's modulus) on the contact pressure, the acrylic pipes that has Young's modulus of 0.4 x 10^6 psi (2.76 GPa) were replaced by steel pipes with Young's modulus of 29 x 106 psi (200 GPa). The simulation results showed that (Figure 7.1) at the same displacements, the contact pressures generated at the steel pipe-seal interfaces are higher than the contact pressure generated at acrylic pipe-seal interfaces. This observation can be linked to the higher stiffness of the steel pipe. It is evident from Figure 7.1 that at 2 mm, 2.5 mm, and 3 mm displacements, the contact pressures in case of using steel pipes are higher by around 33%, 36%, and 42% respectively than in case of using acrylic pipes.

7.1.1.3 Effect of Friction

Drag and friction forces are very important parameters that need to be carefully considered when deploying liners in horizontal and deviated wells. Therefore, this scenario is developed to assess the effect of friction on the elastomers contact pressure. The coefficient of friction is varied between (0 and 1). Simulations were run at a constant displacement of 2 mm. Figure 7.2 shows that increasing friction coefficient between elastomer and pipe slightly reduces the contact pressure. However, the reduction is within the error margin of the model. The reduction can be attributed to the partial loss of the setting load that was dissipated to overcome the friction. As a result, less seal volumetric compression (expansion) and contact pressure are generated. Based on this observation, it can be recommended that in field applications, prior to set the liner hanger, the host casing should have a smooth contaminants-free surface.

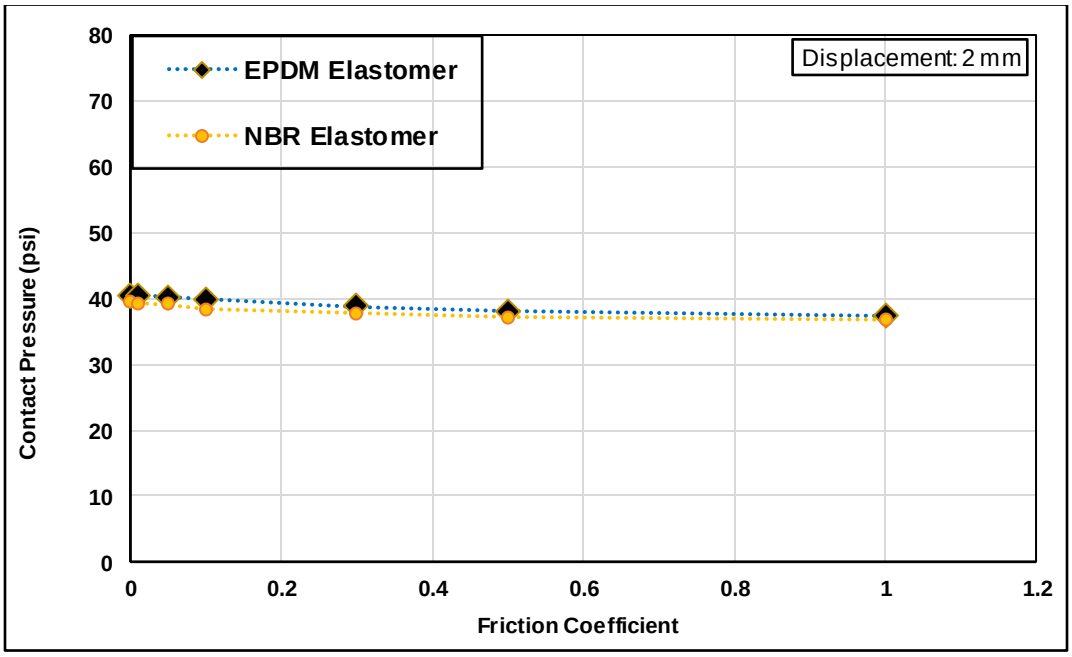

Figure 7.2: Effect of friction coefficient on contact pressure

7.1.2 Elastomers Performance Under Chemical Swelling Conditions

Elastomers' energization using swelling is a growing technology. To understand the elastomers sealing behavior when they are exposed to a swelling agent, FEA was conducted in this study. Prior to simulations, small specimens of EPDM and NBR (shown in Figure 6.4) were immersed in a surfactant for 7 days. After this swelling period, the specimens cord diameter was measured at three recovery days, and reported readings were used as input parameters for the model. Simulation results demonstrated that more swelling leads to an increase in elastomer cord diameter, which results in higher compression /contact pressure at the elastomers-pipes interfaces as shown in Figure 7.3. The results also demonstrated that as the elastomer starts recovering with time, the contact pressure also starts decreasing. It is important to point out that NBR specimen swells more than EPDM specimen, thus resulting in a higher seal contact pressure compared to EPDM. Although NBR shows superior sealability, it is more susceptible to chemical degradation. The hardness of NBR was reduced by 35% whereas the hardness of EPDM was only reduced by 15%. NBR hardness reduction is beyond the maximum limit (20%) specified by Norsok standard M-710 (2014). Therefore, the structural integrity of NBR samples is compromised due to swelling conditions considered in this study.

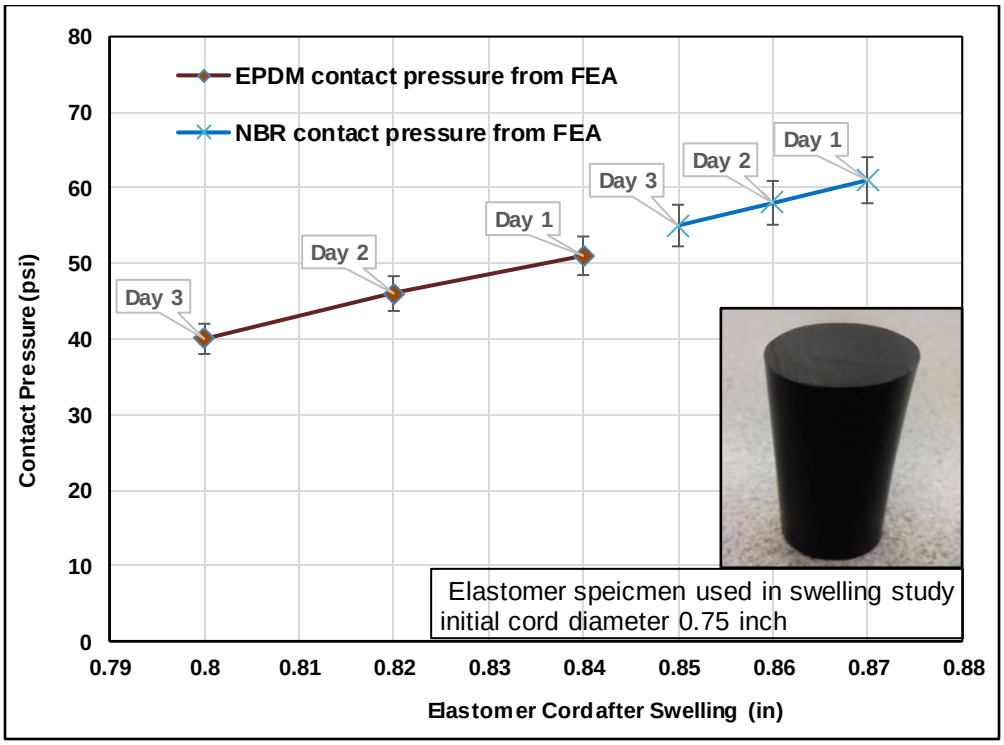

Figure 7.3: Effect of swelling on contact pressure

7.1.3 Validation of Modeling Results

To validate the model, the contact pressures from simulations were compared to the contact pressures estimated from the experimental sealability tests. In the case of experiments, the contact pressure between seal and pipe was indirectly estimated by injecting nitrogen at various increasing pressure until leakage is observed. The injection pressure at which leak is observed can be considered as representative of actual contact pressure at the seal-pipe interface. In this study, the model was validated using two experimental scenarios: normal and swelling conditions. The validation methods are described in the following sections.

7.1.3.1 Validation of Elastomers Performance Under Normal Conditions

The cord diameter of elastomer O-rings procured for this study was measured. It was about 1 mm greater than the actual annulus clearance of 0.75 in. between the setup two concentric acrylic pipes.

Therefore, simulations were re-run with the actual value of the cord diameter in order to establish a fair comparison between simulations' and experiments' results. The 1 mm increase in the cord diameter led to elastomer-pipes interference as shown in Figure 7.4. Resolving this interference, the contact pressures from simulations were 40 psi and 41 psi for NBR and EPDM respectively without requiring external torque. Increasing the torque i.e. energization displacement, contact pressure rises linearly up to 2.5 mm displacement. It is notable that the EPDM sample exhibits contact pressure slightly greater than the NBR sample.

When the experimental sealability test was conducted at 40 psi without applying any external energization, no leakage was observed in either of the elastomer samples. This test confirmed that the actual contact pressure at the seal-pipe interface is greater or equal to 40 psi. Increasing the torque values/displacement did not result in a leak at 40 psi as shown in Figure 7.4. According to the FEM prediction, EPDM and NBR can offer contact pressures during the experimental pressure tests up to 61 psi and 58 psi, respectively. However, the pressure test was maintained constant at 40 psi (see Figure 7.4) during the experiments for safety precautions.

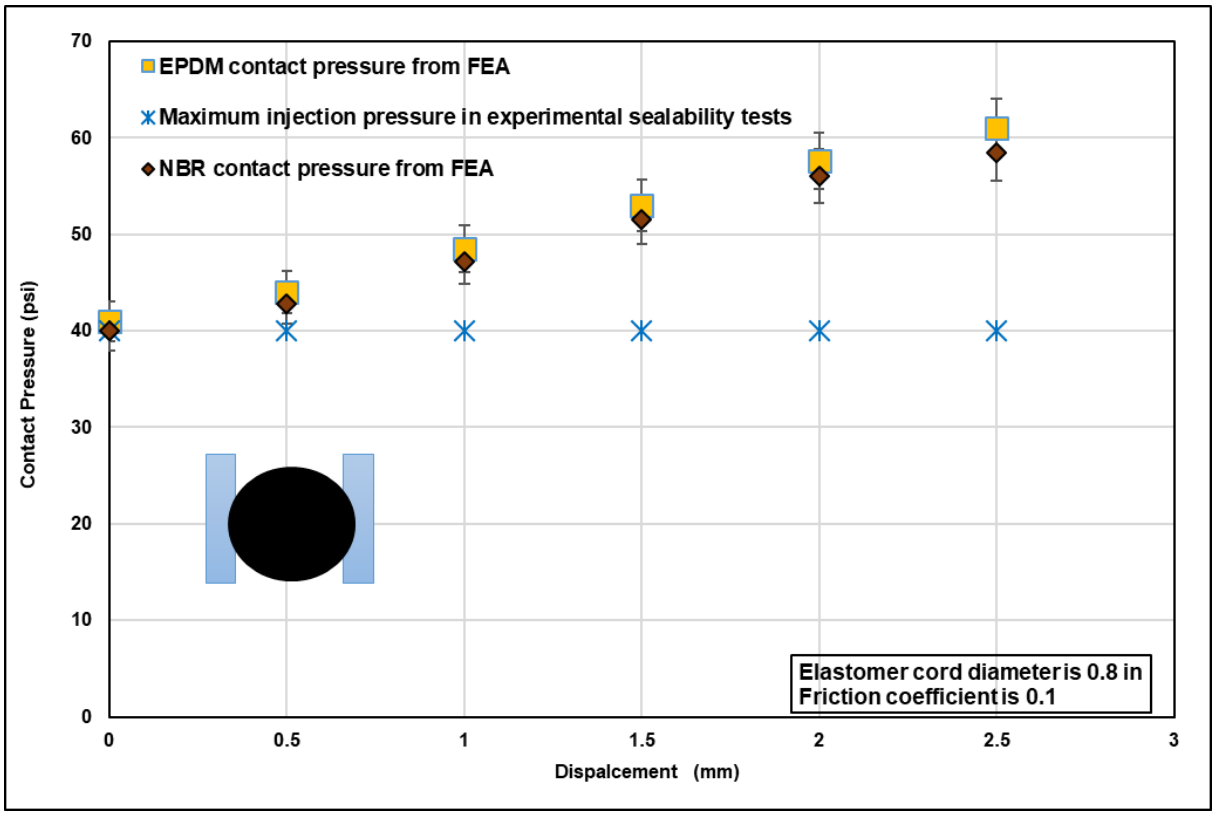

Figure 7.4: **Comparison between FEA simulation and Experimental Test for contact pressure of EPDM and NBR elastomers**

7.1.3.2 Validation of Elastomers Performance Under Swelling Conditions

The increase in the cord diameters of EPDM and NBR elastomers reported during the recovery periods as shown in Figure 7.5. Reported values are used as inputs for the FEM to predict contact pressures. Simulation results revealed that due to pre-stress caused by chemical swelling. EPDM provided a contact pressure of 50, 45, and 41 psi for day 1, day 2, and day 3 respectively as shown in Figure 7.6 (upper dotted lines). Based on these results, it was decided that the experimental pressure test should not exceed 40 psi because of the pipes of the setup made of acrylic materials that could not withstand high pressure.

To validated the FEM, laboratory tests were performed using the setup shown in Figure 4.5 to assess the sealability of EPDM and NBR after they were immersed in a surfactant for a week. During this chemical swelling period, the diameter and cord diameter of each elastomer

sample were increased as shown in the table included in Figure 7.5. Under these swelling conditions, experimental pressure tests were conducted over three days of recovery periods in order to examine the elastomer sealing behavior. EPDM elastomers were tested at 40 psig and 30 min holding time after being removed from the surfactant. The test was repeated for the next two days of recovery. Figure 7.6 (lower graph) shows that for EPDM, no leak was observed during day 1, day 2, and day 3. This indicates a contact pressure of 40 psi or greater.

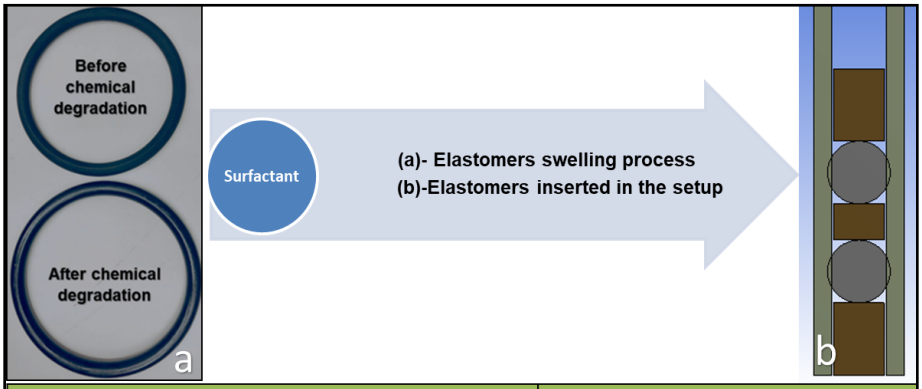

	EPDM Elastomer			NBR Elastomer		
Recovery Date	Day 1	Day 2	Day 3	Day 1	Day 2	Day 3
Cord after Swelling	0.84 in (21.34 mm)	0.82 in (20.83 mm)	0.80 in (20.32 mm)	0.87 in (22.10 mm)	0.86 in (21.84 mm)	0.85 in (21.59 mm)
Increase in cord	0.09 in (2.3 mm)	0.07 in (2 mm)	0.05 in (1.3 mm)	0.12 in (3 mm)	0.11 in (2.8 mm)	0.1 in (2.5 mm)
Expansion	12%	10%	7%	16%	14.5%	13.3%

Figure 7.5: **Elastomers swelling and recovery process**

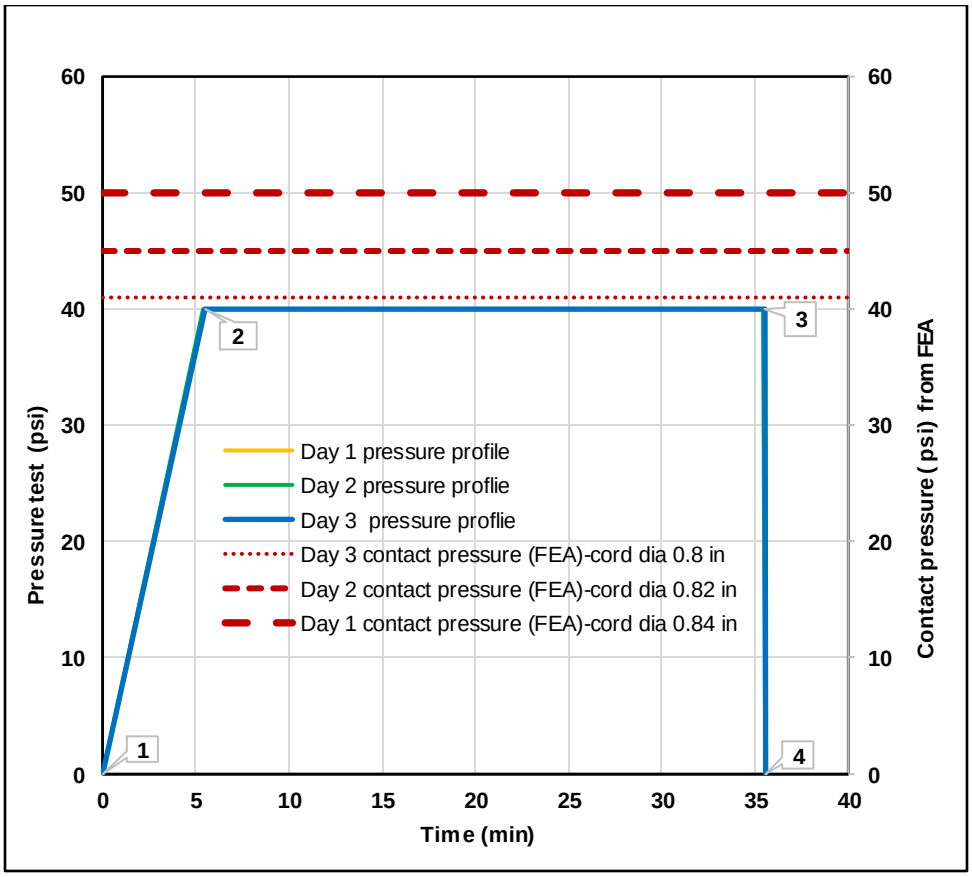

Figure 7.6: EPDM pressure tests on Day 1, Day 2 and Day 3 after exposure to a surfactant (lower graph), and EPDM contact pressures on Day 1, Day 2 and Day 3 after exposure to a surfactant (3 dotted lines)

The contact pressure predicted by the FEA model for NBR is 61, 58, and 55 psi on day 1, day 2, and day 3, respectively. It should be noted the contact pressures obtained from the FEA for NBR are higher than those obtained from EPDM. This observation correlated with NBR higher volumetric swelling compared to EPDM (shown in Figure 7.5) and hence yielded higher contact pressure. To validate the FEM, NBR elastomers were subjected to experimental pressure tests using the same procedure and consecutive intervals (days) followed during the testing of EPDM elastomers. Results of three days of tests were plotted in the lower graph of Figure 7.7. No leak was observed at 40 psig pressure test as predicted by the FEM.

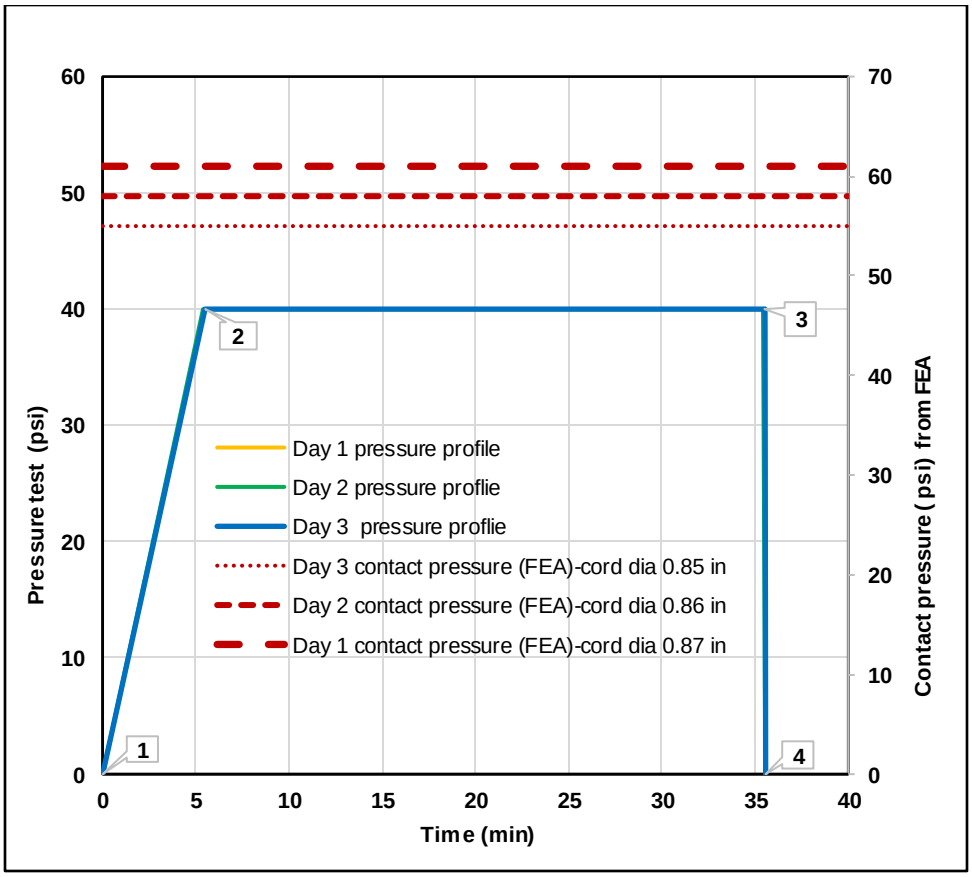

Figure 7.7: NBR pressure tests on Day 1, Day 2 and Day 3 after exposure to a surfactant (lower graph), and NBR contact pressures on Day 1, Day 2 and Day 3 after exposure to a surfactant (3 dotted lines)

7.2 Simulation Results of Liner Hanger Dual Barrier System

7.2.1 Effect of Curing Times on the Cement Mechanical Properties

7.2.1.1 Preliminary Simulations and Analytical Validation

Preliminary simulations result of radial and hoop stresses were compared with the values calculated from the analytical method. In the analytical calculations, Lamé modified equations presented by Patel and Salehi (2019b) were used to determine the radial and hoop stresses. Radial and hoop stresses from FEA and analytical methods were plotted in Figure 7.8 (A) and (B) respectively. Figure 7.8 (A) shows that at the cement-inner pipe (liner) interfaces, a fair match

between radial stress from FEA and analytical results was observed. The FEA results deviated by 3% to 3.8% from the analytical values. The hoop stress values at cement-inner pipe (liner) interfaces from FEA and analytical method were also compared and found to be in a fair agreement, as shown in Figure 7.8 (B). The FEA results deviated by 3.6% to 4 % of the values calculated using the analytical method.

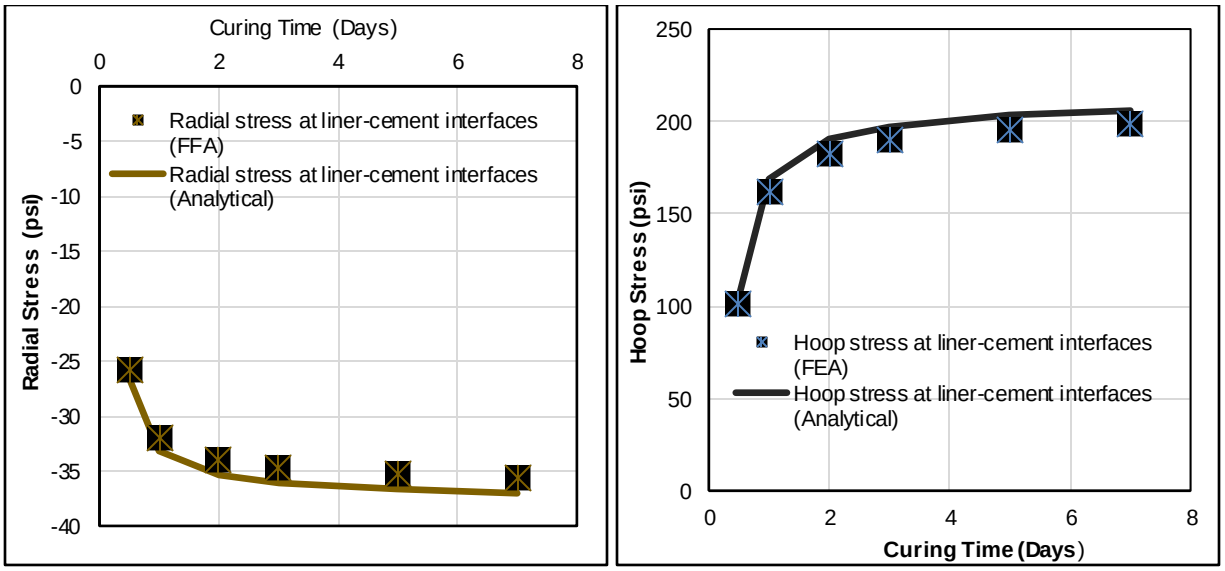

(A) **(B)**

Figure 7.8: Comparison of radial (A) and hoop (B) stresses magnitudes determined by FEA and analytical

7.2.1.2 FEA Verification Using Results from Experimental Work

Following the model validation using analytical methods, the stresses were simulated at different curing times (12 h, 24 h, 48 h, 72 h, 5 days, and 7 days). The simulation's objective is to investigate the effect of WOC on the cement sealability. Sealability was examined by comparing the values of the radial, hoop, and shear stresses that were generated at liner-cement interfaces with UCS, TS, and SBS, respectively. Figure 7.9 shows that when applying an internal pressure of 40 psi, the radial stresses at liner-cement interfaces are very low for all WOC intervals. It is clear that at a pressure of 40 psi, the cement will not fail by crushing as the radial stress values are too far from the UCS values.

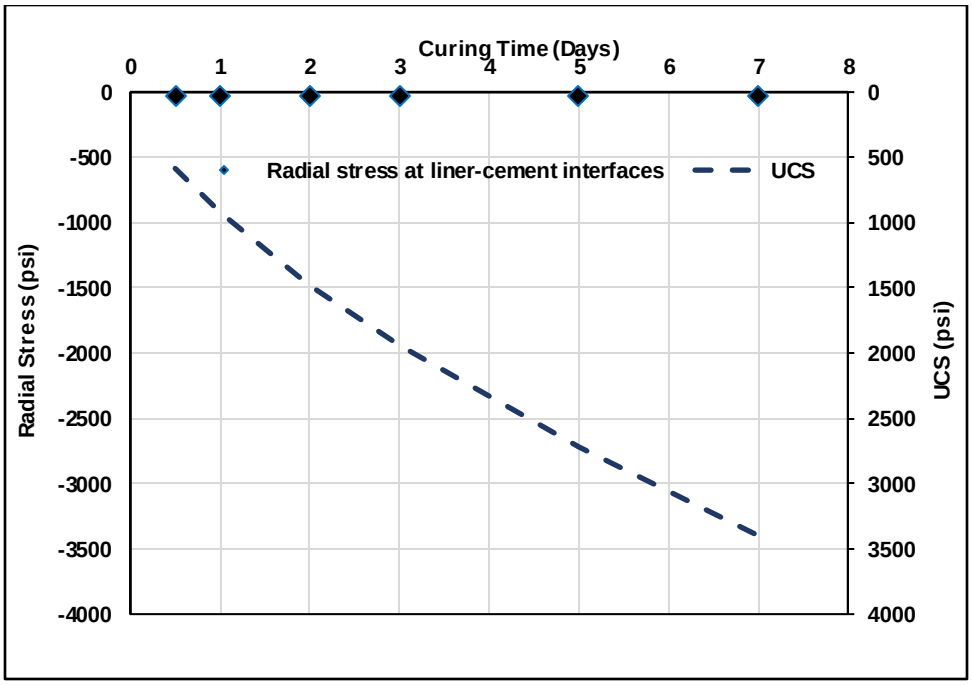

Figure 7.9: Radial stress at different WOC intervals

Figure 7.10 shows that hoop stress increases as WOC intervals increase. The results revealed that the cement failed by radial cracking due to the high concentration of hoop stress, particularly at 12-72 h WOCs. The failure occurred because the values of the hoop stresses during theses WOCs are higher than the tensile strength. This fact is supported by the cracks that appeared at the cement surface (shown in Figure 7.11 (A)) and the pressure decline (Figure 7.12) that was observed during the experimental tests in which the cement was subjected to 40 psi pressure test. It is concluded from these results, that cement is prone to failure due to radial cracks. This observation matches with previous studies that indicate high probability of cement failure in tension (Mueller and Eid 2006; Lavrov and Torsæter 2016; Patel et al. 2019b).

Figure 7.10 shows a linear relationship between the axil/shear stress and WOC intervals. The cement failed by interfacial debonding because the shear stress exceeded the cement-pipe interfacial shear bonding strength specified by Carter and Evans (1962). This result was also verified by the leakage that occurred during the experimental pressure test conducted at 40 psi

using the setup shown in Figure 7.11 (A) and (B). In this test, several leakage points were observed at cement-inner pipe interfaces. However, fewer leakage points were seen at cement-outer pipe interfaces, as illustrated in Figure 7.11(B). This observation is supported by the studies conducted by Ahmed et al. (2019a); Patel and Salehi (2019b), in which the authors reveal that debonding is more likely to occur at cement-inner pipe (liner) interfaces.

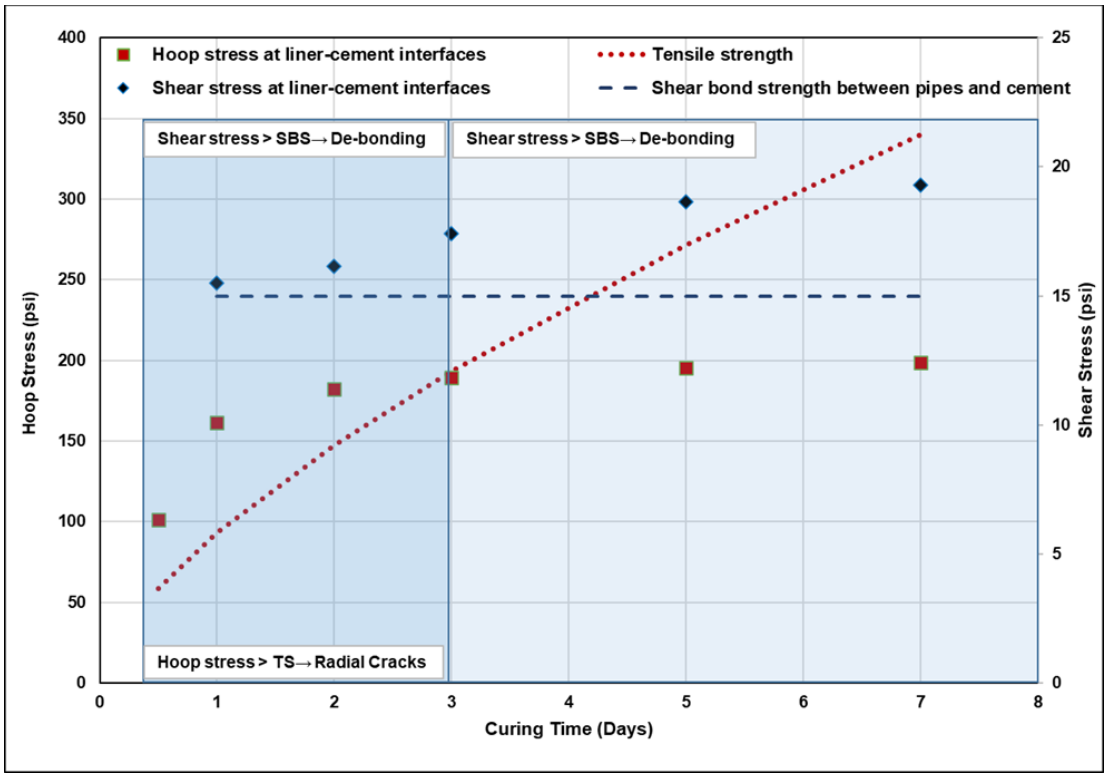

Figure 7.10. Hoop and shear stresses at different WOC intervals

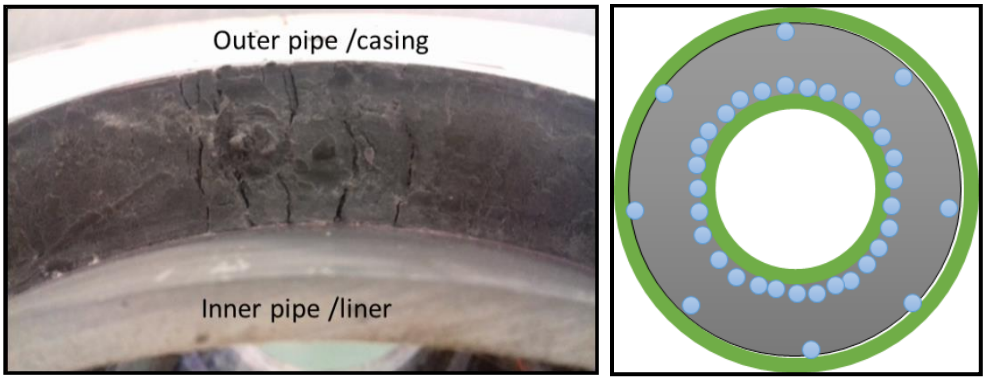

(A) **(B)**

Figure 7.11: Radial cracks (a) and leak (b) occured during experimental pressure tests

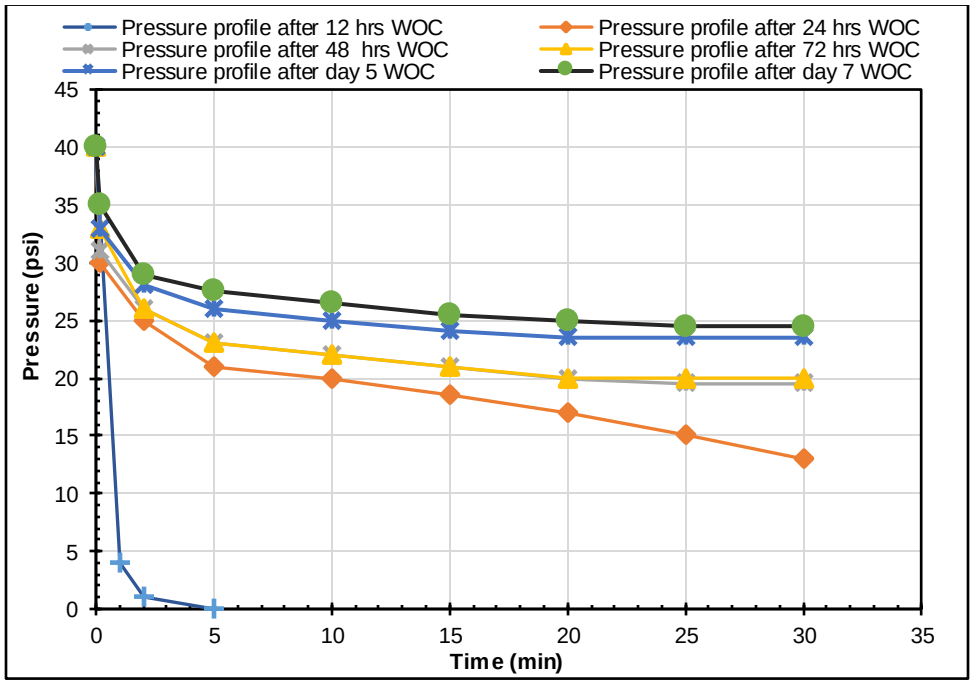

Figure 7.12. Pressure decline at 40 psi obtained from experimental work at various curing times

7.2.2 Effect of Wellbore Pressure Variation

During the life cycle of a well, cement may experience high inner casing pressure variations that can be attributed to the integrity tests (e.g. pressure test, negative pressure test, formation integrity test, leak-off test, and extended leak-off test) and wellbore pressure variation during drilling operations, perforation operations, and stimulation operations. The increase of the inner casing pressure can induce extra compression to the radial stress and tension to the hoop stress as well as compression or tension to the axial stress. As a result, crushing, radial cracks, debonding, and shear failure can occur individually or collectively within the bulk cement and /or at casing-cement-rock (Bois et al. 2011; Lavrov and Torsaeter 2016).

To investigate the effect of the wellbore pressure variations upon the annular cement integrity, the model created in this study (Figure 6.5(A) and (B)) was subjected to pressure loads

of 500, 1500, 5000, 8000, 10000, and 15000 psi. The pressure variations considered represent realistic pressure fluctuations that a shallow liner serves in a low, medium, and high pressure wells could confront. The diameters of the surface/shallow liner and host casing are commonly 18 and 22 in. respectively. The cement curing time also varied (12 h, 24 h, 48 h, 72 h, 5 days, and 7 days) to provide in-depth investigations on cement short terms integrity. Under these conditions, several simulations were run and the results of radial, hoop, and axial stresses are plotted in Figure 7.13, Figure 7.14, and Figure 7.15 respectively to enable identifying the potential failure modes and the operation boundaries.

Figure 7.13 shows that the compressive radial stress at liner-cement interfaces induced from wellbore pressure up to 500 psi cannot compromise the zonal isolation at the interfaces up to 7 days because the magnitudes of the radial stress are less than the UCS. This conclusion also applies for wellbore pressure of 1500 psi after 24 h and up to 7 days WOC as well as for wellbore pressure 5000 psi and 7 days WOC. However, the zonal integrity can be compromised (the area below the UCS line) at a wellbore pressure of 1500 psi at 12 h, wellbore 5000 psi and 12, 24, 48, 72 h, and 5 days WOC and for the rest of the high wellbore pressure at any curing time. Under these conditions, the cement is failed by crushing as illustrated in Figure 3.8 because the magnitudes of the radial stress are higher than the UCS.

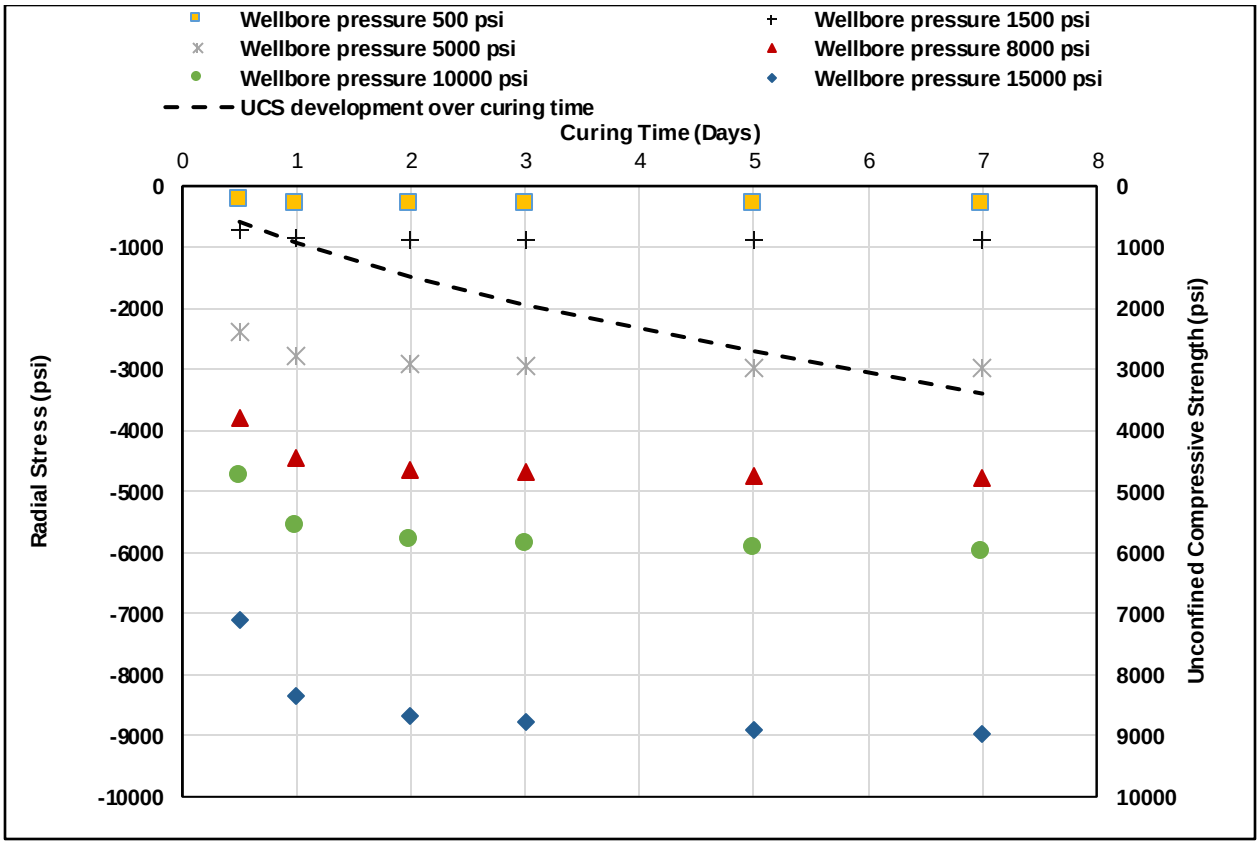

Figure 7.13: Radial stress at liner-cement interfaces at various wellbore pressures and WOC

The radial stress cannot be used alone to evaluate cement integrity. Therefore, further simulations were run to determine the magnitudes of hoop stress. Figure 7.14 compares the magnitudes of hoop stress with the tensile strength at liner-cement interfaces. It is obvious that hoop stresses at liner-cement interfaces caused by wellbore pressure up to 500 psi cannot jeopardize the cement sealability after 24 h WOC and up to 7 days because the magnitudes of the hoop stress are less than the tensile strength. In case of wellbore pressure of 1500 psi, integrity is maintained up to 48 h WOC only. The cement sealability is likely to be lost for the rest of the pressures and respective WOCs because the magnitudes of hoop stress exceeded the tensile strength. The failure by high hoop stress would be in the form of radial cracks as illustrated in Figure 3.7 and Figure 3.8.

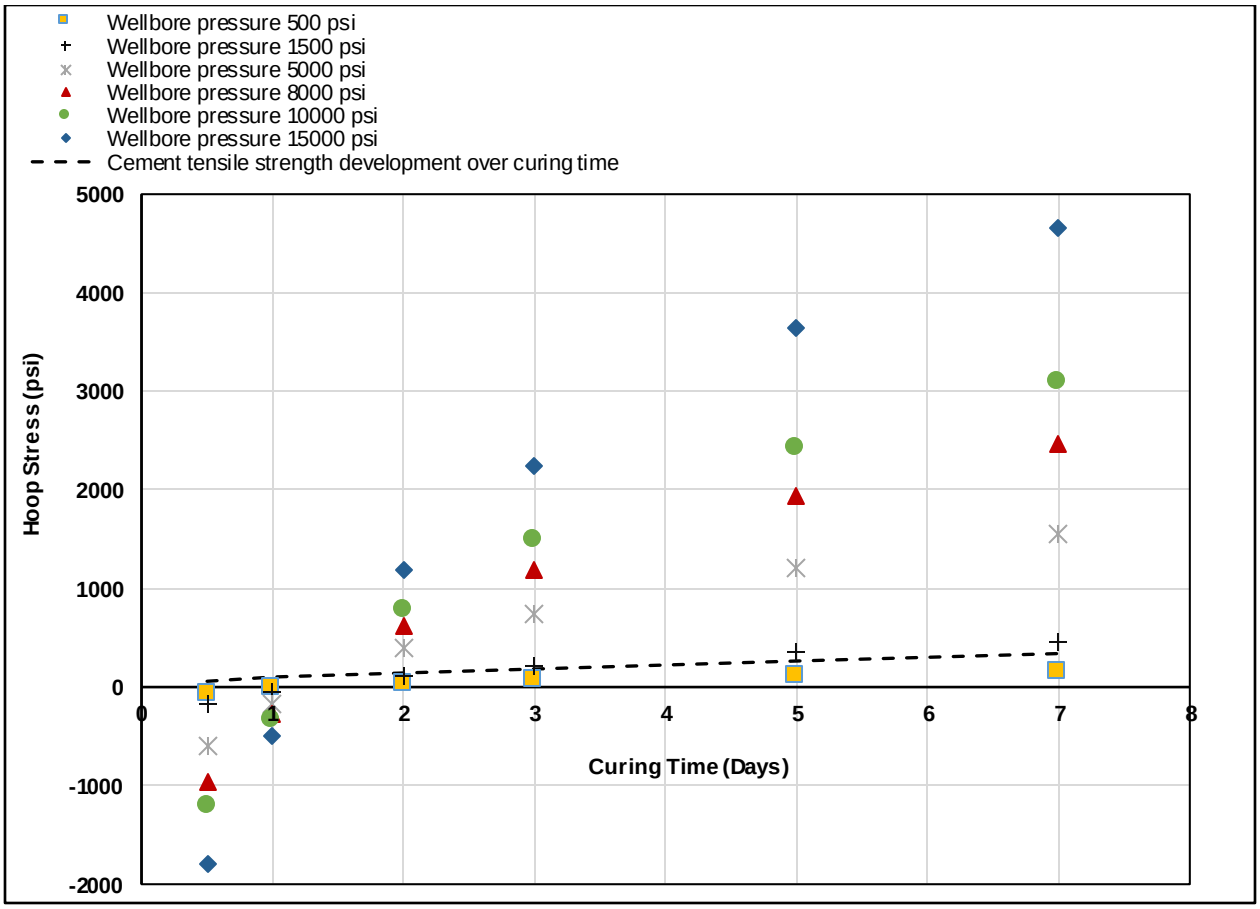

Figure 7.14. Hoop stress at liner-cement interfaces at various wellbore pressures and WOC

Beside radial and hoop stresses, axial/shear stress is an important parameter to characterize the cement performance. The simulation results presented in Figure 7.15 show that interfacial shear bonding strength at liner-cement interfaces can withstand shear stresses resulting from pressures loads of 500 and 1500 psi as well as from pressure of 5000 psi between 24 to 72 h WOC only. However, a failure in form of cracks / debonding as illustrated in Figure 3.7 and Figure 3.8 is likely to occur from the rest of the pressure loads at their respective WOCs because at these pressures, the magnitudes of the shear stress exceeded their anticipated interfacial bonding

strength. In this study, the bond strength values are reported after 24 h and assumed to be constant for all the WOC intervals. This assumption is made based on the study performed by Teodoriu et al. (2018 and 2019). In all, it can be concluded that hoop stress caused the most failure situations, followed by radial, and axial stresses as inferred by the risk failure matrix shown in Figure 7.16. The matrix is created based on information extracted from the figures presented in this section. The failure caused by hoop stress is attributed to the lower values of cement tensile strength. Therefore, additives to enhance tensile strength is highly recommended. The target tensile strength would depend on the maximum expected pressure load at the designed installation depth.

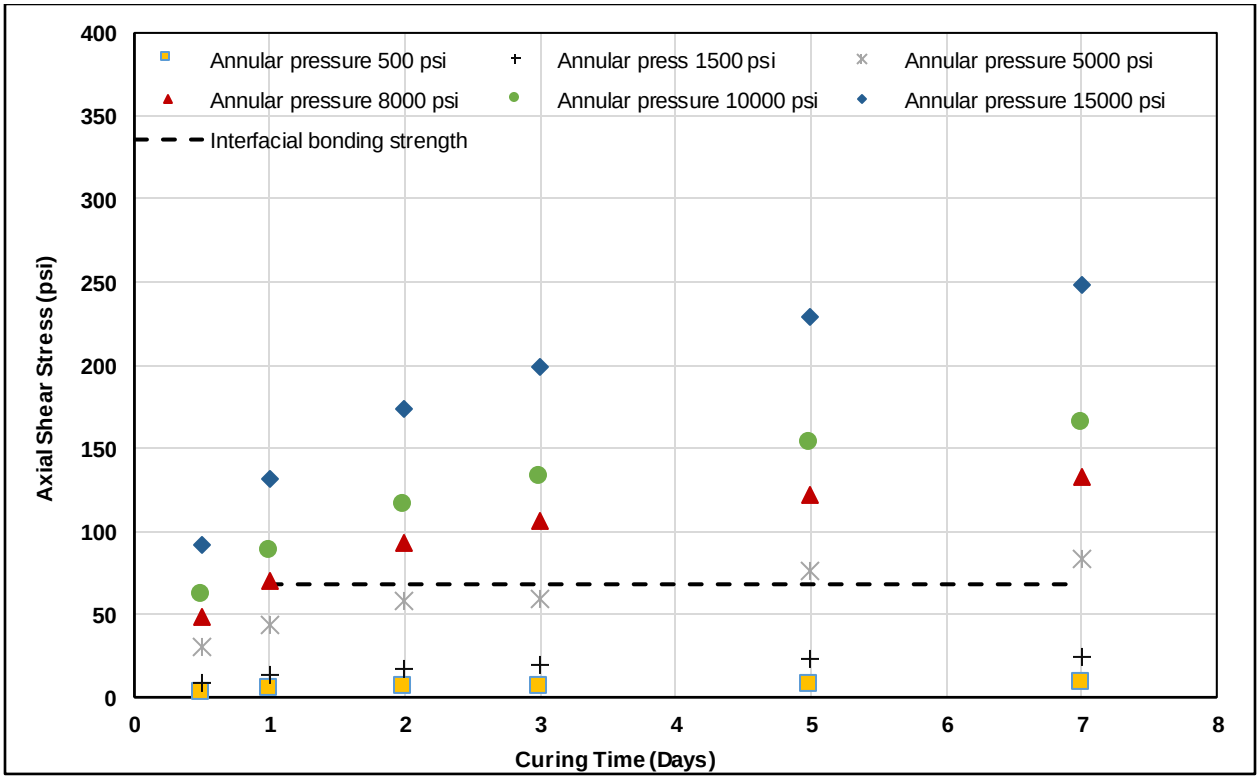

Figure 7.15. Axial / shear stress at liner-cement interfaces at various wellbore pressures and WOC

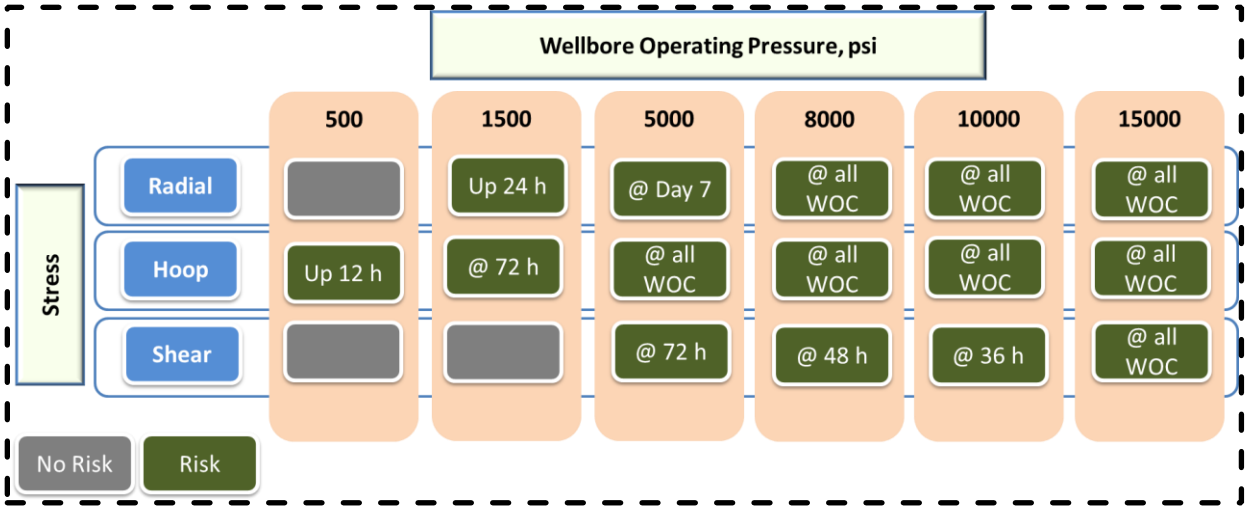

Figure 7.16: Risk of failure matrix for a shallow liner cement at different pressures and curing intervals

7.2.3 Effect of Depth

Figure 7.17 compares the performance of a neat Class H cement sheath for shallow, intermediate, and production liners as illustrated earlier in Figure 1.1. The objectives of this comparison are to investigate the effect of the depth upon the cement sealability, characterize the modes of failures, and rank the liners in terms of the risk of failure that may assist in designing the appropriate cement formulations. Figure 7.17 shows that when the pressure of a shallow liner is up to 500 psi, the radial stress acting at the liner- cement interface is slightly higher than the UCS and the cement is prone to failure by crushing. However, as the UCS develops over the curing time, the radial stress becomes less than the UCS. At a wellbore pressure up to 3000 psi, the intermediate liner cement is not expected to experience failure. This conclusion is supported by the fact that the radial stress is less than the UCS at any curing interval, although the UCS is slightly decreased after 24 h according to cement retrogression at 230 °F. For wellbore pressure and temperature of 4500 psi and 300 °F, the production liner can maintain its integrity in the range of 12-23 h curing times. After that, the cement is highly potential to failure by crushing according to the rapid drop in the

UCS resulting from cement retrogression. From this analysis, it can be concluded that based on the assumptions and simulations performed in this study, the cement sheath in the production liner is more prone to failure. Next is shallow liner while the intermediate liner is not expected to fail.

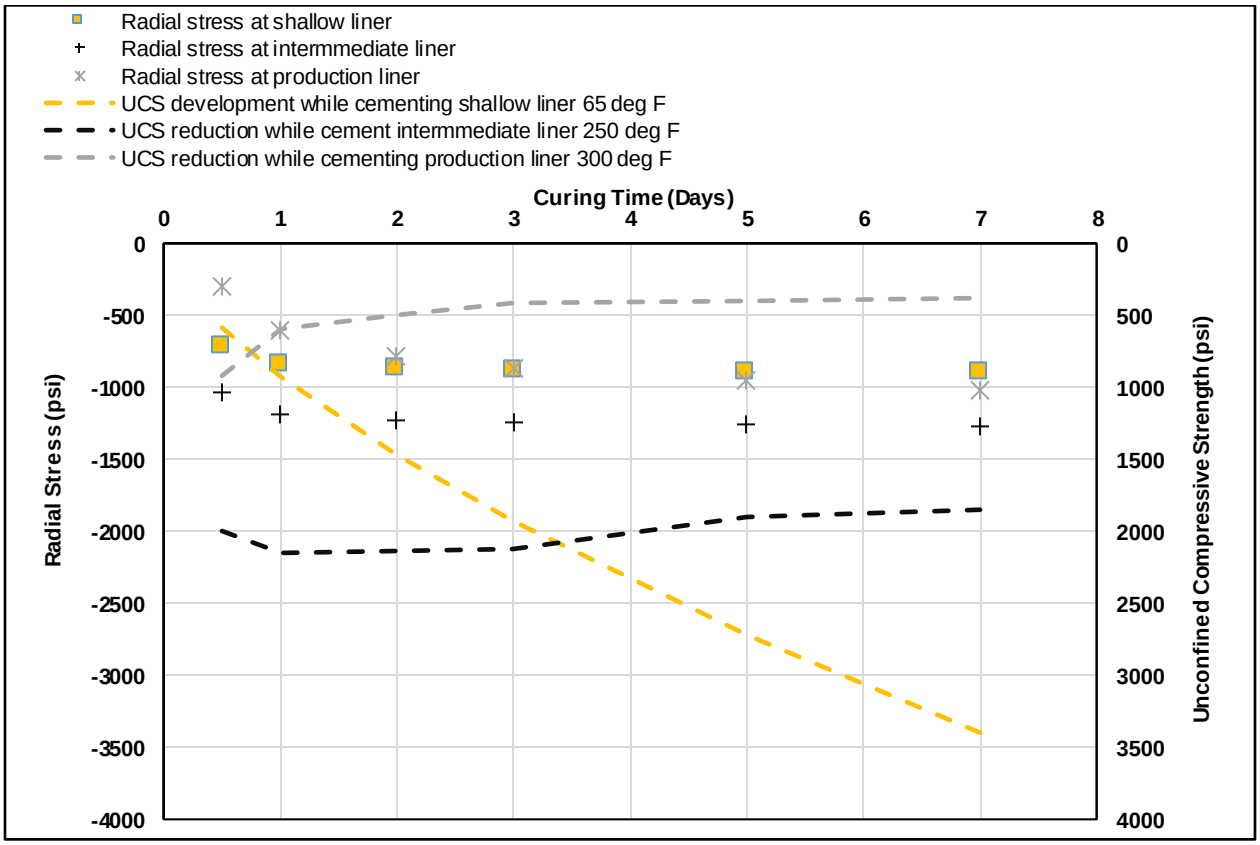

Figure 7.17: Radial stress acting on cement-liner interfaces of dual barrier system of shallow, intermediate and production liners

Hoop stress is very important for evaluating the cement integrity. Figure 7.18 presents hoop stress for shallow, intermediate, and production liners. The Figure shows that the cement sheath of a shallow liner may fail after 12 h, 72 h, 5 days, and 7 days curing times due to the radial cracks resulting from hoop stress exceeding tensile strength. The cracks may not exist at 24 h and 48 h. As shown in Figure 7.18, the intermediate liner has a failure trend similar to the shallow liner

(failed at same curing times). However, the failure may be worse because the cement retrogression creates a bigger gap between the magnitudes of the hoop stresses and their anticipated tensile strength over the curing intervals. The production liner cement can tolerate hoop stress at 12 h curing time, however, the cement retrogression at 300 °F negatively impacted the tensile strength as shown in Figure 7.18. Hence, the cement is highly susceptible to failure after 12 h and the gap between the hoop and the tensile strength becomes much bigger compared to the shallow and intermediate liners. Based on this analysis, it is obvious that the failure probability of the liner cement sheath tends to increase as the wellbore depth increases. It is also worth mentioning that the failure resulting from hoop stress over inducement is more severe than the failure by crushing resulted from radial stress. It recommended that cement for intermediate and production liners of deep wells must be designed to enhance and prevent retrogression strength. A tool to predict the cement failure matrix of different types of liner dual barrier systems was presented in Figure A1, Appendix C.

Axial/shear stress is also very important for cement performance evaluation. However, the effect of liner depth on shear stress could not be studied due to the lack of sufficient data on cement shear bond strength at the cement-pipe interface at elevated temperatures (250 and 300 °F).

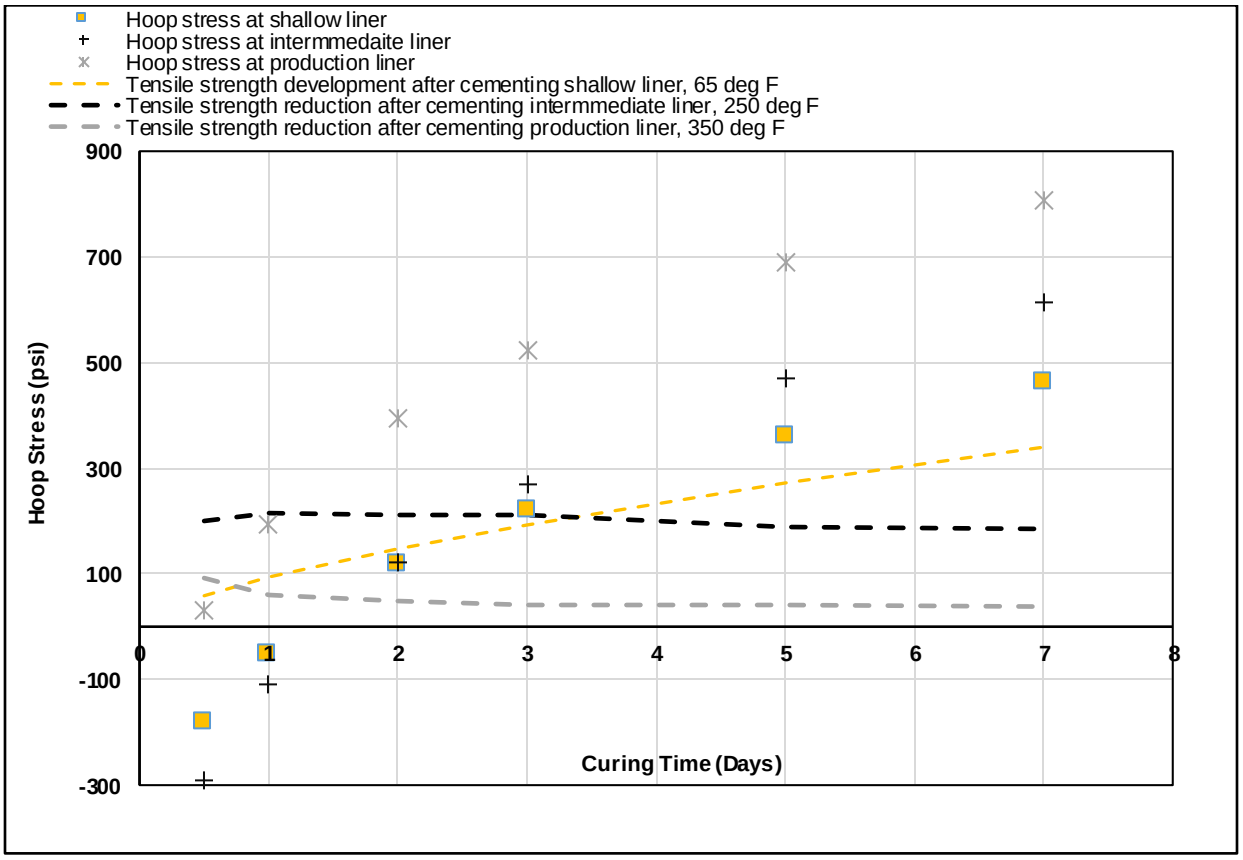

Figure 7.18. Hoop stress acting on cement-liner interfaces of dual barrier system of shallow, intermediate and production liners

Chapter 8: Summary, Conclusions, and Recommendations

8.1 Summary

The identification of the primary barrier in the liner hanger dual barrier in field applications has raised serious concerns that continuously challenge the industry and regulators. There is a lack of procedures, guidelines, and standards that exclusively deal with testing and qualification of dual barrier components system (seal assembly and cement sheath) independently in order to determine which of them can act as a primary barrier. The selection of appropriate elastomeric sealing materials is a major challenge because no single elastomer type available can serve in all the downhole conditions. This issue is backed by the fact that 18% of offshore wells around the world have some form of liner hangers seal failure. As for cement, although many gas migration control additives are used in attempts to prevent gas migration, this problem remains a challenge for the oil and gas industry due to the uniqueness of each well. These issues still pose challenges that need to be addressed by industry and regulatory agencies. The outcomes of this research are intended to provide an improvement in the well integrity in terms of proposing solutions to the issues of liner hanger dual barrier and filling some gaps in current liner hangers' qualifications and testing procedures.

8.2 Conclusions

The testing of liner hanger seal assembly and cement sheath as a dual barrier system is challenging for the oil and gas industry. Based on the experimental and numerical investigations conducted in this study to evaluate the performance of the liner hanger elastomeric seal and cement sheath, the following conclusions have been drawn:

1. Elastomeric seal assembly can act as a primary barrier in the liner dual barrier hanger system in case it is selected, designed, manufactured, qualified, deployed, and tested properly.

However, it should be noted that the performance of the elastomers (EPDM and NBR) evaluated in this study was performed at room temperature. In addition, there is limited information on the seals' chemical compound, physico-mechanical properties, and friction at the seals-acrylic pipes interfaces.

2. For the specific testing protocols developed in this study to investigate the elastomers performance, the results revealed that the order of dominant failure mechanisms that adversely impact the elastomer performance from high to low is CO_2 > mechanical defect > cyclic load > swelling.
3. Pressure cycling is paramount for seal performance evaluation. Technically, the performance of the liner hanger seal assembly under pressure cycling loads depends on the type of elastomeric materials, energization force, and the number of pressure cycles.
4. Prolonging the pressure test duration from 30 minutes to 60 minutes may not assist in a better evaluation of elastomers' performance as independent barriers. However, it is important to point out that the tests conducted in this study did not fully mirror the actual downhole conditions.
5. The results of the FEA from this study showed that the order of parameters that influence the elastomer contact pressure (sealability) from high to low is compression ratio > pipes Young's modulus > elastomer's Young's modulus > friction coefficient.
6. The selection of elastomer material based on evaluation of one or a limited number of parameters may not provide a full characterization about its sealing behavior. Fitness-for-service of an elastomeric seal must be determined holistically by considering all available information on the seals' chemical properties, physico-mechanical properties, and design

specifications. In addition, considering the operation conditions, and compatibility with the downhole environment.

7. For cement sheath to be considered a primary barrier element in a dual barrier zonal isolation system, it must contain a specific anti-gas migration additive in addition to other cement additives.
8. The experimental results from this study revealed that cement integrity was significantly influenced with WOC time, pipe material, and pipes' surface roughness.
9. Results from the experimental and numerical work conducted in this study showed that the cement sheath is more prone to failure by debonding. Debonding is more likely to occur at the cement-inner pipe (liner) interfaces compared to cement-outer pipe (casing) interfaces.
10. The results from FEA performed in this study revealed that liner cement is most likely to fail under tensile hoop stress in forms of radial cracks and/or debonding. Therefore, cement tensile strength is the most critical mechanical property that needs to be controlled carefully.
11. Based on the FEA simulations performed to assess failure of the dual barrier systems of shallow, intermediate, and production liners, it can be concluded that the order of liner hanger dual barrier cement risk of failure from high to low is production > shallow > intermediate. The failure of the production liner cement can be attributed to its retrogression at elevated temperature (above 230 °F) that is usually encountered in deep and ultra-deep wells.

8.3 Recommendations and Future Work

The following recommendations have been made based on the reviews, findings, and conclusions presented in this study:

1. The experimental work in this study was performed at room temperature and relatively low testing pressure (40 psig) because the setup made from acrylic pipes that cannot withstand

pressure and temperature close to those existing in downhole. It is highly recommended to test the elements of the liner hanger dual barrier system (seal assembly and cement) for the anticipated downhole temperature and pressure.

2. Liner hanger elastomer seals are recommended to be subjected to a pressure cycling test before being deployed in the downhole. This test is not recommended in current standards and regulations although some studies revealed that elastomers are prone to failure under pressure cycling conditions.
3. Elastomer energization/setting is critical for seal integrity. It is recommended to consider a very precise tolerance of the radial dimension of an elastomer seal during the design of a liner hanger seal assembly.
4. It is recommended to use cement with gas migration control additive(s) for isolation of shallow gas formation zones and abnormal pressure intervals.
5. Cement for intermediate and production liners of deep and ultra-deep wells should be designed to withstand retrogression at elevated temperatures.
6. Additives to enhance cement tensile strength are highly recommended to prevent its failure according to over inducement of the hoop stress which can result in radial cracks propagation.

Following are some of the future research work proposed based on the results, analyses, and conclusions of this study:

1. Further research should be explored to assess the possibility of testing the sealing system and the cement sheath independently in field application.
2. Further studies are highly recommended to evaluate the performance of more types of seals such as HNBR, FKM/Viton, FEPM/Alfas, and FFKM/Kalrez that are also commonly used in liner hanger sealing assembly.

3. Axial/shear stresses are very important for cement performance evaluation. More research to determine cement shear bond strength at the cement-pipe interface at elevated temperatures is highly imperative to enable a comprehensive investigation of cement performance.
4. More studies are needed to develop gas migration models that consider the complex behavior and the unsteady nature of the gas under actual downhole conditions.

Nomenclature

Acronyms

API	American Petroleum Institute
ASTM	American Society for Testing & Materials
BOP	Blowout Preventer
BSEE	Bureau of Safety and Environmental Enforcement
CFR	Code of Federal Regulations
EPDM	Neoprene ethylene propylene diene monomer
FEPM	Fluorocarbon/ Tetrafluoro ethylene/ Propylene rubber
FFKM	Perfluoroelastomer
FKM	Fluoroelastomer
HNBR	Hydrogenated Nitrile Butadiene Rubber
ISO	International Organization for Standardization
LWOC	Loss of Well Control
MP 295	Main Pass Block 295
NACE	National Association of Corrosion Engineers
NBR	Nitrile Butadiene Rubber
NORSOK	Norsk Sokkels Konkuranseposisjon, “Norwegian Standards”
SSSV	Subsurface Safety Valve
WOC	Wait on Cement

References

Abbas, G., Irawan, S., Kumar, S., Khan, M. N., and Memon, S. 2013. Gas Migration Prevention Using Hydroxypropylmethylcellulose as A Multifunctional Additive in Oil Well Cement Slurry. In: Presented at SPE/PAPG Annual Technical Conference, 26-27 November, Islamabad, Pakistan, SPE 1696643. doi:10.2118/169643-MS.

ABS (ABS Consulting Inc), 2016. 2016 Update of Occurrence Rates for Offshore Oil Spills https://www.bsee.gov/sites/bsee.gov/files/osrr-oil-spill-response-research/1086aa.pdf

ABS, 2018. *Guide for Classification of Drilling Systems*. American Bureau of Shipping. Houston, TX

Agnew, J. W., and Klein, R. S. 1984. The Leaking Liner Top. In: Presented at the SPE Deep Drilling and Production Symposium, 1-3 April, Amarillo, Texas, SPE-12614-MS. https://doi-org.ezproxy.lib.ou.edu/10.2118/0308-0056-JPT.

Ahmed, R., Shah, S., Osisanya, S., Hassani, S., Omosebi, O., Elgaddafi, R., Maheshwari, H., Srivastava, A., Hwang, J., Sharma, M. and Tale, S. 2015. Effect of H_2S and CO_2 in HPHT Wells on Tubulars and Cement, Final Project Report, Prepared under BSEE Project# E12PC00035.

Ahmed, S., Salehi, S. and Ezeakacha, C., 2020a. Review of Gas Migration and Wellbore Leakage in Liner Hanger Dual Barrier System: Challenges and Implications for Industry. *J. Nat. Gas Sci. Eng*. **78**: p.103284. https://doi.org/10.1016/j.jngse.2020.103284

Ahmed, S., Patel, H., Salehi, S., Teodoriu, C., and Ahmed, R. 2020b. Numerical and Experimental Evaluation of Liner Dual Barrier System in Geothermal Wells. Presented at 45th Workshop on Geothermal Reservoir Engineering, 10-12 February, Stanford University, Stanford, California.

Ahmed, S., C Salehi, S., Ezeakacha, C.P. and Teodoriu, C. 2019a. Evaluation of Liner Hanger Seal Assembly and Cement Sheath as A Dual Barrier System: Implications for Industry Standards. *J. Petrol. Sci. Eng* **178**: 1092-1103. https://doi.org/10.1016/j.petrol.2019.04.017

Ahmed, S., C Salehi, S., Ezeakacha, C.P. and Teodoriu, C. 2019b. Experimental Investigation of Elastomers in Downhole Seal Elements: Implications for Safety. *Polym Test.* **76**: 350-364. https://doi.org/10.1016/j.polymertesting.2019.03.041

Ahmed, S., Ezeakacha, C.P. and Salehi, S. 2018. Improvement in Cement Sealing Properties and Integrity Using Conductive Carbon Nanomaterials: From Strength to Thickening Time. In: Presented at SPE Annual Technical Conference and Exhibition, 24-26 September, Dallas, Texas, SPE-19709-MS. https://doiorg.ezproxy.lib.ou.edu/10.2118/191709-MS.

Akhtar, M., Qamar, S.Z., Pervez, T. and Al-Jahwari, F.K. 2018. Performance Evaluation of Swelling Elastomer Seals. J. Petrol. Sci. Eng. **165**: 127-135.https://doi.org/10.1016/j.petrol.2018.01.064

Alzebdeh, K., Pervez, T. and Qamar, S.Z. 2010. Finite element simulation of compression of elastomeric seals in open hole liners. *J. Energy Res. Tech* **132** (3), 031002. https://doi.org/10.1115/1.4002244

Al-Buraik, K., Al-Abdulqader, K. and Bsaibes, R.1998. Prevention of Shallow Gas Migration Through Cement. In: Presented at the 1998 IADC/SPE Asia Pacific Drilling Conference, 7-9 March, Jakarta, Indonesia, IADC/SPE 47775-MS. https://doi.org/10.2118/47775-MS.

Al-Hiddabi, S.A., Pervez, T., Qamar, S.Z., Al-Jahwari, F.K., Marketz, F., Al-Houqani, S. and van de Velden, M. 2015. Analytical Model of Elastomer Seal Performance in Oil Wells. Appl. Math. Model. 39 (10-11), 2836-2848. https://doi.org/10.1016/j.apm.2014.10.028

Allan, M.L. and Philippacopoulos, A.J., 1998. Literature Survey on Cements for Remediation of Deformed Casing in Geothermal Wells (No. BNL-66071). Brookhaven National Lab., Dept. of Applied Science, Upton, NY, U.SA.

Al-Ramadan, M., Salehi, S., Kwatia, G., Ezeakacha, C. and Teodoriu, C. 2019. Experimental Investigation of Well Integrity: Annular Gas Migration in Cement Column. *J. Petrol. Sci. Eng.* **179**, 126-135. https://doi.org/10.1016/j.petrol.2019.04.023

Al-Yami, A. S., Nasr-El-Din, H. A., and Al-Humaidi, A. S. 2009. An Innovative Cement Formula to Prevent Gas-Migration Problems in HT/HP Wells. In: Presented at SPE International Symposium on Oilfield Chemistry, 20-22 April, The Woodlands, Texas, SPE-120885-MS. https://doi-org.ezproxy.lib.ou.edu/10.2118/120885-MS.

Al-Yami, A. S., Nasr-El-Din, H. A., and Al-Humaidi, A. S. 2008. Investigation of Water Swelling Elastomers: Advantages, Limitations, and Recommendations. In: Annual Technical Conference and Exhibition, 21-24 September, Denver, Colorado, SPE-114810-MS. https://doi-org.ezproxy.lib.ou.edu/10.2118/114810-MS.

API BULL E3, *Wellbore Plugging and Abandonment Practices.*, second edition. 2018.Washington, DC: API.

API RP 19 LH, *Recommended Practice for Liner Hangers*, first edition. 2019.Washington, DC: API.

API RP 59, *Standard for Well Control Operations,* second edition.2018. Washington, DC: API.

API RP 65-1, *Standard for Isolating Cementing Shallow-water Flow Zones in Deepwater Wells,* second edition. 2018. Washington, DC: API.

API RP 96, *Recommended Practice for Deepwater Well Design and Construction*, first edition. 2013.Washington, DC: API.

API RP 10B-2, Recommended Practice for: Testing well cements, second edition. 2013 Washington, DC, API

API STD 53, Standard for Well *Control Equipment Systems for Drilling Wells,* fifth edition. 2018.Washington, DC: API.

API STD 65-Part 2, *Standard for Isolating Potential Flow Zones During Well Construction*, second edition. 2010. Washington, DC: API.

API 17TR8, *Technical Report for High-pressure High-temperature Design Guidelines*, first edition. 2015. Washington, DC: API.
API 16 A, *Specification for Drill-Through Equipment*, first edition. 2017. Washington, DC: API.

ASTM D1415, *Standard Test Method for Rubber Property—International Hardness*. 2018. ASTM International, West Conshohocken, PA, USA.

ASTM D412, *Tensile Set of Rubber and Thermoplastic Elastomers*. 2012. ASTM International, West Conshohocken, PA, USA.

ASTM D6147, *Standard Test Method for Vulcanized Rubber and Thermoplastic Elastomer—Determination of Force Decay (Stress Relaxation) in Compression*. 2019. ASTM International, West Conshohocken, PA, USA.

ASTM D395, *Standard Test Methods for Rubber Property—Compression Set.* 2018. ASTM International, West Conshohocken, PA, USA.

ASTM D471-16a, *Standard Test Method for Rubber Property—Effect of Liquids.* 2016. ASTM International, West Conshohocken, PA, USA.

Bauer, P. 1965. Investigation of Leakage and Sealing Parameters. Technical Report AFRPL -TR-153, IIT Research Institute, Air Force Propulsion Laboratory, Air Force System Command, Edwrads, Califiornia.

Beirute, R.M., 1984. The phenomenon of free fall during primary cementing. In: Presented at SPE Annual Technical Conference and Exhibition, 16-19 September, Houston, Texas, USA. SPE-13045-MS. https://doi-org.ezproxy.lib.ou.edu/10.2118/13045-MS

Blizzard, W. A. 1990. Metallic Sealing Technology in Downhole Completion Equipment. *Journal of Petroleum Technology.* **42** (10). SPE 19195-PA doi:10.2118/19195-PA.

Bihua, X., Bin, Y. and Yongqing, W. 2018. Anti-Corrosion Cement for Sour Gas (H_2S-CO_2) Storage and Production of HTHP Deep Wells. *Applied geochemistry* **96**:155-163. doi: 10.1016/j.apgeochem.2018.07.004

BOEMRE, 2011. Report Regarding the Causes of the April 20, 2010 Macondo Well Blowout. The Bureau of Ocean Energy Management, Regulation and Enforcement.

Bois, A. P., Garnier, A., Rodot, F., Sain-Marc, J., and Aimard, N., 2011. How to prevent loss of zonal isolation through a comprehensive analysis of microannulus formation. SPE Drilling & Completion. 26(01), pp.13–31. SPE-124719-PA. http://dx.doi.org/10.2118/124719-PA

Bosma, M., Ravi, K., van Driel, W. et al. 1999. Design Approach to Sealant Selection for The Life of The Well. In: Presented at SPE Annual Technical Conference and Exhibition, 3-6 October, Houston, Texas, USA. SPE-56536-MS. https://doi.org/10.2118/56536-MS.

Bour, D.L. and East, L.E., 1988. Expansion: anti-fluid migration technology solves south Texas fluid migration problems. In: Presented at SPE/IADC Drilling Conference, 28 February-2 March, Dallas, Texas, SPE-17259-MS. https://doi-org.ezproxy.lib.ou.edu/10.2118/17259-MS

Brown, P. R.2002. *Rubber Product Failure*. Rapra Publishing.

BSEE, 2016. Annual Report. Bureau of Safety and Environmental Enforcement, Washington, DC. https://www.bsee.gov/sites/bsee.gov/files/bsee_2016_annual_report_v5_final_january2017.pdf

BSEE, 2014. OC-FIT Evaluation of Seal Assembly & Cement Failures Interim Summary of Findings. Internal QC-FIT Report #2014-02. Bureau of Safety and Environmental Enforcement, Washington, DC.
https://www.bsee.gov/sites/bsee_prod.opengov.ibmcloud.com/files/technical-presentations/blowout-prevention/qc-fit-report-apache-liner-seal.pdf

Byrom, T.G., 2013. *Casing and liners for drilling and completion*. Elsevier.

Calloni, G., Moroni, N. and Miano, F., 1995. Carbon black: a low cost colloidal additive for controlling gas-migration in cement slurries. In: Presented at SPE International Symposium on Oilfield Chemistry, 14-17 February, San Antonio, Texas, SPE-28959-MS.
https://doi-org.ezproxy.lib.ou.edu/10.2118/28959-MS

Cameron., 2018. Diverter solutions for jack-ups and floaters.
https://www.products.slb.com/-/media/productsslb/files/brochure/drilling/diverter-br.ashx

Carter, L.G., Slagle, K.A. and Smith, D.K., 1968. Resilient Cement Decreases Perforating Damage. In: Presented at the API Mid-Continent Dist. Div of Production Spring Meeting Amarillo, TX.

CFR, 2016. Code of Federal Regulations, Title 30, Mineral Resources, Office of the Federal Register National Achieves and Records Administration, US DOT.

Coker, O. D., Harris, K. L., and Williams, T. A., 1992. Preventing shallow gas migration in offshore wells: the performance of lead cements. In: Presented at European Petroleum Conference, 16-18 November, Cannes, France, SPE 24978-MS.
https://doi-org.ezproxy.lib.ou.edu/10.2118/24978-MS

Dao, B., Biezen, E., Vijn, J.P. and Pham, T. 2006. Process for Controlling Gas Migration During Well Cementing. U.S. Patent 7,060,129.

Davies, R.J., Almond, S., Ward, R.S., Jackson, R.B., Adams, C., Worrall, F., Herringshaw, L.G., Gluyas, J.G. and Whitehead, M.A. 2014. Oil and Gas Wells and Their Integrity: Implications For Shale And Unconventional Resource Exploitation. *Marine and Petroleum Geology* **56**: 239-254. http://dx.doi.org/10.1016/j.marpetgeo.2014.03.001

De Andrade, J. and Sangesland, S., 2016. Cement sheath failure mechanisms: numerical estimates to design for long-term well integrity. *J. Petrol. Sci. Eng.* **147**, pp.682-698. http://dx.doi.org/10.1016/j.petrol.2016.08.032

Denison, C.R., Fiore, C.J., Krakowski, F.J. 2018. Application of Wear-Resistant Elastomer to Significantly Improve Service Life of Telescopic Joint Packers. In: Presented at Offshore Technology Conference, 30 April - 3 May, Houston, TX, OTC-28918-MS. https:// doi.org/10.4043/28918-MS.

DOI, 2016. Follow-up on MC-295 Loss of Well Control Report. U.S. Department of Interior, Bureau of Safety and Environmental Enforcement. Washington, DC.

Dolog, R., Ventura, D., Khabashesku, V. and Darugar, Q. 2017. Nano-Enhanced Elastomers for Oilfield Applications. In: Presented at Offshore Technology Conference, 1-4 May, Houston, Texas, OTC-27609-MS. https://doi.org/10.4043/27609-MS.

Drecq, P., and Parcevaux, P. A., 1988. A Single technique solves gas migration problems across wide range of conditions. In: Presented at the SPE International Meeting on Petroleum Engineering, 1-4 November, Tianjin, China, SPE 17629 -MS. https://doi-org.ezproxy.lib.ou.edu/10.2118/17629-MS

DuPont., 2013. Putting science to work, high performance materials: Oil and Gas Industry.

DuPont., 2017. Oil and gas product selector guide.

Dusseault, M. B., Gray. M. N., Nawrock. P.A. 2002. Why Oil Wells Leak: Cement Behavior and Long-Term Consequences. In: Presented at the SPE International Oil and Gas Conference and Exhibition, 7-10 November, Beijing, China, SPE-64733-MS. https://doi.org/10.2118/64733-MS.

Dusseault, M. B., Jackson. R. E., MacDonald. D. 2014.Towards A Road Map for Mitigating the Rates and Occurrences of Long-Term Wellbore Leakage. http://geofirma.com/wp-content/uploads/2015/05/lwp-final-report_compressed.pdf.

Elhard, J.D., Duguid, A. and Heinrichs, M. 2017. Research on Safety Technology Verification for Materials and Pressure High Temperature (HPHT) Continental Shelf (OCS), High Corrosions in the US Outer Material Evaluation. Technical Assessment Program Report (TAP 767AA) Prepared

for Bureau of Safety and Environmental Enforcement. https://www. bsee. gov/tap-technical-assessment-program/research-onsafety-technology-verification-for-materials-and

Evers, R., Koloy, T.R. and Abrahamsen, T. 2013. Design Methodology for Swellable Elastomer Packers for Well Construction Operations. In : Presented SPE Annual Technical Conference and Exhibition, 30 September-2 October, New Orleans, Louisiana,SPE-166499-MS. https://doi.org/10.2118/166499-MS.

Feather, K. 2011. Better Well Integrity. In: Presented at US-Norway Technology Partnership Conference, Minimizing Oil Spills & Discharges to Sea, 30 March, Houston, TX.

Flitney, R. K., 2014. *Seals and Sealing Handbook*, sixth edition, Elsevier.

Gray, K.E., Podnos, E. and Becker, E., 2009. Finite-element studies of near-wellbore region during cementing operations: Part I. *SPE drilling & completion*. 24(01), pp.127-136.

GE., 2019. Pressure Control General Catalog .GE Oil & Gas. https://docplayer.net/25364998-General-catalog-ge-oil-gas-pressure-control.html

Goins Jr, W.C. and Ables, G.L.1987. The causes of shallow gas kicks. In: Presented at SPE/IADC Drilling Conference, 15-18 March, New Orleans, LA, IADC/SPE 16128. https://doi.org/10.2118/16128-MS.

Grace, D. R. 2017. *Blowout and Well Control Handbook*, second edition, Elsevier.

Hallaiburton.,2015. Upstream Technology. Raising the bar for liner hangers.

Hebert, R. N. 1986. Liner Cementing Techniques and Case Histories Offshore Western Gulf of Mexico. In: Presented at the IADC/SPE Drilling Conference, 10-12 February, Dallas, Texas, SPE-14777-MS. https://doi-org.ezproxy.lib.ou.edu/10.2118/14777-MS.

Hirasuna, A. R., Friese, G. J., and Stephens, C. A. 1983. A Proven Elastomer Compound for Extremely Hostile Geothermal and Oilfield Environments. Presented at the IADC/SPE Drilling Conference, New Orleans, Louisiana, 20-23 February. IADC/SPE 11407. doi:10.2118/11407-MS.

Hopkins, H.A., 2016. API Response to BSEE Report #2014-02, QC-FIT Evaluation of Seal Assembly and Cement Failures Interim Summary of Findings, Washington, DC, API.

ISO 16530-1: 2017, Petroleum and natural gas industries—Well integrity—Part 1, Life cycle governance, first edition. 2017. Geneva, Switzerland: ISO.

ISO 13702: 2015, Petroleum and natural gas industries—Control and mitigation of fires and explosions on offshore production installations—Requirements and guidelines, second edition. 2015. Geneva, Switzerland: ISO.

Jackson, J and Smith, P. 2006. Development of an Expandable Drill-In Liner Hanger for Use in Problem-Well Scenarios: Case History. In: Presented at the 2006 Offshore Technology Conference, 1-4 May, Houston, Texas, OTC-18158-MS. https://doi.org/10.4043/18158-MS.

Jafariesfad, N., Geiker, M.R., Gong, Y., Skalle, P., Zhang, Z. and He, J., 2017. Cement sheath modification using nanomaterials for long-term zonal isolation of oil wells. *J. Petrol. Sci. Eng*. **156**: 662-672. doi: 10.1016/j.petrol.2017.06.047

James, S.G. and Boukhelifa, L., 2006. Zonal isolation modelling and measurements-past myths and todays realities. In: Presented at Abu Dhabi International Petroleum Exhibition and Conference, -8 November, Abu Dhabi, UAE. SPE-101310-MS. https://doi-org.ezproxy.lib.ou.edu/10.2118/101310-MS.

Jutten, J.J., Parcevaux, P.A. and Guillot, D.J. 1989. Relationship between Cement Slurry Composition, Mechanical Properties, and Cement Bond Log Output. *SPE Production Engineering* **4** (01), SPE-16652-PA. https://doi-org.ezproxy.lib.ou.edu/10.2118/16652-PA

Kimanzi, R., Patel, H., Khalifeh, M., Salehi, S. and Teodoriu, C., 2019. Potentials of nano-designed plugs: Implications for short and long term well integrity. In: Presented at *ASME 2019 38th International Conference on Ocean, Offshore and Arctic Engineering*. American Society of Mechanical Engineers Digital Collection.

King, G.E. and King, D.E. 2013. Environmental Risk Arising from Well-Construction Failure - Differences between Barrier and Well Failure and Estimates of Failure Frequency Across Common Well Types, Locations and Well Age. In: Presented at the SPE Annual Technical and Exhibition Conference, 30 September -2 October, New Orleans, Louisiana, SPE 166142-MS. https://doi.org/10.2118/166142-MS.

Hook, F.E., Dow Chemical Co, 1969. *Aqueous cement slurry and method of use*. U.S. Patent 3,483,007.

Hopkins, H.A., 2016. API Response to BSEE Report #2014-02, QC-FIT Evaluation of Seal Assembly and Cement Failures Interim Summary of Findings, Washington, DC, API.

Kosinowski, C. and Teodoriu, C. 2012. Study of Class G Cement Fatigue Using Experimental Investigations. In: Presented at SPE/EAGE European Unconventional Resources Conference and Exhibition, 20-22 March, Vienna, Austria, SPE-153008-MS. https://doi.org/10.2118/153008-MS.

Kristiansen, T.G., Dyngeland, T., Kinn, S., Flatebø, R. and Aarseth, N.A. 2018. Activating Shale to Form Well Barriers: Theory and Field Examples. In: Presented at the SPE Annual Technical Conference and Exhibition, 24-26 September, Dallas, Texas, SPE-191607-MS. https://doi-org.ezproxy.lib.ou.edu/10.2118/191607-MS.

Kruszewski, M. and Wittig, V. 2018. Review of failure Modes in Supercritical Geothermal Drilling Projects. *Geothermal Energy*, **6** (1) : 28. https://doi.org/10.1186/s40517-018-0113-4

Lakes, R. 1993. Advances in Negative Poisson's Ratio Materials. *Advanced Materials* ***5***(4):293-296

Lavrov, A., Torsæter, M. (2016), Physics and mechanics of primary well cementing, Springerbriefs in petroleum geosciences and engineering, Springer. Doi:10.1007/978-3-319-43165-9

Ma, M., Jia, W., Bu, Y., Guo, S., 2014a. Study on Rubber Seal Design of a Swellpacker in Oil Well Cementing. Open Access Libr. J. Study **01**, 1–8. https://doi.org/10.4236/oalib.1101082

Ma,W., Qu, B and Guan., 2014b. Effect of the Friction Coefficient for Contact Pressure of Packer Rubber. *J. Mechanical Engineering Science*, **228** (16):2881–2887. doi: 10.1177/0954406214525596

Mackenzie, G., and Garfield, G. L. 2007. Wellbore Isolation Intervention Devices Utilizing a Metal-to-Metal Rather Than an Elastomeric Sealing Methodology. Presented at the SEP Annual Technical Conference and Exhibition, Anaheim, California, 11-14 November. SPE 10979-MS. doi:10.2118/109791-MS.

Marco Rubber & Plastic Inc. 2018. O-Ring Failure Analysis Guide. https://www.marcorubber.com/o-ring-failure.htm (Accessed 10 November 2019).

MMS, 2002. Minerals Management Service. Losses of well control. http://www.mms.gov/incidents/blowouts.htm.

Mohamed, A.O. and Al-Zuraigi, A. 2013. Liner Hangers Technology Advancement and Challenges. In: Presented at the SPE Middle East Oil and Gas Show and Conference, 10-13 March Manama, Bahrain, SPE-164367-MS. https://doi.org/10.2118/164367-MS.

Moore, M.J., Campo, D.B., Hockaday, J. and Ring, L., 2002. Expandable Liner Hangers: Case Histories. In: Presented at Offshore Technology Conference, 6-9 May, Houston, Texas, OTC 14313-MS. https://doi.org/10.4043/14313-MS.

Morries, D., Levine, J and Hudson, C. 2015. Seal Assembly/Cement Failure Technical Evaluation. In: API's 2015 Exploration and Production Standards on Oilfield Equipment and Materials Summer Meeting, 23 June, San Francisco, California. https://www.bsee.gov/sites/bsee.gov/files/public-comments/safety/bsee-seal-assembly-cement-failure-technical-evaluation-june-23-2015.pdf

Mueller, D. and Eid, R., 2006. Characterizing Early-Stage Physical Properties, Mechanical Behavior of Cement Designs. In: Presented at IADC/SPE Drilling Conference, 21-23 February, Miami, Florida, USA, SPE-98632-MS. https://doi-org.ezproxy.lib.ou.edu/10.2118/98632-MS.

Muncrief, R. E., LaFollette, R. E., and Rainbolt, C. G., 1984. Techniques for successful liner cementing in the Anadarko Basin. In: Presented at Deep Drilling and Production Symposium, 1-3 April, Amarillo, Texas, SPE-12627-MS. https://doi-org.ezproxy.lib.ou.edu/10.2118/12627-MS

NACE MR0175-1., 2015. General principles for selection of cracking-resistant materials. NACE International, Houston, TX.

NACE TM0187., 2011. Evaluating Elastomeric Materials in Sour Gas Environments. NACE International, Houston, TX.

NACE TM0192. 2012. Evaluating Elastomeric Materials in Carbon Dioxide Decompression Environments. NACE International, Houston, TX.

NACE TM0297-HD. 2017. Effects of High-Temperature, High-Pressure Carbon Dioxide Decompression on Elastomeric Materials. NACE International, Houston, TX.

Najipoor, M., Haroonabadi, L and Dashti, A. 2008. Assessment of failures of nitrile rubber vulcanizates in rapid gas decompression (RGD) testing, Polym. Test. **72** (2018) 377-385 https://doi.org/10.1016/j.polymertesting.2018.11.002

Nath, F., Kimanzi, R.J., Mokhtari, M. and Salehi, S., 2018. A novel method to investigate cement-casing bonding using digital image correlation. *Journal of Petroleum Science and Engineering*, ***166***, pp.482-489. DOI: 10.1016/j.petrol.2019.106806

Nelson, E. B. (Ed.). (1990). *Well cementing*. Newnes.

Nida, R., 2005. Liner hanger system increases installation success. *Drilling Contractor*. **61**(2). http://iadc.org/dcpi/dc-maraprl05/March05-expand.pdf

NORSOK Standard D-010., 2013. Well Integrity in Drilling and Well Operations, rev. 4, Lysaker, Norway: Standards Norway.

NORSOK M-710., 2014. Qualification of Non-Metallic Materials and Manufacturers – Polymers, rev 3. Lysaker, Norway: Standards Norway.

Patel, H., Salehi, S., Ramadan, A., and Teodoriu, C. 2019a. Review of Elastomer Seal Assemblies in Oil & Gas Wells: Performance Evaluation, Failure Mechanisms, and Gaps in Industry Standards. *J. Petrol. Sci. Eng*, **179** : 1045-1062. https://doi.org/10.1016/j.petrol.2019.05.019

Patel, H., Salehi, S., Teodoriu, C. and Ahmed, R., 2019b. Performance Evaluation and Parametric Study of Elastomer Seal In Conventional Hanger Assembly. *J. Petrol. Sci. Eng* **175**: 246-254. https://doi.org/10.1016/j.petrol.2018.12.051

Patel, H., Salehi, S and Teodoriu, C., 2019c. Assessing Mechanical Integrity of Expanding Cement. In: Presented at SPE Oklahoma City Oil & Gas Symposium, April 9-10, Oklahoma City, OK. SPE 195225. https://doi.org/10.2118/195225-MS.

Patel, H., and Salehi, S. 2019a. Investigation of Elastomer Seal Energization: Implications for Conventional and Expandable Hanger Assembly. *Energies* **12** (4): 763. https://doi.org/10.3390/en12040763.

Patel, H. and Salehi, S. 2019b. Development of an Advanced Finite Element Model and Parametric Study to Evaluate Cement Sheath Barrier. *Journal of Energy Res Tech,* **141**(9): 092902. doi:10.1115/1.4043137.

Payne, C.W., Warneke, J.S. and Kaculi, J.T. 2016. Liner Hanger Rating Methodologies Validated with Physical Testing. In: Presented at Offshore Technology Conference, 2-5 May, Houston, Texas, OTC-26945-MS. https://doi-org.ezproxy.lib.ou.edu/10.4043/26945-MS.

Per Holand, 2017. Research on Loss of Well Control Occurrence and Size Estimators, Phase I and II. Report (ES201471/2) Prepared for Bureau of Safety and Environmental Enforcement.

Persson, B. N. J and Yang, C., 2008. Theory of the Leak-Rate of Seals. *J. Physics: Condensed Matter* **20** (31): 315011. doi:10.1088/0953-8984/20/31/315011

Pervez, T., Qamar, S.Z., Siddiqui, R.A., van de Velden, M., 2009. Effect of exposure on material response of a swelling elastomer. Arch. Mater. Sci. Eng. **37**, 77–84

Pervez, T., Seibi, A., Al-Hiddabi, S., Al-Jahwari, F.K., Qamar, Z.S. and Marketz, F. 2007. Solid Tubular Expansion in Horizontal Wells. In: Presented SPE Middle East Oil and Gas Show and Conference, 11-14 March, Manama, Bahrain, SPE-105704-MS. https://doi.org/10.2118/105704-MS.

Peyvandi, A., Taleghani, A. D., Soroushian, P. and Cammarata, R. 2017. The Use of Low-Cost Graphite Nanomaterials to Enhance Zonal Isolation in Oil And Gas Wells. In: Presented at the SPE Annual Technical Conference and Exhibition, 9–11 October, San Antonio, Texas, SPE-187105-MS. https://doi.org/10.2118/187105-MS.

Pleasants, C., Joseph, B., Glynn, J., Munshi, A. and Knebel, M. 2014.Successful Installation of a Completion System For Gas Migration Prevention. In: Presented at Offshore Technology Conference-Asia, Kuala Lumpur, Malaysia. 25-28 March. OTC-24831-MS. https://doi-org.ezproxy.lib.ou.edu/10.4043/24831-MS.

PPE (Precision Polymer Engineering).2019.https://www.prepol.com/solutions/why-do-o-rings-fail-a-brief-guide-to-o-ring-failure-mode (Accessed 10 November 2019)

Pour, M.M. and Moghadasi, J., 2007. New Cement formulation that solves gas migration problems in Iranian South Pars field condition. Presented at the 15th SPE Middle East Oil & Gas Show and Conference, Bahrain International Exhibition Centre, Kingdom of Bahrain. 11-14 March. SPE-105663-MS. https://doi.org/10.2118/105663-MS

Prince, P.K. 1990. Current Drilling Practice and The Occurrence of Shallow Gas. *J. Safety in Offshore Drilling,* (**35**):3-25.

PSA, 2013. Norwegian Petroleum Safety Authority. Principles for Barrier Management in the Petroleum industry. http://www.ptil.no/getfile.php/1319891/PDF/Barrierenotatet%202013%20engelsk%20april.pdf.

PSA, 2006. Norwegian Petroleum Safety Authority. Principles for Barrier Management in The Petroleum Industry.

Ramosa, R.M. and Camusc, A.S., 2017. Borehole cement sheath integrity-numerical simulation under reservoir conditions. *Mecánica Computacional*. p. 193-225

Ravi, K., Bosma, M. and Gastebled, O., 2002. Improve the economics of oil and gas wells by reducing the risk of cement failure. In: Presented at IADC/SPE Drilling Conference, 26-28 February, Dallas, Texas. SPE-74497-MS.
https://doi-org.ezproxy.lib.ou.edu/10.2118/74497-MS.

Rogers, M. J., Dillenbeck, R. L and Eid, R. N. 2004. Transition Time of Cement Slurries, Definitions and Misconceptions, Related to Annular Fluid Migration. In: Presented at the SPE Annual Technical Conference and Exhibition, 26-29 December, Houston, TX, SPE-90829-MS. https://doi.org/10.2118/90829-MS.

Royer, E.S. and Turney, R.A. 2019. HPHT Expandable Liner Hanger Technology with Superior Pressure Integrity. In: Prasented at Offshore Technology Conference. Offshore Technology, 6-9 May, Houston, Texas, OTC-29494-MS. https://doi-org.ezproxy.lib.ou.edu/10.4043/29494-MS.

Sabins, F. L., Tinsley, J. M. and Sutton, D. L. 1982. Transition Time of Cement Slurries Between the Fluid And Set States. *SPE J*. 22(06), 875-882. http://dx.doi.org/10.2118/9285-PA.

Saleh, F. K., Salehi, S., & Teodoriu, C. 2019. Experimental Investigation of Mixing Energy of Well Cements: The Gap Between Laboratory and Field Mixing. *J. Nat. Gas Sci Eng.* **63**: 47-57. https://doi.org/10.1016/j.jngse.2019.01.004.

Saleh, F. K., Rivera, R., Salehi, S., Teodoriu, C. and Ghalambor, A. 2018. How Does Mixing Water Quality Affect Cement Properties. Presented at the SPE International Conference and Exhibition on Formation Damage Control, Lafayette, Louisiana, 7–9 February. SPE-189505-MS. https://doi.org/10.2118/189505-MS

Salehi, S., Ezeakacha, C.P., Kwatia, G., Ahmed, R. and Teodoriu, C. 2019. Performance Verification of Elastomer Materials in Corrosive Gas and Liquid Conditions. *Polym Test* **75**: 48-63. https://doi.org/10.1016/j.polymertesting.2019.01.015.

Simpson, D. A., 2017. Practical Onshore Gas Field Engineering.

Skalle, P. 2012. *Pressure Control During Oil Well Drilling*, third edition, Ventus Publishing ApS.

Sklet, S., 2005. *Safety Barriers on Oil and Gas Platforms Means to Prevent Hydrocarbon Releases*. PhD thesis. Norwegian University of Science and Technology , Trondheim, Norway.

Skogdalen, J.E., Utne, I.B. and Vinnem, J.E., 2011. Developing Safety Indicators for Preventing Offshore Oil and Gas Deepwater Drilling Blowouts. *J. Safety science.* (**49**):1187-1199.
doi:10.1016/j.ssci.2011.03.012

Strand, G. 2017. *Well Safety: Risk Control in the Drilling Phase of Offshore Wells*. PhD thesis. Norwegian University of Science and Technology , Trondheim, Norway.

Speer, M., 2006. Introduction to wellhead systems. In: In: Lake, L.W. (Ed.), Petroleum Engineering Handbook, vol. 2. Society of Petroleum Engineers, Richardson, Texas pp. 344–369 Chap. 8.

Talabani, S., and Hareland, G. 1995. New Cement Additives that Eliminate Cement Body Permeability. In: Presented at SPE Asia Pacific Oil and Gas Conference, 20-22 March, Kuala, SPE 29269-MS. https://doi-org.ezproxy.lib.ou.edu/10.2118/29269-MS.

Tavares, F., Rocha, J. and Calado, V., 2013, October. Study of the influence of cement slurry composition in the gas migration. In: Presented at Offshore Technology Conference, 29-31 October, Rio de Janeiro, Brazil, OTC-24420-MS. https://doi-org.ezproxy.lib.ou.edu/10.4043/24420-MS

Thorbjornsson, I. 2016. Deliverable Candidate Materials for Couplings and Casings, Geowell, Grant Agreement No. 654497;2016.

Torbergsen, H.E.B., Haga, H.B., Sangesland, S., Aadnøy, B.S., Sæby, J., Johnsen, S., Rausand, M. and Lundeteigen, M.A. 2012, December. An Introduction to Well Integrity. In: Presented at Norwegian Oil and Gas Association's Well Integrity Forum (WIF), Norwegian University of Science and Technology (NTNU), Universitet i Stavanger (UIS).

Teodoriu, C., Ichim, A., and Falcone. G., 2018. Estimation of cement thermal properties through the three-phase model with application to geothermal wells. *J. Energies.* **10** (11), 28-39. doi:10.3390/en11102839

Verbakel, R., Salazar, J., and van Aerssen, M., 2016. Optimized cement systems and placement techniques for tight clearance liners. In: Presented at the SPE Bergen One Day Seminar , 20 April, Bergen, Norway, SPE-180001-MS. https://doi-org.ezproxy.lib.ou.edu/10.2118/180001-MS

Van Dort, R., 2009. Metal-to-Metal Seals Meet Downhole Hazard Demands. *J. Petrol. Technol.* **61** (01): 24–26. SPE-0109-0024-JPT. https://doi.org/10.2118/0109-0024-JPT

Visakh, P.., Sabu, T., Arup, K.C., Mathew, A.P., 2013. Advances in Elastomers I, Advanced Structural Materials. Springer. https://doi.org/10.1007/978-3-642-20925-3

Walker, J., 2009. Elastomeric seals & components for the oil & gas industry.

Walker, J., 2017. Elastomer Engineering Guide.

Walvekar, S. and Jackson, T. 2006. Expandable Technology Improves Reliability of Conventional Liner Hanger Systems. In: Presented at the IADC/SPE Drilling Conference, 21-23 February, Miami, Florida, SPE-99186-MS. https://doi.org/10.2118/99186-MS.

Watson, T.L. and Bachu, S. 2007. Evaluation of The Potential for Gas and Co_2 Leakage Along Wellbores. In: Presented at the SPE E&P Environmental and Safety Conference, 5-7 March, Galveston, Texas, SPE 106817. https://doi.org/10.2118/106817-PA.

Welch, J.C., Newman, C.R., Gerrard, D.P., Mazyar, O.A., Mathur, V., Thieu, V. 2012. Nano-enhancement of elastomers for improved downhole barrier performance. In: Presented at SPE Deepwater Drilling and Completions Conference, 20-21 June, Galveston, TX, SPE-147409-MS. https://doi.org/10.2118/147409-MS.

Williford, J and Smith, P. 2007. Expandable Liner Hanger Resolves Sealing Problems and Improves Integrity in Liner Completion Scenarios. In: Presented at the SPE 2007 Production and Operations Symposium, 31 March-3 April, Oklahoma City, Oklahoma, SPE-106757-MS. https://doi.org/10.2118/106757-MS.

Williford, J., Rice, P. and Ray, T. 1999. Selection of Metallurgy and Elastomers Used in Completion Products to Achieve Predicted Product Integrity for the HP/HT Oil and Gas Fields of Indonesia. Presented: In SPE Asia Pacific Oil and Gas Conference and Exhibition, 20-22 April, Jakarta, Indonesia, SPE-54291-MS. https://doi.org/10.2118/54291-MS

Worldwide oilfield Machine., 2019. BOP Replaceable Seat Seal Assembly. https://womgroup.com/product/replaceable-seat-seal-assembly/

Wu, B., Doble, R., Turnadge, C. and Mallants, D. 2016. Well Failure Mechanism and Conceptualization of Reservoir-Aquifer Failure Pathways. In: Presented at the SPE Asia Pacific Oil & Gas Conference and Exhibition,25-27 October, Perth, Australia, SPE-182460-MS. https://doi.org/10.2118/182460-MS.

Zeng, J., Gao, D., Wang, Y. and Fang, J., 2019. Evaluation Method for Cement Sheath Sealing Failure Under Sustained Casing Pressure. *Chemistry and Technology of Fuels and Oils*. pp.1-12. DOI 10.1007/s10553-019-01007-7

Zhang, L., Dzombak, D. A., Nakles, D. V., Hawthorne, S. B., Miller, D. J., Kutchko, B. G., Lopano, C. L. and Strazisarc B, R. 2013. Characterization of pozzolan-amended wellbore cement exposed to CO_2 and H_2S gas mixtures under geologic carbon storage conditions. *Int. J. Greenhouse Gas Control* **19** (11): 358-368. http://dx.doi.org/10.1016/j.ijggc.2013.09.004

Appendix A: Guidelines for Pressure Test of Different Barriers

Table A. 1 Pressure test guidelines for wellbore main barriers (Data are extracted from CFR 2016)

Barrier		Minimum Test Pressure		Holding Period
Cemented Casing	Drive or structural	Not required		30 minutes [1]
	Conductor	200 psi		
	Surface, intermediate, and production	70 % of its minimum internal yield		
Drilling liner (and liner-lap)		Equal to the anticipated pressure to which the liner will be subjected during the formation pressure-integrity test		30 minutes
Production liner (and liner-lap)		500 psi above the formation fracture pressure at the casing shoe into which the liner is lapped		30 minutes
Diverter-sealing element and diverter valves[2]		200 psi		Not mentioned
BOP[4] system (this includes the choke manifold, kelly valves, inside BOP, and drill-string safety valve)		Low-pressure test	200-300 psi	5 minutes[3]
		High-pressure test (ram type)	Rated working pressure or 500 psi above MASP	5 minutes[3]
		High-pressure test (annular type)	70 % of rated working pressure	5 minutes[3]

Notes:

1- The pressure must not decline 10% during the holding period.

2- After the diverter installation and test, another pressure test must be conducted within 7 days.

3- For surface BOP, 3 minutes are acceptable.

BOP must be pressure tested when installed and before two weeks have elapsed since last test.

Appendix B: Comparison between Elastomers Used in Liner Hangers

Table A.2: Common elastomers used in liner hangers

Type	Family	Applications	Working Conditions	Manufacturer/ Reference
NBR	Nitrile	**RS**: Petroleum oils and fuels, water and glycols **Not RS**: Ketones, H_2S esters and amines	-For lower duties -Low to medium down-hole temperature (-50°C to 120°C)	James Walker/ Walker, (2009)
HNBR	Hydrogenated Nitrile	**RS**: Petroleum oils and fuels, water and glycols **Not RS**: Strong acids and halohydrocarbons	-Slightly better tolerance than standard nitrile -Down-hole temperature (-55°C to 160°C)	James Walker/ Walker, (2009)
Viton	Fluoroelastomer (FKM)	**RS**: Petroleum oils and fuels, acids, halohydrocarbons and phosphate esters **Not RS**: Ketones, amines, hot water and steam	-Medium to high down-hole temperature (200°C to 315°C) -Resistant to H_2S -Economical solution in high-temperature and harsh-chemical environments	James Walker/ Walker, (2009) DuPont/ DuPont, (2013) DuPont, (2017)
Aflas	Tetrafluoroethylene (FEPM)	**RS**: Sour petroleum oils and fuels, acids, bases, amines and steam **Not RS**: Halohydrocarbons	-Medium to high down-hole temperature, 5°C to 205°C -Resistant to H_2S -Swellable when used in oil-based fluids	James Walker/ Walker, (2009) AFLAS/ DuPont, (2013) DuPont, (2017)
Kalrez	Perfluoroelastomer (FFKM)	**RS**: Sour petroleum, acids, bases, MTBE and ketones **Not RS**: Alkali metal solutions	-HP/HT applications -Maximum application temperature (325°C) - Maximum application pressure (45000 psi)	James Walker/ Walker, (2009) DuPont/ DuPont, (2013) DuPont, (2017)

Note: RS = Recommended Service

Appendix C: Tool to Predict Cement Failure Matrix of Different Liner Dual Barrier Systems

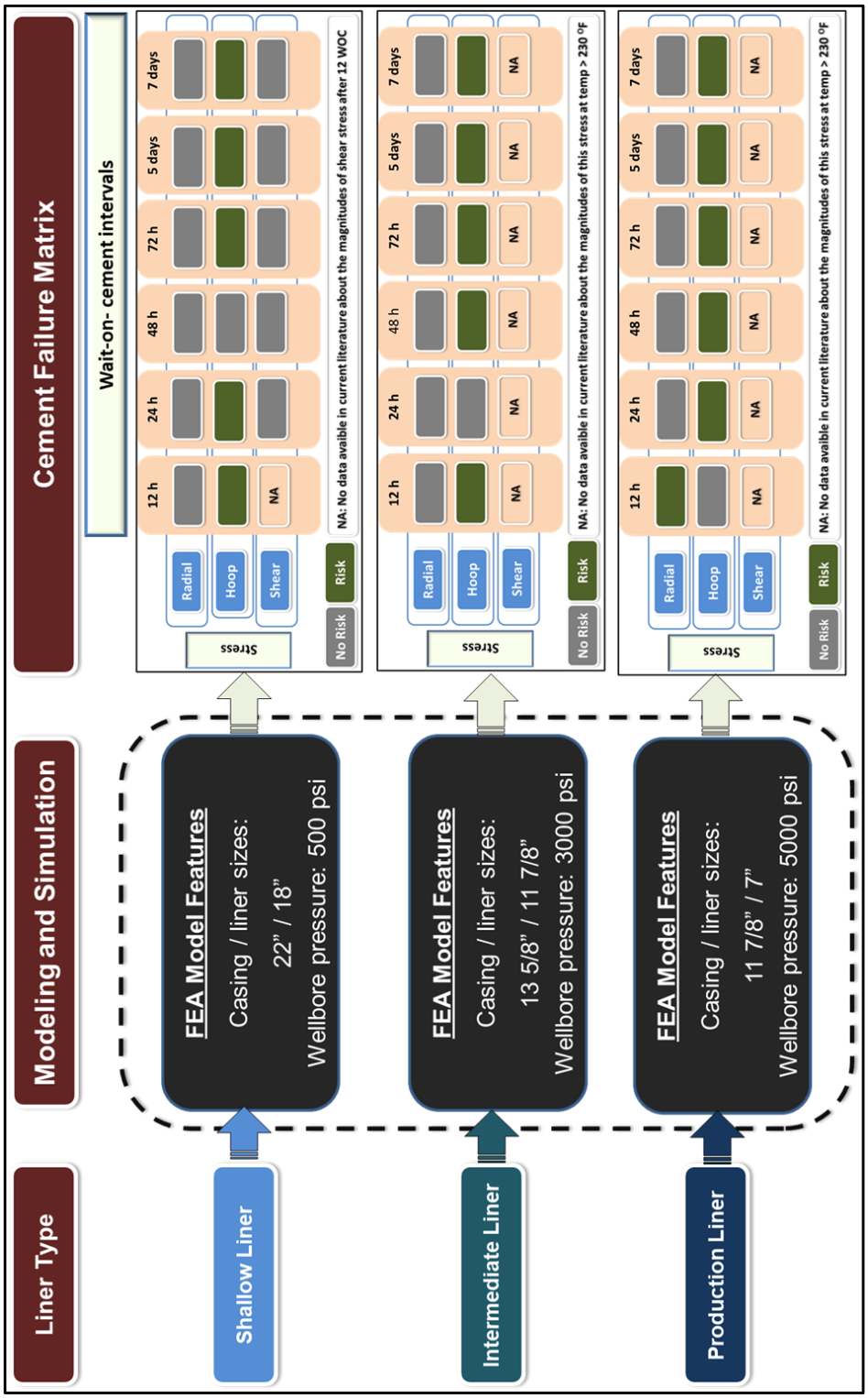

Figure A 1: Cement Failure Matrix at different liner hangers (Shallow, intermediate, and production)